FLAMMABILITY CHARACTERISTCS OF LIGHT HYDROCARBONS AND THEIR MIXTURES AT ELEVATED CONDITIONS

A Dissertation

by

NING GAN

Submitted to the Office of Graduate and Professional Studies of
Texas A&M University
in partial fulfillment of the requirements for the degree of

DOCTOR OF PHILOSOPHY

Chair of Committee,	M. Nazmul Karim
Co-Chair of Committee,	Dragomir B. Bukur
Committee Members,	Mahmoud M. El-Halwagi
	Eric L. Petersen
Head of Department,	M. Nazmul Karim

December 2018

Major Subject: Chemical Engineering

ABSTRACT

Accurate data of flammability limits for flammable gases and vapors are needed to prevent fires and explosions. The flammability limit is the maximum or minimum fuel concentration at which a gas mixture is flammable in a given atmosphere. Even though investigations of flammability limit have been carried out for decades, data are still scarce and sometimes unavailable. Through years of study, people have developed estimation and approximation methods for the prediction of flammability limit. However, these methods exhibit significant variations, especially at elevated temperatures and pressures.

This research focuses on the flammability limits of light hydrocarbons (methane, propane, and ethylene) and their binary mixtures at normal and elevated conditions. The flammability limits of pure light hydrocarbons, and binary mixtures were determined experimentally at the temperature up to 300 ℃ and initial pressure up to 2atm. The experiments were conducted in a closed cylindrical stainless steel vessel with upward flame propagation. The combustion behavior and different flammability criteria were compared and the 7% pressure increment was determined as the most appropriate criterion for the test. Experimentally measured pure hydrocarbon flammability limits are compared with existing data in the literature to study the influence of temperature, pressure, and apparatus set. An estimation model was developed for the prediction of pure light hydrocarbon flammability limit at elevated conditions.

For binary mixtures, experiment data were compared with predictions from Le Chatelier's Rule to validate its application at elevated conditions. It was discovered that Le Chatelier's rule works fairly well for the lower flammability limit of mixtures only. The explanation of the difference between upper flammability limit predictions with experimental data was investigated through the reaction pathway analysis using ANSYS CHEMKIN software. It was proved that for the upper flammability limit test, ethylene was more reactive than methane and propane in the combustion process. Finally, a modified Le Chatelier's rule model was developed and validated using experimental data.

DEDICATION

To my mother, Lichan Chen and my father, Boxuan Gan, who always believe in me and give all their love to me.

To my fiancée, Lei Shi, who encouraged me every day during my Ph.D. study.

.

This is a tribute to the three of you.

ACKNOWLEDGEMENTS

I would like to express my deepest gratitude to my advisor, Dr. M. Nazmul Karim, for all his guidance, advice, and help through these years of study and work. Besides the instructions in the class, guidance in the work, he is also a true mentor in my life who teaches me to be a better person. During my Ph.D. study, he has provided tremendous professional suggestions and countless opportunities for me. I am grateful and honored to be one of his students.

I would like to thank my committee co-chair, Dr. Dragomir Bukur, for his support of my research. Without him, the path of this research and study would be a lot more difficult. Also I would like show my appreciation to my committee members, Dr. Mahmoud El-Halwagi, and Dr. Eric Petersen, for their advice, availabilities and commitments.

I would like to acknowledge Dr. Hans Pasman for his detailed advice and insightful ideas relating to my research. He is the person who taught me the fundamental concepts of combustion and guided me through my research.

I must thank Randy Marek for his invaluable help in building and modification of my flammability apparatus. Discussions and communications with Randy helped me establish the basic understanding of experiment equipment design.

I would like to thank Dr. Chad Mashuga, who helped me in the initial stage of my research. Many of my research ideas came from Dr. Mashuga's guidance.

Thanks also go to my friends and colleagues at Texas A&M University. Special thanks go to the members and staff of the Mary Kay O'Connor Process Safety Center, especially to Valerie Green for her care and help during my daily life.

There are not enough words to thank my parents, Lichan Chen and Boxuan Gan, for their love and unconditional support, for being the reason to motivate me moving forward and becoming better.

CONTRIBUTORS AND FUNDING SOURCES

Contributors

This work was supervised by a dissertation committee consisting of Professor M. Nazmul Karim, Professor Dragomir Bukur, Professor Mahmoud El-Halwagi of the Department of Chemical Engineering, and Professor Eric Petersen of the Department of Mechanical Engineering.

All work for the dissertation was completed independently by the student.

Funding Sources

Graduate study was supported by a fellowship from Texas A&M University and a dissertation research fellowship from Mary Kay O'Connor Process Safety Center.

TABLE OF CONTENTS

Page

LIST OF FIGURES

Page

LIST OF TABLES

Page

1. INTRODUCTION

1.1 Introduction and background

Combustible gases like hydrogen and hydrocarbons are widely used in industry. For the safe handling of combustible or flammable gases and vapors, it is imperative to understand their properties [1]. Knowing flammability limits and related information is crucial since serious fires and gas explosions may occur within the flammable range. Figure 1 shows an example of the consequences that resulted from unintentional propylene release. The incident Williams Olefins explosion [2] occurred on June 13, 2013 at Geismar, Louisiana. In this incident, propylene vapor cloud formed quickly through the leak of a liquid cracker and was ignited by a damaged heat exchanger.

Figure 1 Williams olefins explosion at Geismar plant (Reprinted from CSB's investigation report of Williams Olefins plant explosion and fire case study) [2]

Flammability characteristics including flammability limits, ignition requirements and burning rates may change under various conditions. Available data are not always

adequate for use in a particular application [3] since most of them have been obtained at room temperature and lower pressure range.

1.2 Motivations and objectives

Research of flammability limits for combustible gases started since 1817 [4] and has been improving ever since. Typical flammability research can be categorized based on different factors including: fuel: single vs. multiple, ambient condition/elevated condition, in air/in controlled atmosphere. In the past years, research mainly focused on the single fuel divisions. Even though investigations have extended into other divisions, data for flammability limits are still scarce and sometimes unavailable.

In industry, many of the process and operations requires understanding of the flammability behavior since the reactions take place in the fuel rich region with more than one species (fuel, inert gas or oxidizer) being present, where flammability limits data are limited. It is the ultimate goal to maximize the reaction efficiency while staying safe. To avoid entering flammable zone, people have developed estimation and approximation methods to predict flammability characteristics. However, the estimation and approximation methods such as Le Chatelier's rule, may not be accurate and they only apply to certain ranges and circumstances. For example, the experimental flammability limits of unsaturated hydrocarbon (ethylene, propylene, etc.) mixtures deviate from the predicted value of Le Chatelier's rule [5] (See Figure 2).

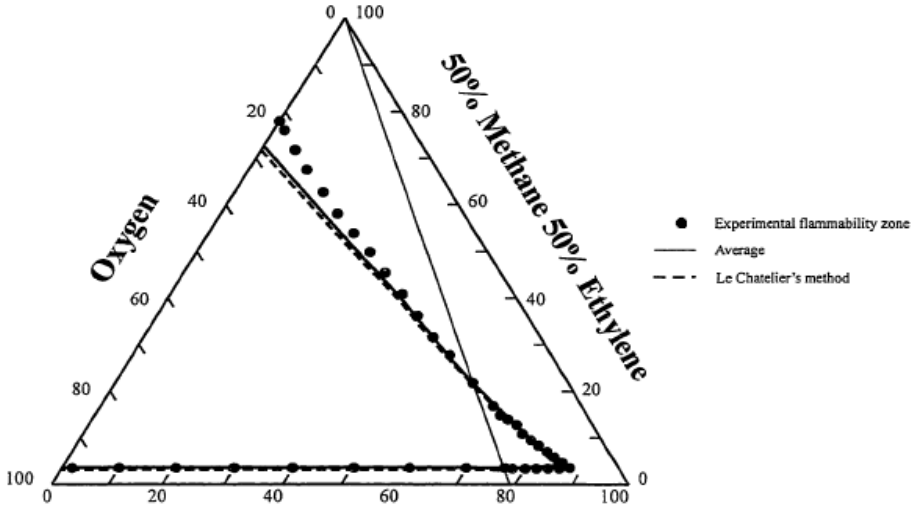

Figure 2 Experimental data and Le Chatelier's rule prediction for 50% methane and 50% ethylene flammability limits (Reprinted from Mashuga CV. Determination of the combustion behavior for pure components and mixtures using a 20 L sphere.) [5]

The prediction of flammability characteristics becomes even more complex when combustible gases are mixed at high temperatures and high pressures. Therefore, it is necessary to verify the mixture rules at elevated conditions and to find out how much do they deviate from experimental data. It is necessary to fill in these gaps and build up comprehensive data sources for flammability limits.

In this research, the first objective is to design and conduct experiments to determine the flammability limits of

a) pure light hydrocarbons (methane, propane, ethylene, etc.) at normal conditions

b) pure light hydrocarbons at elevated conditions (Temperatures: ambient to 300 ℃; Pressures: atmospheric to 3atm).

c) binary mixtures of hydrocarbons at different compositions and normal conditions

d) binary mixtures at elevated conditions.

The goal of experiments is to provide essential data set of flammability limits and using the data set to study apparatus set influence, temperature effect and pressure effect. These studies will be used to develop models to predict flammability limit of pure light hydrocarbons at elevated conditions.

The second part of the research is to conduct numerical data analysis from obtained experimental data for the validation of mixture rules such as Le Chatelier's rule and Calculated Adiabatic Flame Temperature (CAFT) model. The prediction results will be compared with experimental data to examine the validity of mixture rule at elevated conditions. If necessary, modifications on the mixture rule will be performed so that more accurate models can be provided for industrial applications.

1.3 Dissertation organization

This dissertation is based on the research program in the flammability laboratory of the Mary Kay O'Connor Process Safety Center at Texas A&M University.

This dissertation includes seven chapters:

Chapter 1 presents the motivations, objectives, and the organization of this dissertation.

Chapter 2 introduces the background information and literature review related to this work, which includes the definition of flammability, the flammability dependence on various factors such as temperature, pressure, humidity, gas composition, ignition and apparatus set, as well as the fuel mixture flammability limit.

Chapter 3 covers the experimental setup and the operation procedure used for this research. Detailed description of the equipment and modification of the hardware are provided.

Chapter 4 focuses on the determination of flammability criterion for the non-standard apparatus set used in this work. Combustion behaviors collected from experiments are categorized and used as a semi-quantitative method to distinguish flame propagation capability. Different flammability limit criterion from industrial standard and their corresponding pressure/temperature indices are compared for the selection of the most appropriate measurement criterion for the experiment.

Chapter 5 presents experimental data of pure light hydrocarbon flammability limits. From the comparison of data collected at different initial conditions, apparatus set influence, temperature effect and pressure effect on the pure fuel component are provided. From the analysis of data from temperature effect and pressure effect, a model of flammability limit prediction of pure light hydrocarbons at elevated conditions is suggested.

Chapter 6 summarizes experimental data of binary hydrocarbon flammability limits at different compositions and different reaction conditions. Experimental data are compared with predictions from mixture rule to validate mixture rule effectiveness at

elevated conditions. Detailed reaction mechanism analyses are provided to support experimental data.

Chapter 7 summarizes the conclusions from the work and provides recommendations for future work.

2. BACKGROUND AND LITERATURE REVIEW

2.1 Flammability limit definition

The essence of fire (combustion) or explosion is a rapid exothermic oxidation reaction of an ignited fuel [6]. The basic elements of combustion include fuel, oxidizer, and ignition source, which can be presented as Figure 3. A more recent study suggests that the essence of combustion should be further understood as the fire tetrahedron (Figure 4) [7], in which the element of chain chemical reaction is also necessary to sustain the fire. The fire tetrahedron is a better model that can be used to understand the flame propagation during the combustion process. When the flame propagates, the exothermic oxidation reaction from burned gas will heat up unburned gas to a certain temperature for the ignition to happen. This chain reaction will sustain the fire and allows it to continue until or unless at least one of the elements (fuel, oxidizer, ignition source, chain reaction) is removed. On the other hand, the differences between fires and explosions are mainly related to the rate of energy release. Since the fire and explosion in this study are generated from the combustion of vapors and gases, the reaction mechanism of fire and explosion can be simply determined as the oxidation chemical reaction of light hydrocarbon with air.

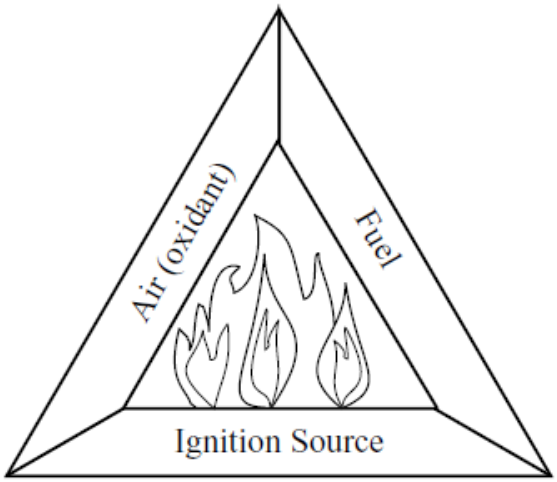

Figure 3 The fire triangle (Reprinted from Daniel A. Crowl, Joseph F. Louvar. Chemical process safety: fundamentals with applications. 3rd ed.) [6]

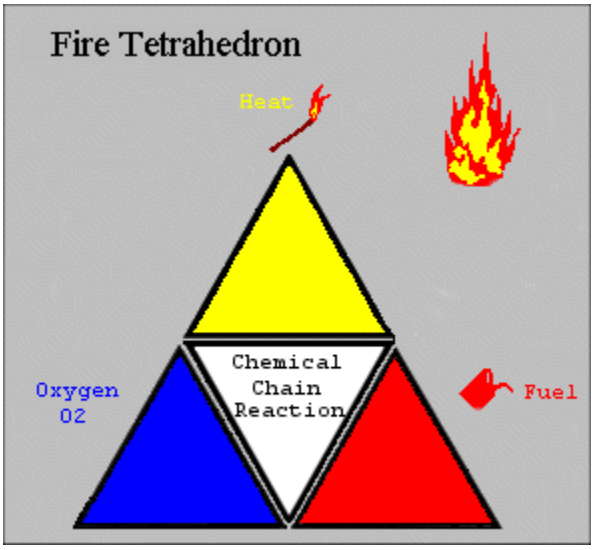

Figure 4 The fire tetrahedron (Reprinted from Safelincs-Ltd. Information about the Fire Triangle/Tetrahedron and Combustion.) [7]

Studies of flammable gas characteristics have been conducted for decades. To prevent unwanted fire and gas explosions, or to ensure that fuel gas mixtures of

combustion reaction remain in the safe zone, knowledge of gas and vapor flammability is required.

Among all of the flammability indices, one of the most important parameters is the flammability limit [8], which is defined as the volume percentage concentration of a flammable substance (mostly gases and vapors) in air that can produce a fire or explosion when an ignition source is present.

Each flammable gas substance can only be ignited within a certain fuel concentration range, which is capped by a lean limit and a rich limit, including: 1) the lower flammability limit [9] (LFL), the minimum concentration of a combustible substance that is capable of propagating a flame through a homogeneous mixture of the combustible substance, and a gaseous oxidizer under the specified conditions of the test; 2) upper flammability limit [9] (UFL), the maximum concentration of a combustible substance that is capable of propagating a flame. In the U.S. and Europe, different industrial standards are implemented to experimentally measure the flammability limit using certain apparatus and criterion.

2.2 Flammability limit dependence

Flammability limit of gases and vapors is not a constant. It can be affected by various factors including:

i. condition of the gas mixtures, such as the mixture temperature, initial pressure before ignition, humidity, etc.,

ii. composition of the gas, such as the oxidizer type, oxidizer concentration, inert gas species, etc.;

iii. ignition, which include ignition source, ignition energy, direction of flame propagation;

iv. apparatus or enclosure used for the experiment, both the dimension and shape of the test vessel will have influence on the measurement results.

Therefore, in reporting results from flammability limit studies it is important to include specifications of the experimental apparatus, the criterion of flammability, and the experimental conditions. In the following section, literature about flammability limit dependence on each influencing category is explained.

2.2.1 Dependence on gas condition - Temperature

Research by Coward and Jones [10] indicated that the flammability limit of most fuels varies linearly as temperature increases (Figure 5). In general, the flammability region widens (UFL increases and LFL decreases) when the initial temperature of the gas mixture increases (Figure 6). By collecting and analyzing flammability limit data of light hydrocarbons, Zabetakis generated two equations for LFL (Equation 1) and UFL (Equation 2) to quantify the temperature impact on flammability limit [3]

$$\frac{LFL_T}{LFL_{25}} = 1 - 0.000784 \times (T - 25) \quad (1)$$

$$\frac{UFL_T}{UFL_{25}} = 1 + 0.000721 \times (T - 25) \quad (2)$$

where, LFL_{25} and UFL_{25} are flammability limits at room temperature (25 ℃). LFL_T and UFL_T are flammability limits at test temperature T (℃). These two correlations, which

are generated based on the theory that the flame temperature is constant at the lower limit [11], use 1300 ℃ as the approximate flame temperature and can fit in the data generated using upward flame propagation. However, equation 1 and equation 2 are very approximate and only work for a very limited number of hydrocarbons over a limited temperature range. Especially, the higher alkanes (hexane, heptane, and octane) do not follow these equations, and the reason is that nonlinearities arise due to cool-flame ignitions with some gases at some temperatures [12].

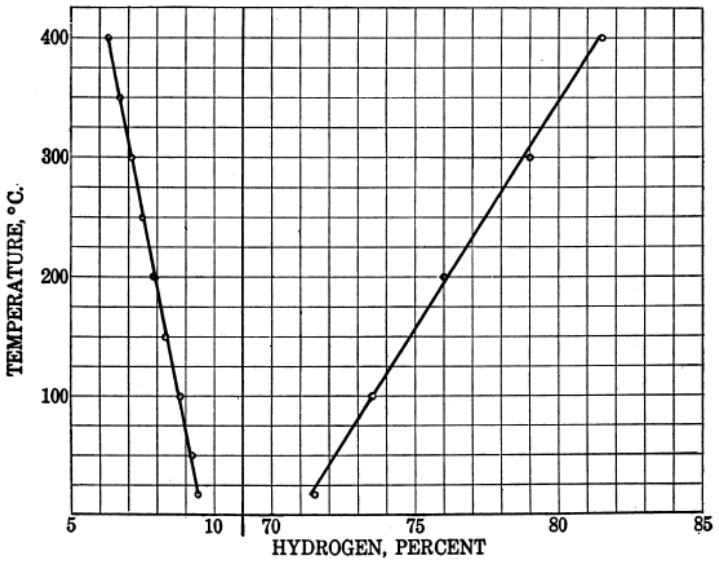

Figure 5 Temperature effect on hydrogen flammability limits (Reprinted from Kuchta JM. Investigation of fire and explosion accidents in the chemical, mining, and fuel-related industries) [12]

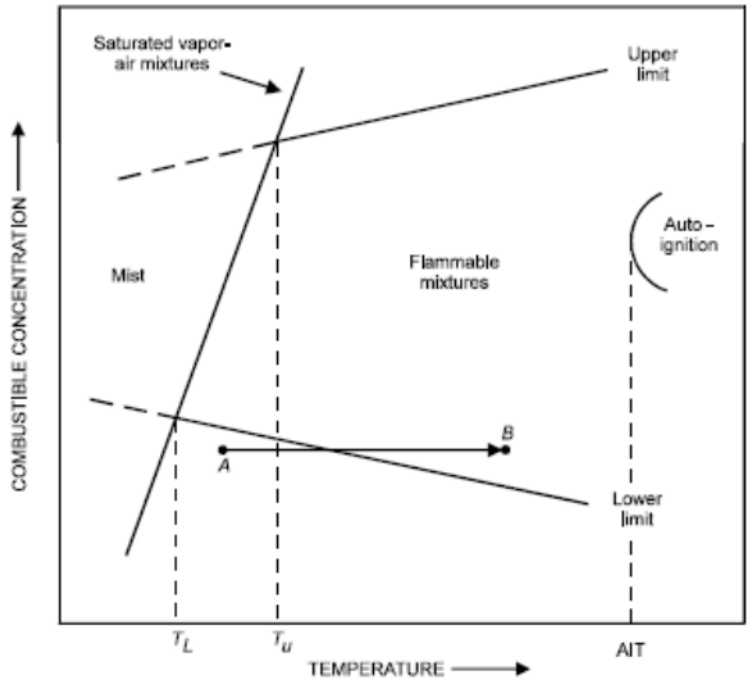

Figure 6 Effect of temperature on flammability limit of a combustible vapor in air (Reprinted from Zabetakis MG. Flammability Characteristics of Combustible Gases and Vapors.) [3]

To find the best model that fits the measurement data, Zabetakis, Lambiris and Scott[13] suggested the modified Burgess-Wheeler law, for the effect of temperature on the LFL and UFL of hydrocarbons in the absence of cool flames, as shown in Equation 3 and Equation 4,

$$LFL_T = LFL_{25} - \frac{0.75}{\Delta H_c}(T - 25) \quad (3)$$

$$UFL_T = UFL_{25} + \frac{0.75}{\Delta H_c}(T - 25) \quad (4)$$

where ΔH_C is the net heat of combustion (kcal/mole) and T in ℃.

2.2.2 Dependence on gas condition - Pressure

It is suggested by previous research that pressure effect (when P>1bar) on flammability limits is small for LFL, while UFL increases significantly with increase in pressure [6]. An empirical expression for UFL as a function of pressure was developed by Zabetakis [3], as shown below (Equation 5)

$$UFL_P = UFL + 20.6 \times (logP + 1) \quad (5)$$

Besides the empirical relation suggested by Zabetakis, Jones and coworkers[10] also found that both LFL and UFL could be expressed as a function of the logarithm of the initial pressure (Equation 6 and Equation 7)

$$L = 4.9 - 0.71 \times logP \quad (6)$$

$$U = 14.1 + 20.4 \times logP \quad (7)$$

However, the influence of pressure on flammability limits is not as simple as the temperature effect. Unlike the temperature effect, where the flammability region increases with increase in temperature, this is not always observed with the increase in the initial pressure. The widening of the flammability range with increase in the initial pressure was observed only with some of the light hydrocarbon species. For some gases like pentane and heptane, the flammability range widens with an initial increase of pressure, which usually happens below 0.2 bar, then the flammability range narrows till the pressure reaches 0.4 bar; the flammability limits of such gas species will remain constant until the pressure reaches 1 bar, then with further increases in pressure, the flammable range widens again (Figure 7) [3].

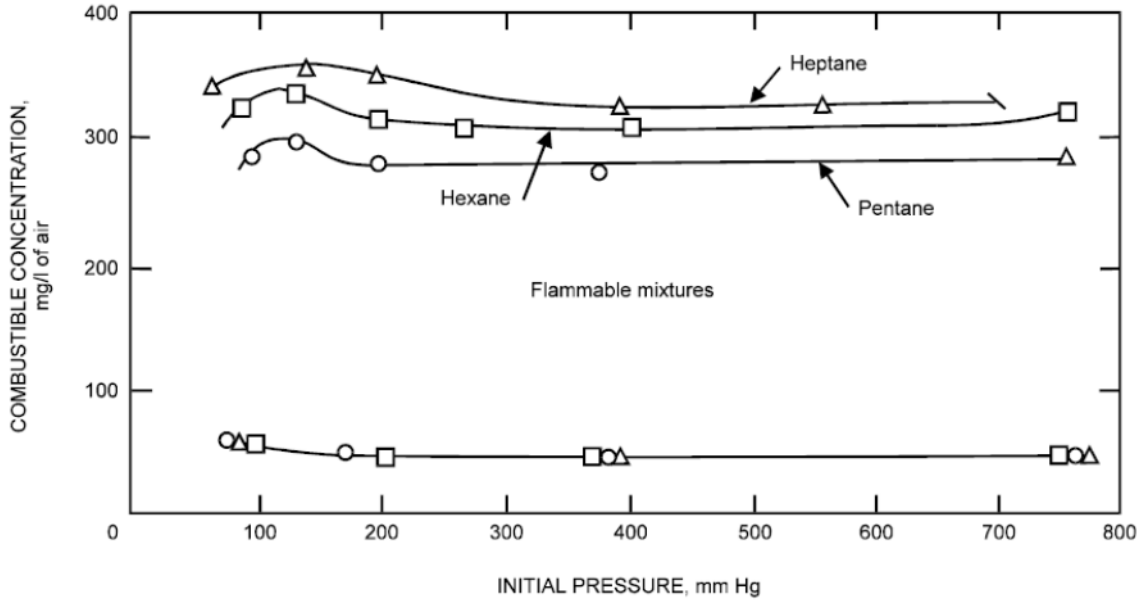

Figure 7 Effect of pressure on limits of flammability of Pentane, Hexane, and Heptane in Air at 26 °C (Reprinted from Zabetakis MG. Flammability Characteristics of Combustible Gases and Vapors.) [3]

The pressure effect on the flammability can be related to the fuel species and it has been found that combustion reaction mechanism plays an important role. Therefore, with existing literature data for flammability limit at elevated pressure, it is difficult to predict pressure effect on pure component precisely, and even more so for fuel mixtures.

2.2.3 Dependence on gas condition - Humidity

Unlike temperature effect and pressure effect on the flammability limit, the humidity does have influence on the flammability limit but only to a certain extent. Research on the humidity effect shows that when the humidity increases the range of the

flammable range will be narrower because water vapor can dilute the flammable mixture and isolate the oxygen [14]. There are two reasons, on one hand, the water steam can play a role in diluting the concentration of the flammable gas and separating the oxygen molecules from roundly contacting the combustible gas molecules, on the other hand, the evaporated water steam molecules may also collide with the fuel molecules to reduce its activating energy, thus reducing the danger of explosion, therefore improving the safety in utilization of the flammable gases.

However, investigation by Kondo [15] indicated that humidity does not affect much the flammability limits of fuel like ammonia, HFC-32, or HFC-143a. However, the flammability limits of some halogenated fuels like HFO-1234yf and HFO-1234ze, does depend on humidity of air. For example HFO-1234ze, which is non-flammable in dry air, becomes flammable if humidity becomes larger than 10% at ambient temperature.

Since the fuel species used in this work are limited to light hydrocarbons only and the combustion does generate water/steam in the reaction, the humidity effect is mainly taken as a dilution in the heat transfer and more inert gas (inhibition of flame propagation). Therefore, in this study the humidity effect will not be considered as a major issue in the flammability limits dependency.

2.2.4 Dependence on gas composition

Typically, the flammability of a combustible gas can be presented as a flammability triangle diagram (Figure 8). At any point on the flammability triangle

diagram, concentration of fuel, oxygen and inert gas is plotted on three axes in vol% with a sum of 100%. As shown in Figure 8, the air line represents combinations of fuel and air and it intersects with the nitrogen axis at 79% nitrogen which is the composition of air. While the intersection of air line with flammable zone is the lower flammability limit and upper flammability limit in air. However, both upper limit and lower limit are not constant, as the concentration of nitrogen decreases, the flammable range widens. Contrary to this, if the oxygen concentration decreases, the upper limit and lower limit will intersect at a concentration, which is defined as the limiting oxygen concentration (LOC).

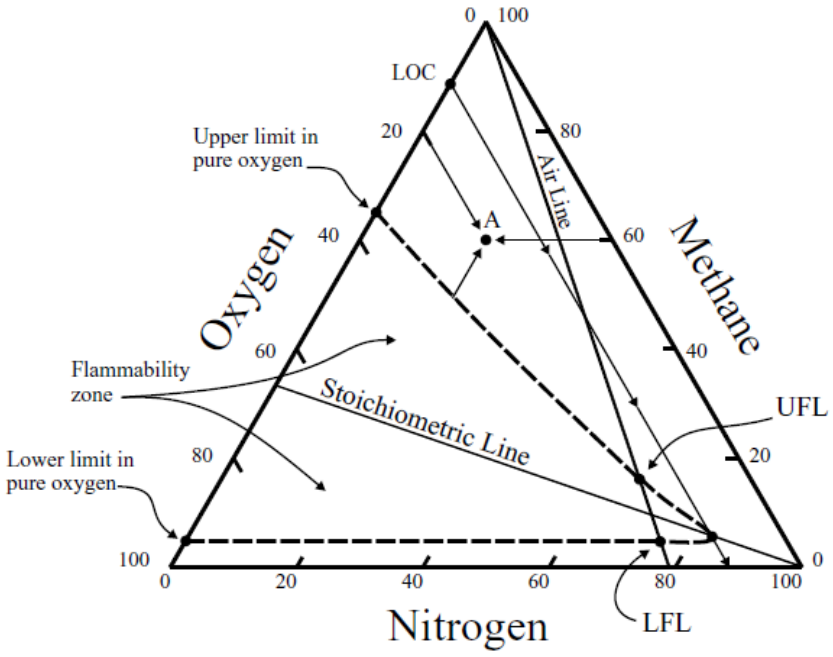

Figure 8 Flammability triangle diagram (Reprinted from Daniel A. Crowl, Joseph F. Louvar. Chemical process safety : fundamentals with applications. 3rd ed.) [6]

Previous study [16] on the inert gas effect on flammability indicated that not only addition of inert gas will narrow the flammable range, but also that the flammability limit is affected by the inert gas species. Research by Zhao [16] showed that LFLs of light hydrocarbon as well as their binary mixtures remain almost constant with addition of nitrogen, while UFLs decrease dramatically. All of the binary hydrocarbon mixtures LFLs and UFLs are linearly related to the additional nitrogen concentrations except ethylene mixture. On the other side, study by Mitu [17] showed that inert additives have a strong influence on the laminar burning velocity, and maximum flame temperature. With additional inert additives, dilution effect gets stronger while laminar burning velocity and maximum flame temperature decrease. Among all inert additives, CO2 is the most effective one, followed by N2, Ar and He. It is found that the high heat capacity and heat dissipation rate of carbon dioxide compared with nitrogen, argon and helium are the main contributors to the effectiveness of this inert gas.

2.2.5 Dependence on ignition

The flame propagation direction, which is typically determined by the location of the ignition source in the vessel, is another important parameter influencing flammability limits. For experimental test, three most commonly seen flame propagation directions are upward, horizontal, and downward. When the combustion process is triggered by the ignition, the flame will propagate in all directions. But due to buoyancy effect, the heated and expanded combustion products, which have lower density than unburned fuel mixtures, will tend to rise and introduce upward convective currents. Therefore, flame

propagation upward requires less energy than the downward ones. Previously, experiments were carried out with three propagation directions in the same cylindrical vessel for methane-air and ammonia-air mixtures [10]. It was found that the flammable range is the largest (lower LFL and higher UFL) with upward propagation followed by horizontal propagation, then downward propagation [10]. Therefore, when cylindrical vessels are used to determine the flammability limits, upward flame propagation (bottom ignition source) is recommended for more conservative results.

Ignition source and ignition energy is another factor affecting the experimentally determined flammability limits. The ignition should be energetic enough to provide sufficient energy to induce flame propagation. As shown in Figure 9, usually the minimum ignition energy (MIE), which is the minimum energy input required to initiate combustion, shows up at the stoichiometric ratio of the combustible gas. While for ignition source, different types of igniters including electric arc, sparks, hot wire and open flame are used for flammability test. For the selection of the ignition source type, the most important factor is the delivery of a fixed amount of energy consistently for each test. According to Mashuga [5], sparks caused by exploding fuse wire is the most reliable way of delivering constant ignition energy in the flammability test and the recommended energy is in the range of 10 J to 20J.

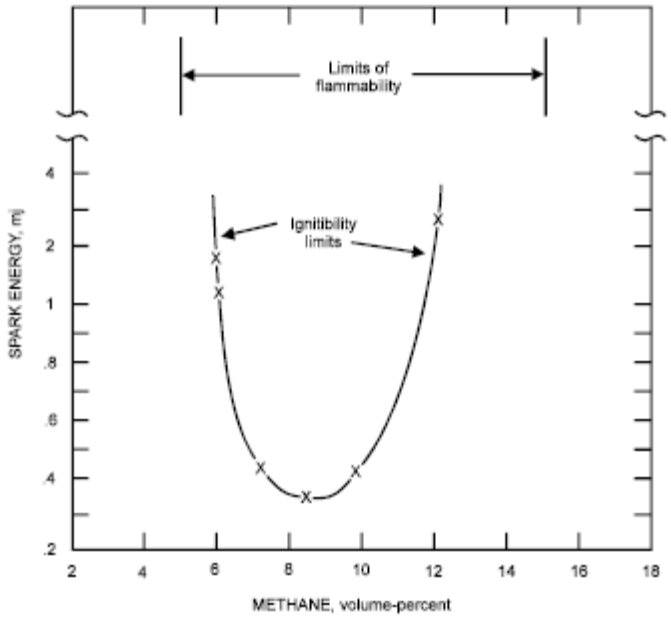

Figure 9 Ignition energy vs methane flammability in air at 1atm, 26 °C (Reprinted from Mashuga CV. Determination of the combustion behavior for pure components and mixtures using a 20 L sphere.) [5]

2.2.6 Dependence on apparatus

Typically, for experimental measurement of flammability limit, cylindrical vessels such as German Federal Institute for Materials Research and Testing (BAM) 6L, Warsaw University of Technology (WUT) 40L [18] or spherical vessels such as 20L sphere can be used. However, the experimental data [18] generated from different types of equipment are different, which indicates that flammability limit is dependent on the apparatus.

In 1950s, Coward and Jones [10] used a cylindrical vertical tube (constant pressure) of 5cm internal diameter to measure the flammability limits for gases and

vapors. But later, Zabetakis [19] suggested that a tube with the diameter of 5 cm is too small for accurate measurement due to the quenching effect. The size of the reaction vessel becomes one of the factors affecting the flammability limits because the propagation of flame requires sufficient energy to be transferred from the burned gas to the adjacent unburned gas. Therefore, vessels designed to measure flammability limits must have large enough diameters so that the quenching effect is eliminated.

Previously, Takahashi [20] had done research related to the effect of different geometry apparatus on the flammability limit including varying the vessel sizes and shapes. In general, the results can be summarized as: (i) for cylindrical vessels with large height and small diameter (L:D>8:1, D<5cm), the flammability limits are highly dependent on the reactor wall quenching effect; (ii) for cylindrical vessels with small heights, the flammability limits are mainly affected by the tendency of hot gas accumulation at the vessel top, heat transfer between burned and unburned gas; (iii) the measured flammability limits will be close to those obtained from open space if the reactor size is large enough.

2.3 Flammability limit of fuel mixtures

Through years of flammability study, estimation methods for predicting flammability limit of fuel mixtures, such as Le Chatelier's rule, Calculated Adiabatic Flame Temperature (CAFT) model, have been developed.

2.3.1 Le Chatelier's rule

Le Chatelier's rule is an empirical formula most widely used to calculate flammability limits of fuel mixtures. The rule states that the mixture flammability limit can be determined based on the flammability limit and composition of each fuel species, as shown in Equation 8 and Equation 9.

$$LFL_{mix} = \frac{1}{\sum_{i=1}^{n} \frac{y_i}{LFL_i}} \quad (8)$$

$$UFL_{mix} = \frac{1}{\sum_{i=1}^{n} \frac{y_i}{UFL_i}} \quad (9)$$

where y_i is the mole fraction of component i on a combustible basis, and LFL_i and UFL_i are the lower flammability limit and upper flammability limit of the i^{th} component in volume percent, LFL_{mix} and UFL_{mix} are the lower flammability limit and upper flammability limit of the gas mixtures.

Le Chatelier's rule was originally developed based on experimental data with lower flammability limits of gas mixtures. Later, Le Chaterlier's rule was extended to upper flammability limit calculation also. Mashuga and Crowl [6] have proved using thermodynamic calculations that the Le Chatelier's rule should be universally applicable in a certain temperature range. However, a few assumptions must be added: i) adiabatic flame temperature rise at the lower flammability limit for all species is same, ii) constant product heat capacities, iii) same number of moles for the initial mixture and final products, and iv) the combustion kinetics is independent and unchanged by other combustible species. At the upper flammability limit where fuel is the majority of the content and oxygen becomes the limiting component, these assumptions are less

reasonable since the heat capacities, gas mole number and adiabatic flame temperature for partial oxidation no longer stay constant. Therefore, the Le Chatelier's rule is expected to predict mixture flammability limit at LFL fairly well, while for UFL the application of the rule depends upon the individual mixtures.

2.3.2 Calculated adiabatic flame temperature (CAFT) model

Another method that can be used to predict the fuel mixture flammability limits is the Calculated Adiabatic Flame Temperature (CAFT) model [21]. The basic principle of CAFT model is based on the total energy balance (Equation 10)

$$\Delta U = W + Q \quad (10)$$

where ΔU is the internal energy of the reaction system, W is work generated by the system, and Q is the total amount of heat. The assumptions of this model include that the flammability limits are thermodynamically related, and chemical equilibrium of oxidation reactions are not taken into consideration. Since no work is done by the system, W is zero. And assuming that there is no heat losses to surroundings, which gives Q = 0. Therefore, the internal energy change ΔU for the constant volume reaction system can be separated to 2 stages: the internal energy change ΔU_c (Equation 11) from the exothermic oxidation reaction at the initial temperature T_i; and the internal energy change ΔU_t (Equation 12) from the initial temperature T_i (K) to the final flame temperature T_f (K) of the mixture of fuels, as shown below.

$$\Delta U_c = \Delta H_c - \Delta nRT_i \quad (11)$$

$$\Delta U_t = \sum_{products} n_i \int_{T_i}^{T_f} C_{vi} dT \quad (12)$$

where ΔH_c is the heat of combustion at the initial temperature, Δn is the total mole number change of the combustion reaction, R is the gas constant, n_i is the number of moles of product component i, and C_{vi} is the heat capacity. And the sum of ΔUc and ΔUt should equal to zero.

In the calculation of flammability limit for fuel mixtures [21], the CAFT model can be simplified as four steps:

a) Experimentally measure the flammability limits of the pure fuels
b) Estimate the AFTs of the pure fuels
c) Estimate the AFT of the mixture of fuels (T_{fmix})
d) Calculate the flammability limit of the fuel mixtures

In the third step, the adiabatic flame temperature for fuel mixture can be calculated using a linear equation that correlates fuel mixture flame temperature with that of its individual combustibles, as indicated in Equation 13 [22]:

$$T_{fmix} = \sum_i^n x_i T_{fi} \quad (13)$$

where, T_{fmix} are the flame temperatures for fuel mixture, T_{fi} is the flame temperature for each fuel component, x_i is the mole fraction of fuel component i.

3. EXPERIMENTAL SETUP AND PROCEDURE

As indicated in the research objectives, one of the major goals is to design and conduct experiments to determine the flammability limits of pure light hydrocarbons and binary mixtures at both normal conditions and elevated conditions. Therefore, appropriate experimental setup and operation procedures are necessary for this study. In this section, detailed experimental setup and procedures will be described.

3.1 Flammability equipment details

The flammability apparatus used in this study is located in Jack E. Brown Building at Texas A&M University. The equipment is located in a continuously vented lab area. The apparatus mainly consists of six parts: (i) gas feeding system, (ii) mixing system, (iii) reaction vessel, (iv) igniter, (v) heating unit and (vi) data acquisition system. Figure 10 is the simplified schematic representation of the apparatus. The apparatus is modified and upgraded based on the original design by Wong [23] and Zhao [16]. With additional parts and improved detectors, the new developed instrument is capable of measuring the flammability limits at initial temperature up to 350 ℃ and initial pressure up to 3 atm. A detailed description of each part is provided below.

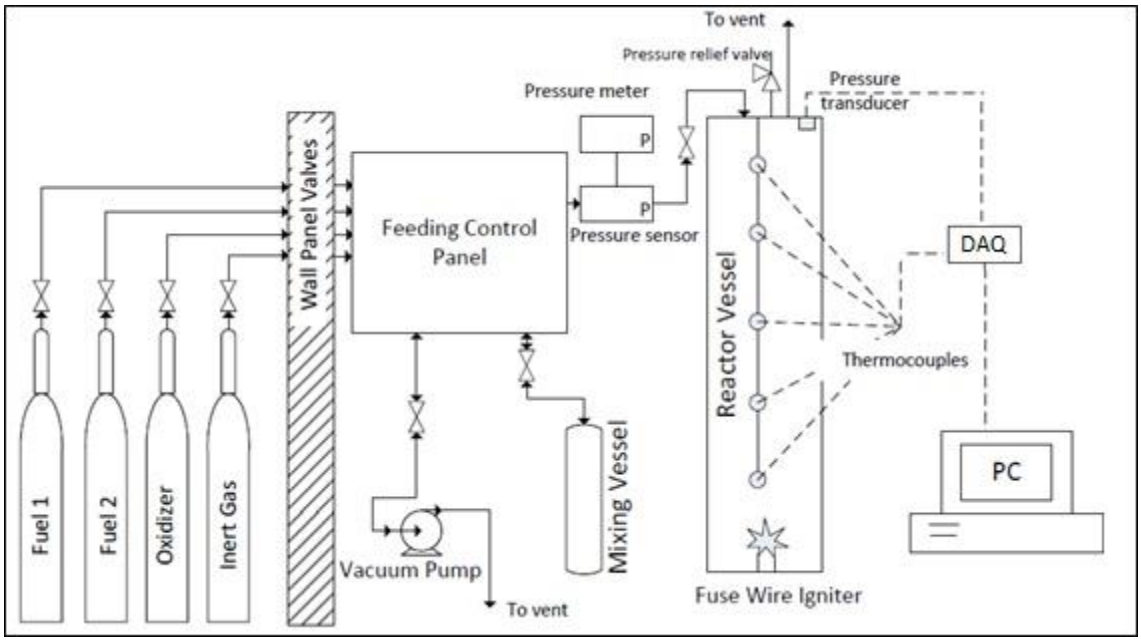

Figure 10 Schematic representation of experimental apparatus

3.1.1 Gas feeding system

The chemicals currently used in this study include hydrocarbon fuels (methane, propane, ethylene and propylene), nitrogen and air. All of these chemicals are supplied from pressurized cylinders in the chemical loading area outside the laboratory (Figure 11). Each pressurized cylinder is connected to an appropriate pressure regulator, then through the double valve gas feed wall panel (built-in feature of laboratories in the building) into the laboratory area.

Figure 11 Chemical supply (Pressurized cylinders) and the wall panel valve

The main feeding system, which includes a manual control manifold, connects to the chemical cylinders, the vacuum pump (Welch Mfg. Duoseal Pump with ultimate vacuum 1.0×10^{-3} mmHg), vent (fume hood), the mixing vessel and the reaction vessel (see Figure 12). The fuel lines, inert gas lines and oxidizer line connecting to the gas loading manifold are equipped with check valves to prevent reverse gas flow in case there is leak in the valves or operator error occurs. The check valves (Swagelok) have 6,000 psig maximum working pressure at normal condition. The junction area from all pressurized cylinders has a pressure transducer (Omega PX613, 0.4 % accuracy with 0.07 %/F thermal zero and span effect) that provides pressure information for gas loading to specified pressure, and control valves that allow isolation of each section from the gas line and each other. The manifold is purged with inert gas (nitrogen) and evacuated between each gas loading step. The vent line can be used for the release of gas contents from the manifold, as well as the reaction vessel or mixing vessel during

different stages of gas loading. The vented gas is directly released into a constant suction laboratory vent to prevent the building up of flammable gases in laboratory. All gas lines (1/4 in tubing, 0.035 in thick) and plug valves (Swagelok, SS-4P4T) in the manifold are constructed of 316 stainless steel with Swagelok compression fittings.

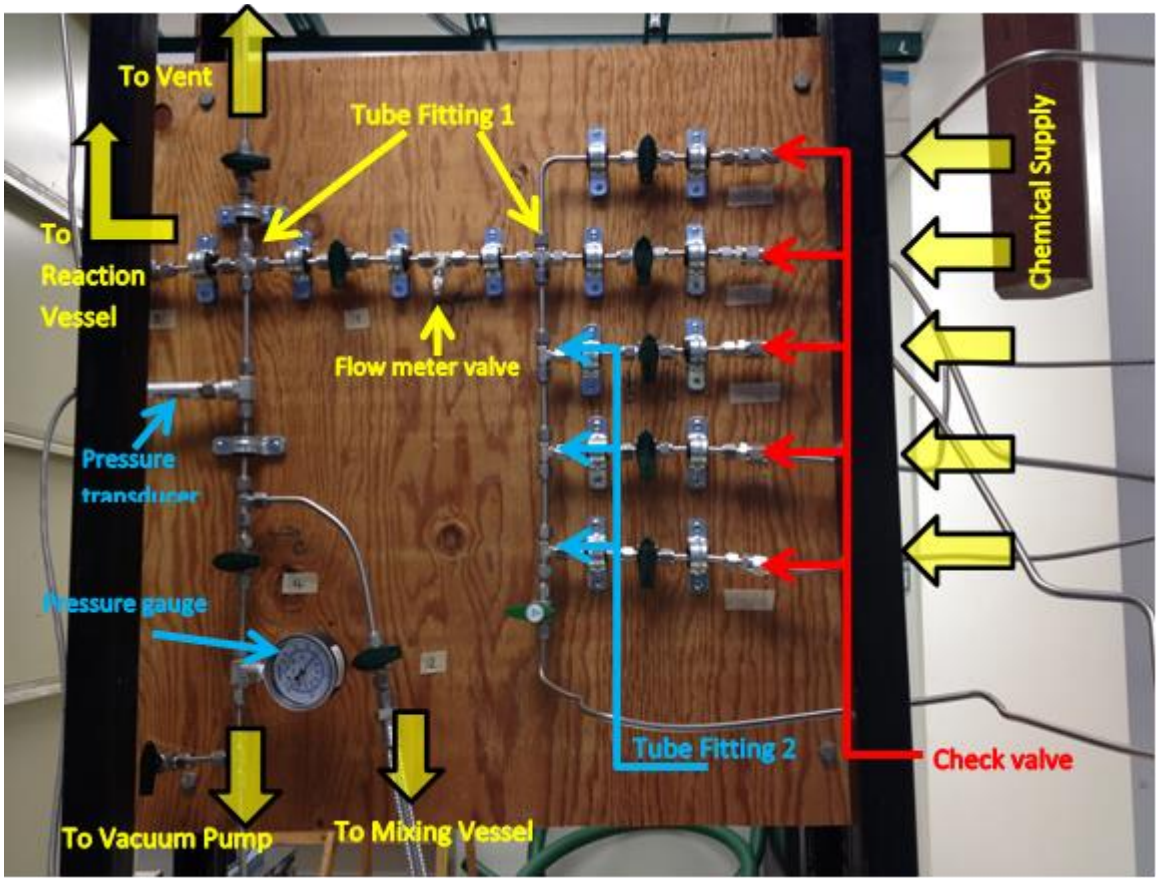

Figure 12 Main control manifold

3.1.2 Mixing system

The mixing system consists of a vacuum pump and an external mixing vessel (See Figure 13). For the external mixer, it imitates the mixing scheme from a portable

sample cylinder designed by Precision General Inc. In this design, the cylindrical vessel contains a cylindrical Teflon block which can slide along inside the vessel. The block diameter is slightly smaller than the cylinder internal diameter, allowing smooth movement of the block. When the vessel is rotated, the block falls toward the lower end. Gases moving between the block and vessel wall create high turbulence zones in front of and behind the moving block, which help facilitate fast mixing of gases. Similarly, in our apparatus, the external mixer consists of a mixing vessel and motor for vessel rotation, both mounted on top of the mixing stand (L ×W ×H: 38 in × 18 in × 21.5 in), which is made of 1.25 in square steel tubing welded together (See Figure 15). The mixing vessel is made of stainless steel (3.88 inch internal diameter and 29.75 inch internal length) with flanges (7/8" thick flanges, 8 bolts, and Buna-n gaskets) screwed at both ends. The mixing element is a cylindrical Teflon block with 3.65 inch diameter, 2.9 inch thickness. The vessel is rotated lengthwise by a steel shaft (clamped on to the vessel), mounted with bearing blocks on top of the mixing stand. A DC motor coupled to the shaft rotates the mixing vessel. The motor is powered by a variable voltage controller (See Figure 14), which enables rotation speed selection by voltage adjustment. The mixing vessel is connected to the gas loading manifold during the loading phase with a quick connect fitting and flexible metal hose. The hose is disconnected from the mixing vessel for rotation during mixing process. For each added gas component (fuel, oxidizer, or inert gas), the vessel is rotated for 5 minutes, approximately 300 inversions.

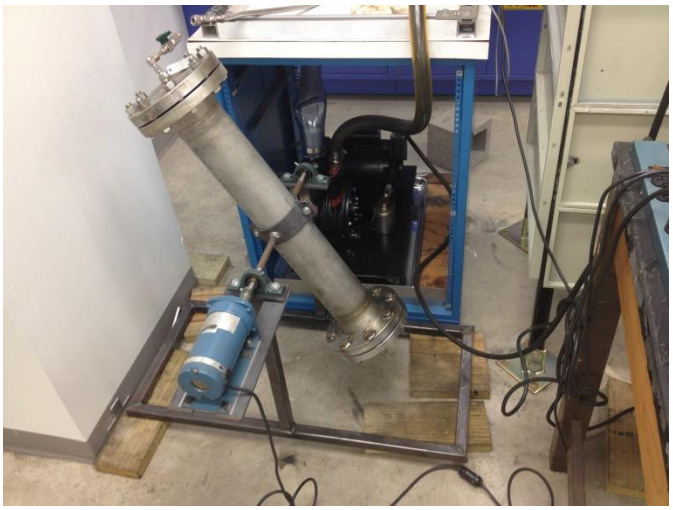

Figure 13 The mixing system

Figure 14 Variable voltage controller

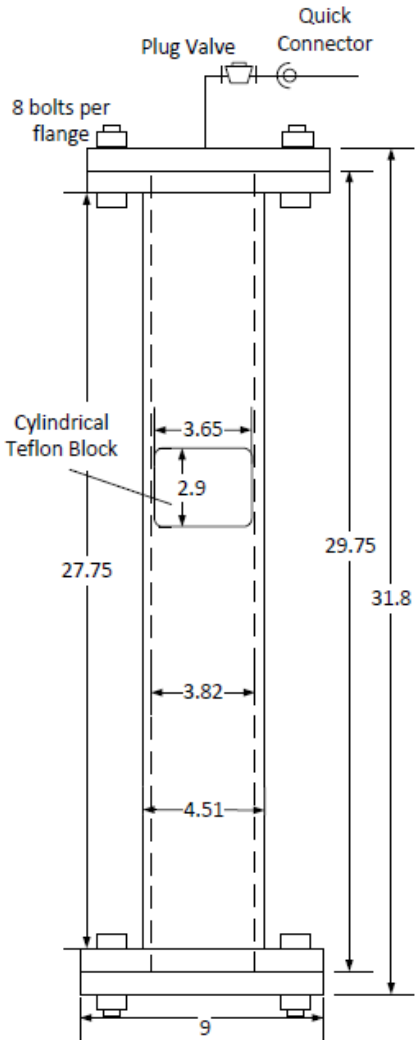

Figure 15 Mixing vessel scheme (Unit: inch)

3.1.3 Reaction vessel

The reaction vessel, similar to the one designed by US Bureau of Mines [10], is a constant volume cylindrical tube made of 316 stainless steel. The reaction system is made of four parts:

i. The hanging plate (Figure 16), which is affixed permanently to the enclosure. A round open window is drilled (D = 4.02in, 10.22cm) in the middle of the plate for the gas line and thermocouples to pass through. The main purpose of using the hanging plate is to hold and support the reaction vessel with 4 sets of bolt and nut so that the reaction vessel itself can be isolated from the enclosure during the experiment. The isolation of the reaction vessel is an upgrade of the hardware from the original design to improve the test capability at high temperature. The modifications of the setup, which include lowering down of the reaction vessel using 4 sets of bolt and nut and installation of the ceramic washers between the nut and hanging plate, allows the reaction vessel to be heated to 300 ℃ without causing overheat scenarios to the enclosure.

ii. The top flange (Figure 17), where the gas feeding, emergency venting and thermocouples will go through into the reaction vessel. A pneumatic valve is installed at the top plate as the barrier to separate gas content from reaction vessel to the control panel. Also a pressure relief valve with set pressure of 500 psi (35bar) is installed to prevent overpressure scenarios.

iii. The reaction vessel body, which is a schedule 40, 4 inch nominal (11.43 cm O.D., 10.22 cm I. D.), 100 cm long, 316 stainless steel cylinder with welded flanges (17.78 cm O.D., 1.778 cm thick, 12 threaded bolt holes) at both ends. The reaction vessel has a volume of 8.2 liter.

iv. The bottom flange (Figure 18), where the ignitor and the evacuation gas line are installed. The bottom flange and the top flange are bolted directly to the reactor body. The vessel is sealed against vacuum and pressure with customized graphite gasket, (Graphite/Buna-N Sheet Gasket, 1/16" Thick).

For the installation and maintenance, two sets of hooks, which are attached to a counterweight pulley system, are connected with the top plate for lowering down and dis-assembly of the reaction vessel (Figure 19). Figure 20 shows the reaction vessel mounted on the enclosure.

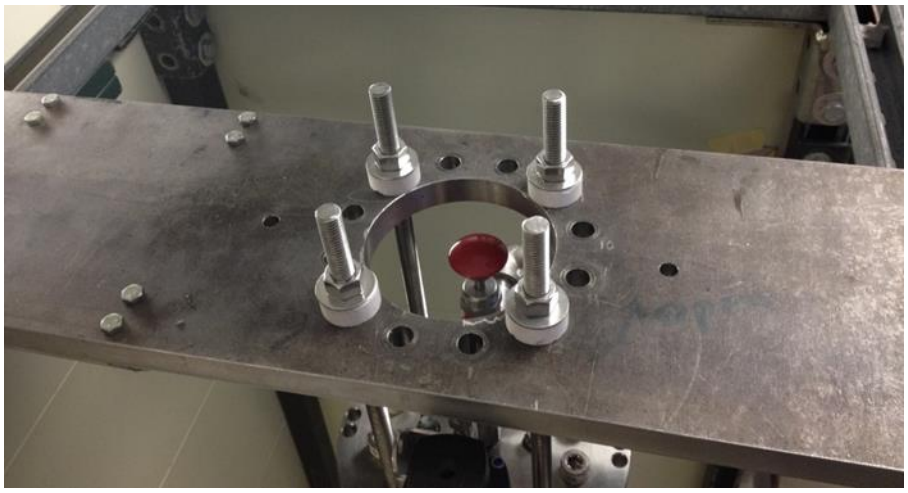

Figure 16 Hanging plate

Figure 17 Top flange and line connections

Figure 18 Bottom flange

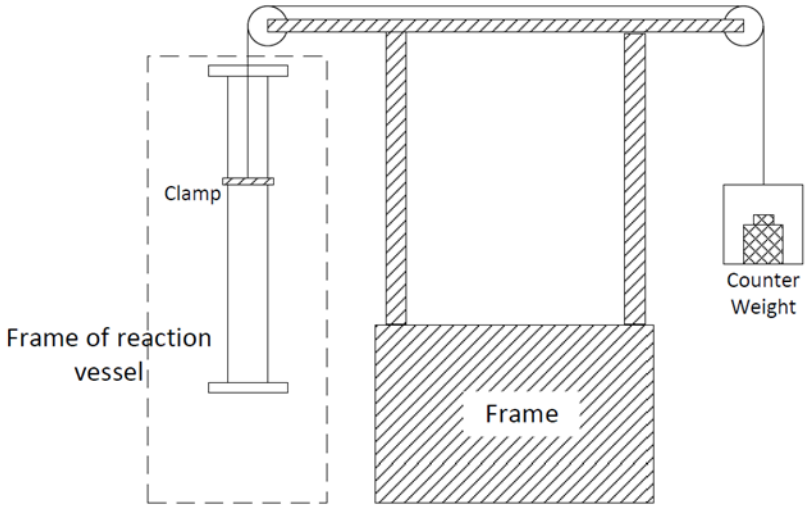

Figure 19 Scheme of counter weight pulley system

Figure 20 Reaction vessel mounted in the safety enclosure

3.1.4 Igniter

The ignition system used in this experiment is similar to that outlined in ASTM E 918-83 standard [24]. Demonstrated by Mashuga [5], this ignition system is capable of inputting 10 J of energy with repeatable power delivery. The ignition source is a 10 mm piece of AWG 40 tinned copper wire, vaporized by a 500 VA isolation transformer (Hammond 171 E) at 115 V AC switched on with a zero-crossing solid-state relay (Omega, model SSRL240DC100) so that the current is delivered beginning at the zero point of the AC cycle each time. Figure 21 shows the igniter system circuit.

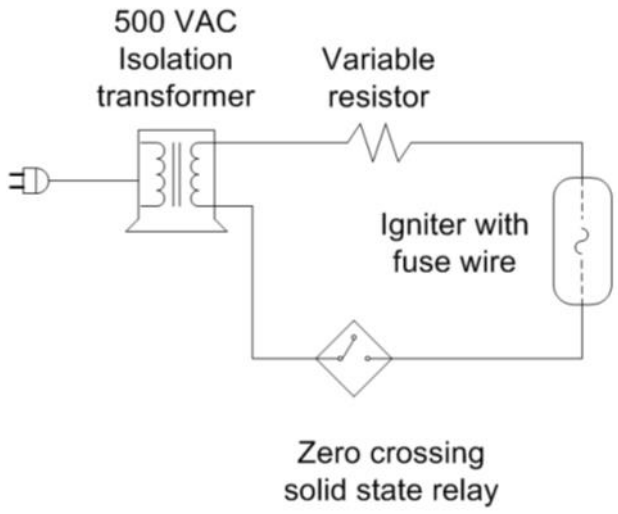

Figure 21 Igniter system circuit.

The igniter (Figure 22), which is installed at the bottom of the reaction vessel, consists of a 35cm long mineral insulated cable (MI cable, sheath 316, 6 type K conductor) and a Conax compression fitting (single element sealing compression fitting, grafoil). Top part of the igniter (Figure 23) is used as the wire holder and the bottom section of the igniter is connected to the energy source. The wire holder section has 6 rods evenly spread at each direction and the distance between the tips of each rod is fixed as 1 cm. Every two rod tips are used to wrap and hold the fuse wire. The pressure seal is accomplished by inserting the igniter into the port and tightening the screw. Compression fitting is tested and proved to be leak proof at the condition of 300 ℃ and 30atm. Figure 23 shows the igniter design.

Figure 22 Igniters

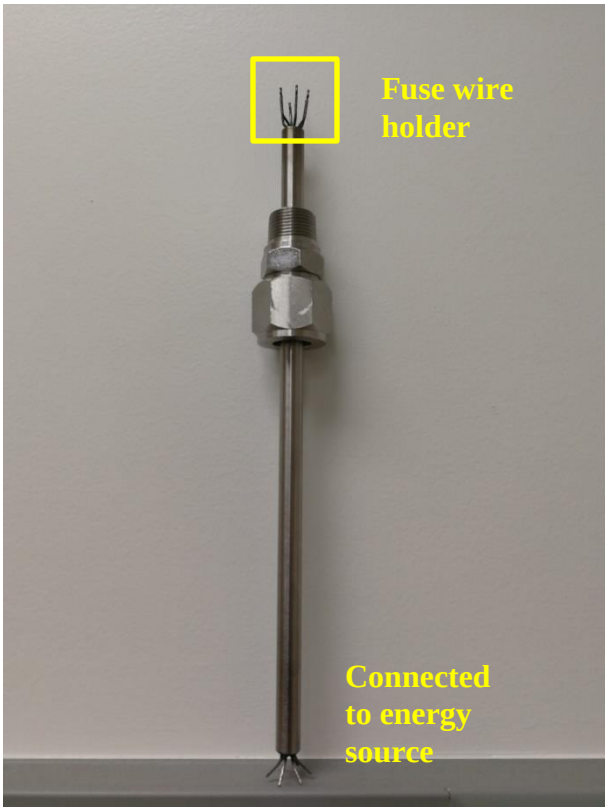

Figure 23 Ignitor connections

3.1.5 Heating unit

The temperature control of the reaction vessel is mainly achieved by using high temperature heating tape and temperature controller box (Figure 24). The heating tape (Omega, STH102-060/Heat element plus, BWH17x080x) is connected with temperature controller box to switch on/off the voltage input. A total of five thermocouples (Omega, KMTSS-040G, Figure 25) are installed outside the reaction vessel at different positions (bottom plate, lower section, middle section, upper section and top plate) to monitor the temperature and make sure the entire vessel is heated. Fiberfax insulation layer is wrapped and tightened outside the heating tapes to prevent heat loss to the surroundings.

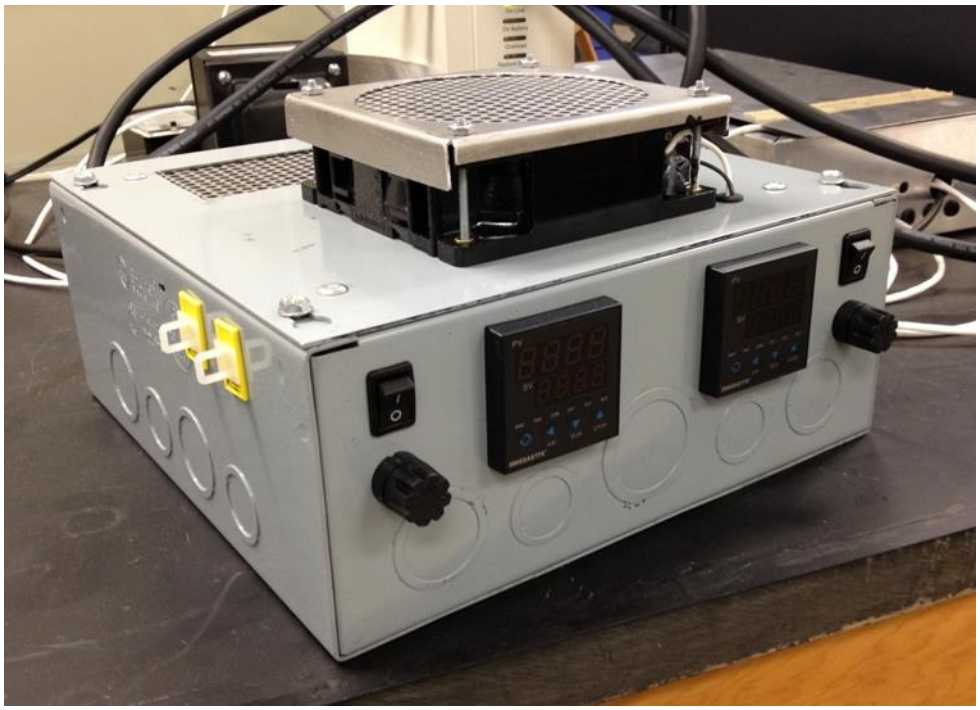

Figure 24 Temperature Controller Box

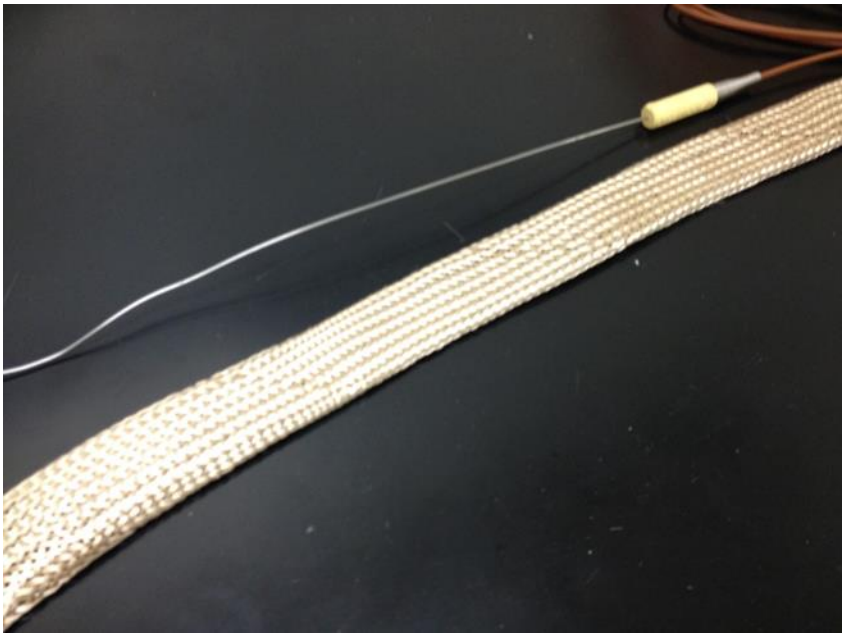

Figure 25 Heating tape and thermocouples

3.1.6 Data acquisition system

During the tests, the experimental data needed include pressure increment and temperature rise. Temperature data and pressure data are generated from thermocouple and pressure sensor as voltage signals and collected by a data acquisition (DAQ) device. Figure 26 shows the sensor configuration in the reaction vessel.

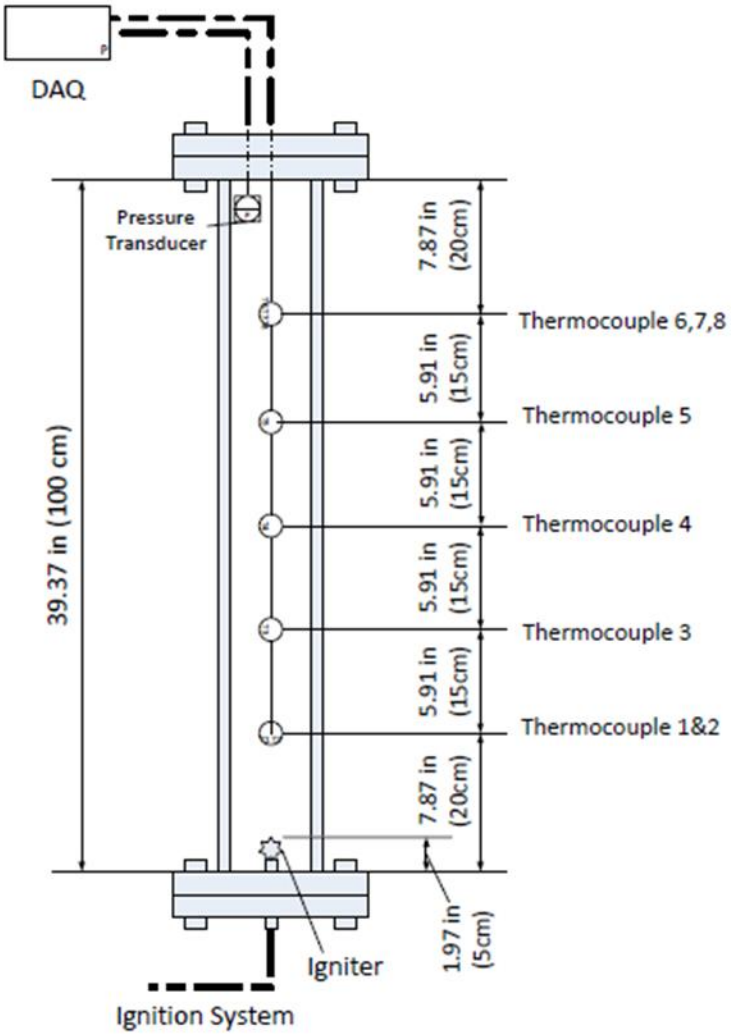

Figure 26 Thermal and pressure sensors in reaction vessel

During the experiment, the pressure increment within the reaction vessel is monitored with a high precision dynamic pressure transducer (Honeywell precision grade, STJE, 0 – 5Vdc output signal, ±0.05 % accuracy, 3 KHz response) mounted on the top plate. The transducer has a measurement range of 0 to 500 psig, with 0 to 5Vdc nominal output signal. The pressure transducer uses a SOLA-HD power supply and the

signal output is amplified and sent to the DAQ device. The transducer is capable to handle maximum flash fire temperature at 3,000 ℉ (1,650 ℃), which is sufficient for test at initial temperature up to 300 ℃. Though the temperature compensation will affect the measurement of pressure at high temperature condition; however, the data acquisition software has been calibrated and adjusted to calculate the exact pressure increment. Calibrations of the pressure transducers are checked every half year to ensure the precision of pressure reading.

The thermal sensors used to measure the position of flame front are eight thermocouples (Transition Junction Style Thermocouple Probes, KMTSS-040U, 0.01 s response time in still air). There are several reasons to use thermocouples instead of thermistors or resistance temperature detectors (RTD). First, thermocouples can withstand at high temperatures, as well as shock and vibrations, the K-type thermocouple can withstand the temperature as high as 1,100 ℃, much higher than thermistors or RTDs. Second, the ungrounded thermocouple has 0.01s response time which is quick enough to detect temperature change during the flame propagation. Third, the diameter of the thermocouple is 0.04 inch, large enough for the thermocouple to tolerate multiple tests without replacement. These advantages have made the K-type thermocouple a necessity for the measurement during combustion events where response time and stability are the major considerations.

The thermocouples are suspended at the center axis inside the reaction vessel at different lengths from the ignition source (20cm, 35cm, 50cm, 65cm and 80cm). The signal end of the thermocouple is connected through the reaction vessel by a multi-

conduct feedthrough (MFT-040-8). Since the flame front generated from combustion may not be in a uniform shape, more than one thermocouple is installed at 80 cm level to monitor the temperature rise in order to confirm that the flame has propagated to the top. During the installation stage, combustion test had been done to prove that if the temperature rise at 80cm level thermocouple was more than 10 ℃, the top of the vessel would receive a temperature rise more than 5 ℃, which means the flame front had reached the top.

Data acquisitions are performed by a desktop computer (Dell® Optiplex 210L, with Windows XP®) equipped with a multifunction temperature and voltage data acquisition device (MCCDAQ, USB 2408 series, 24-bit resolution, 8 inputs, ±0.05% accuracy, Figure 27). Original signal from thermocouple and pressure transducer are delivered into the DAQ device as differential voltages, then amplified and noise reduced. These signals are further transferred to the desktop and calculated using LabVIEW software (National Instruments, version 2013) to reflect the real temperature and pressure readings. Both data measurement and ignition trigger are controlled by a LabVIEW program to ensure identical ignition delay time. Figure 28 and Figure 29 are the block diagram window and front panel of the LabVIEW program.

As shown in Figure 29, the software program is capable to do the smoothing for the data recorded through combustion process. Since the original voltage data from both thermocouples and pressure transducer include noises, and no noise reduce hardware is installed, the pressure and temperature file generated from combustion process will be smoothed by using average of every couple data point recorded. The program itself is

able to provide average value of every 1 to 10 data points (thermocouple voltage reading and pressure transducer voltage reading). Through testing of methane combustion at 5 vol% (flammable/explosive) at room temperature and atmospheric pressure, the average number of data and total data points are compared. As shown in Table 1, the average number of every 5 data point will provide an optimal balance between the accuracy of the data and the total length of the data (number of data).

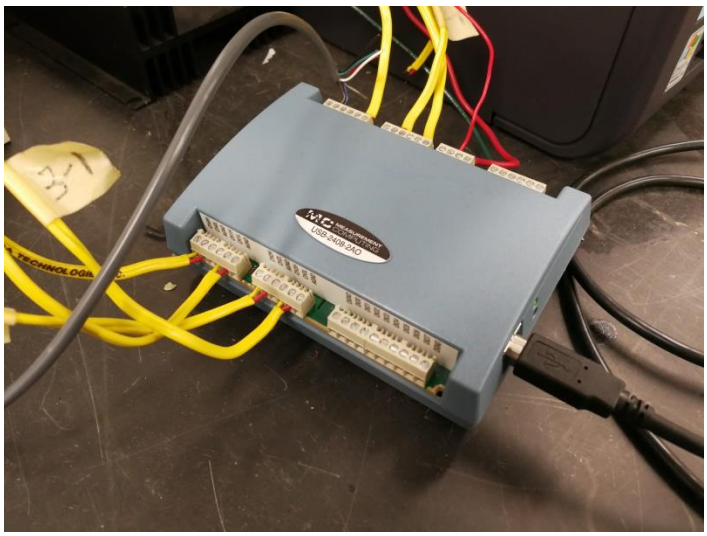

Figure 27 Data acquisition device (MCCDAQ-2408)

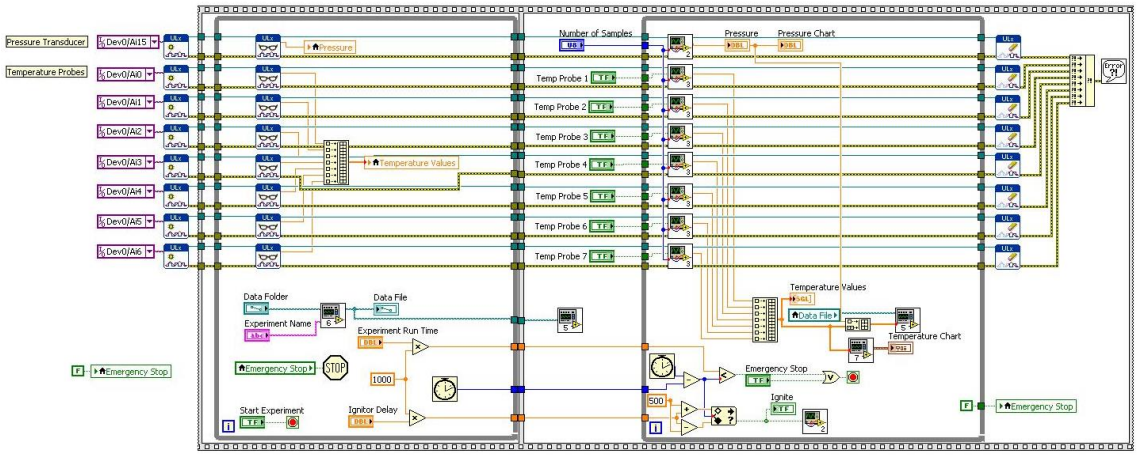

Figure 28 LabVIEW program (block diagram window)

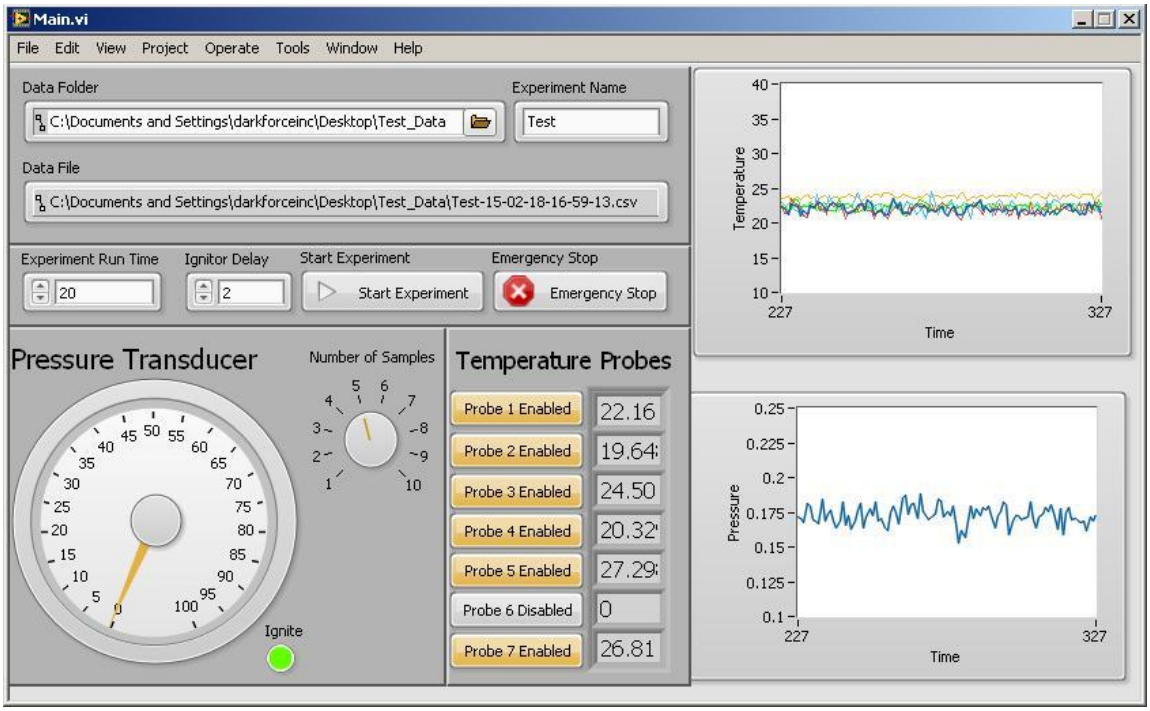

Figure 29 LabVIEW program (front panel)

Table 1 Balance between counts (average of every # of data points) and length of data

Average of every # data points	Total data points	Maximum temperature of combustion (℃)	Maximum pressure of combustion (psi)	Accuracy of data/comments
4	33	100	7.8	A lot of noises in the data
5	27	180	9	No significant vibrations (acceptable)
6	23 (too short, <25)	110	8.2	No significant vibrations (acceptable)
7	21 (too short, <25)	100	7.8	No significant vibrations (acceptable)

3.2 Experimental procedure

Operation of the flammability apparatus operation is a manual process, which includes a series of actions as follow:

a) Preheating of the reaction vessel, this step can take up to 3 hours. Temperature readings from both the controller and the data acquisition program should reach a steady value before any experimental operations.
b) Purge and evacuation of the mixing vessel and control manifold;
c) Preparation of the igniter, wrap and tighten fuse wire, install the igniter to the reaction vessel;
d) Gas loading, must be in the sequence of fuel, inert gas and oxidizer to minimize the existence of flammable/explosive gas mixtures;
e) Mixing gases, mixing vessel will rotate for 5 minutes to ensure the gas content is mixed as homogeneously as possible;
f) Evacuation of the reaction vessel and control manifold;
g) Transfer premixed gas mixture from mixing vessel to reaction vessel; once the pressure of reaction vessel has reached desired value, the gas content will be left still about 2mins to reach equilibrium (quiescent state, Temperature change $\leq \pm 0.05$ °C/min, Pressure change $\leq \pm 0.01$ psi/min).
h) Ignition, triggered by the LabVIEW program, typical ignition delay set as 2s;
i) Data acquisition, data are monitored for 10s, but combustion process usually finish within 300ms;
j) Purge and evacuation of gas mixer, reaction vessel, control manifold and tubing lines.

The fuel/air mixtures used in this experiment are generated using Ultra-high-purity (UHP) grade fuels and UHP-grade air from compressed gas cylinders. To precisely control the concentration of each gas component, fuel and air are loaded on a partial pressure basis. Great care is taken during the gas loading procedure to make sure that the desired fuel concentration is achieved.

To test the mixing effect of the mixer, samples of methane gas mixtures are collected and sent for concentration examination. After the gas mixer is rotated for five minutes, samples of the methane gas mixtures are collected using a gas sample bag and these samples are sent to the Texas A&M University Chemistry Department, analyzed using gas chromatography (GC). Test results prove that the mixing apparatus can precisely control the methane concentration within ±0.1% (target methane centration as 5%, GC results indicated average concentration as 5.005% for 3 tests). Since the loading procedure is done at room temperature and ambient pressure, it is assumed the fuel/air mixtures will behave as ideal gases.

The measurement and data recording are controlled by a written-in-house LabVIEW program. The software program converts the raw data to engineering units and plots data vs. time. Maximum pressure and maximum temperature are obtained from the pressure vs. time traces and temperature vs. time traces, respectively. The reproducibility of the flammability data is checked by repeated tests over a period of time.

4. FLAMMABILITY CRITERIA APPLICATION ON NON-STANDARD VESSEL[1]

The definition of flammability limit is stated as the volume percentage concentration of a flammable substance in air that can produce a fire or explosion when an ignition source is present [9]. However, this statement is relatively brief description without any numbers that can be used to interpret the quantitative indicator of the fire/explosion. Therefore, different researchers worldwide use different definitions of fire/explosion or flame propagation in terms of temperature rise, pressure increment, and flame propagation distance. The table (Table 2) below is a summarized literature review of the existing experimental measurement of light hydrocarbons using different equipment and flammability criteria.

[1] Reprinted with permission from "Application of flammability limit criteria on non-ASTM standard equipment" by Gan, N., Bukur, D. & Mannan, M.S., 2018. J Therm Anal Calorim (2018), P1-14, https://doi-org.ezproxy.library.tamu.edu/10.1007/s10973-018-7413-6 Copyright 2018 Springer International Publishing.

Table 2 Summary of literature review for existing flammability experimental measurement results

Source / Reference	Vessel shape	Vessel dimension	Flammability criterion	Flammability range		
				Methane	Propane	Ethylene
USBM [3]	Cylindrical, glass tube	Length = 1.5m, Diameter = 50mm	Visual flame propagation > 75cm	5 - 15%	2.1 - 9.5%	2.7 - 36%
Cashdollar [25]	Spherical	Volume = 120L, Diameter = 60cm	7% pressure rise	5 - 15.7%	2.05 - 9.8%	-
Mashuga [5]	Spherical	Volume = 20L	7% pressure rise	4.85 - 16.14%	-	2.62 - 30.38%
Kondo [26]	Spherical	Volume = 12L,	Visual flame propagation > 0.5in	4.9 - 15.8%	2 - 10%	2.7 - 31.5%

To have a uniform measurement of fire/explosion and the flame propagation, people have summarized the test condition, test vessel, ignition source, criterion and other related information into standards. In the U.S. and Europe, different standards are implemented to experimentally measure the flammability limit using certain apparatus

and define the corresponding way to determine the onset flammability limit concentration. Examples of the standards for constant volume vessel measurement are given below.

ASTM E 918-83 (USA)

Ignition vessel:	metal cylinder, volume = 1.0 dm^3, diameter > 76 mm
Initial temperature:	room temperature up to 200 ℃
Initial pressure:	atmospheric pressure up 137.9 bar
Mixture status:	Mixture is quiescent when ignited
Ignition source:	fusing wire igniter
Criterion:	pressure rise, Pex/Pi > 1.07
Step size:	selectable
Repetition of tests:	1
Explosion limit:	Mean value between ignition point and non-ignition point

EN 1839 (T) (tube method) [27]

Ignition vessel:	vertical glass tube, inner diameter 80 mm, height 300 mm
Initial temperature:	room temperature up to 200 ℃
Initial pressure:	atmospheric pressure
Mixture status:	mixture is quiescent when ignited
Ignition source:	high voltage spark, duration 0.2 s
Criterion:	flame detachment and spread out in minimum 100 mm
Step size:	10% of sample concentration below 2 mol%,

	0.2 mol% above 2 mol% sample concentration
Repetition of tests:	4
Explosion limit:	last non-ignition point

EN 1839 (B) (bomb method) [28]

Ignition vessel:	closed spherical/cylindrical steel vessel, volume > 5 dm^3
Initial temperature:	room temperature up to 200 ℃
Initial pressure:	atmospheric pressure
Mixture status:	mixture is quiescent when ignited
Ignition source:	high voltage spark 0.2s, fusing wire (10 J – 20 J)
Criterion:	pressure rise of Pex/Pi > 1.05 (5 % of initial pressure)
Step size:	10% of sample concentration below 2 mol%,
	0.2 mol% above 2 mol% sample concentration,
Repetition of tests:	4
Explosion limit:	last non-ignition point

The three standards listed above are most widely used for constant volume vessel test. Among them, the only standard that covers the determination of explosion limits at elevated pressures and temperatures is the ASTM E918-83. Beyond these, there are also many standards including optical observation of flame propagation standards (U.S Bureau of Mines) that can be applied for flammability limit experimental measurement in constant pressure vessel.

From the literature review, it has been confirmed that the flammability limit can be influenced by many factors including temperature [23], initial pressure of the fuel mixtures [3], direction of flame propagation [23], shape and size of the reaction vessel [20], and turbulence [3]. The experimentally measured data using a lab-scale reactor (1L~20L) is different from the test value generated using a plant-scale vessel [18]. The differences between the standards and the equipment used in this work raise the questions: Do these standards work for a non-standard test equipment? Which standard suits our equipment best? Should we mainly focus on pressure elevation? Or should we also consider the flame propagation distance? Can the differences be reconciled given the definitions?

With these questions in mind, we started measurement with methane at ambient temperature and atmospheric pressure. For each test, 5 repetitive experiments were executed to ensure the repeatability of the results. For LFL, test started from 5%, then the concentration of methane was decreased by 0.1% for each step until no temperature and pressure readings is received during the combustion process. For UFL, test started at 14%, then the concentration of methane was increased by 0.2% then 0.1% until there is no temperature or pressure increment. Table 3 shows the results.

Table 3 Methane flammable test at ambient temperature and atmospheric pressure

Gas Species	Desired reaction condition			Flammable?
	Temperature (°C)	Pressure (bar)	Concentration	
CH_4 LFL	20	1	5.0%	Yes
			4.9%	Partial
			4.8%	Partial
			4.7%	No
			4.6%	No
CH_4 UFL	20	1	14.0%	Yes
			14.2%	Yes
			…	Yes
			16.0%	Yes
			16.2%	Yes
			16.4%	Partial
			16.6%	Partial
			16.7%	Partial
			16.8%	No
			16.9%	No
			17.0%	No
			17.2%	No

Based on the fuel concentration, the combustion process will generate different flame propagation distance, pressure increment and temperature rise. According to Wong [23] and Zhao [8], these combustion behaviors can be grouped into 5 categories as a qualitative method to distinguish if the fuel mixture is flammable or not. In the previous work [16], due to instrumentation restriction, only signals from the thermistors and patterns of signal readings were used for the determination of flame propagation. In

this work, to better study and categorize the difference between each combustion behavior, detailed temperature vs. time profile and pressure vs. time profile are provided.

4.1 Combustion behavior

Based on the temperature increment and pressure difference before and after ignition, the combustion behaviors can be separated into 5 categories. Examples of each combustion behavior are collected and presented below.

1) Non-propagation (Figure 30), in this scenario, there is negligible temperature increment and pressure fluctuations after ignition ($\Delta T < 5°C$, $\Delta P < 0.1$ psi (7×10^{-3}bar))

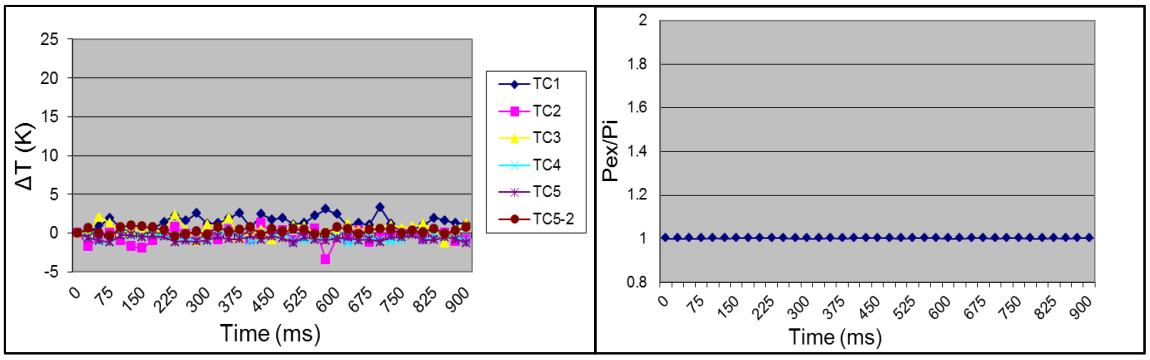

Figure 30 Temperature (left) and pressure (right) profiles for non-propagation combustion (3% methane in air at ambient temperature and 1 atm)

2) Flash combustion (Figure 31): flame propagation reaches the 1st thermocouple (closest one to the ignition source) but terminate before 2nd thermocouple, typically, temperature readings from 1st thermocouple are $\Delta T < 10$ ℃, while the temperature difference between the initial

temperature and temperature recording from 2nd thermocouple is negligible, pressure difference is smaller than or equal to 1 psi (0.07bar);

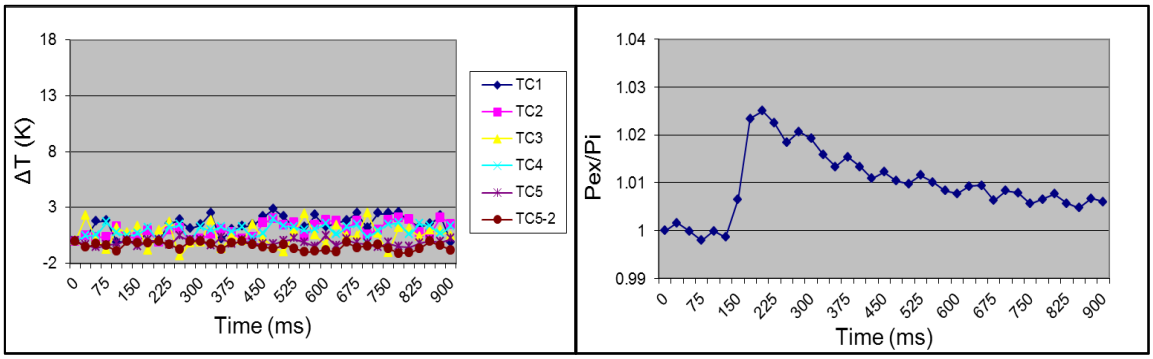

Figure 31 Temperature (left) and pressure (right) profiles for flash combustion (4.5% methane in air at ambient temperature and 1 atm)

3) Discontinuous flame propagation (Figure 32): flame propagates vertically but terminates before it reaches the top of the vessel, some of the thermocouples (more than one) receive signals, pressure difference is larger than 1 psi (0.07 bar);

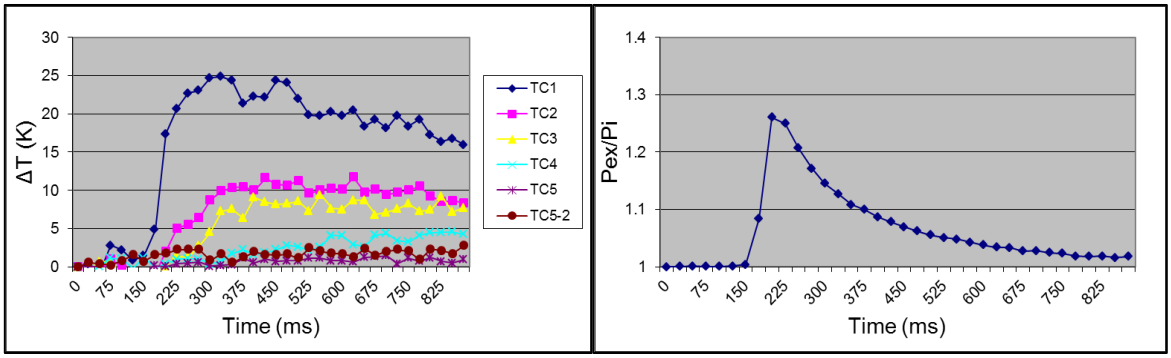

Figure 32 Temperature (left) and pressure (right) profiles for discontinuous flame propagation combustion (4.6% methane in air at 100 °C and 1 atm)

4) Continuous flame propagation (Figure 33): flame does not extinguish before it passes the highest thermocouples (TC5 & TC5-2), it is assumed flame propagates to the top of the vessel, pressure reading gives a sharp peak, both temperature and pressure readings increase smoothly;

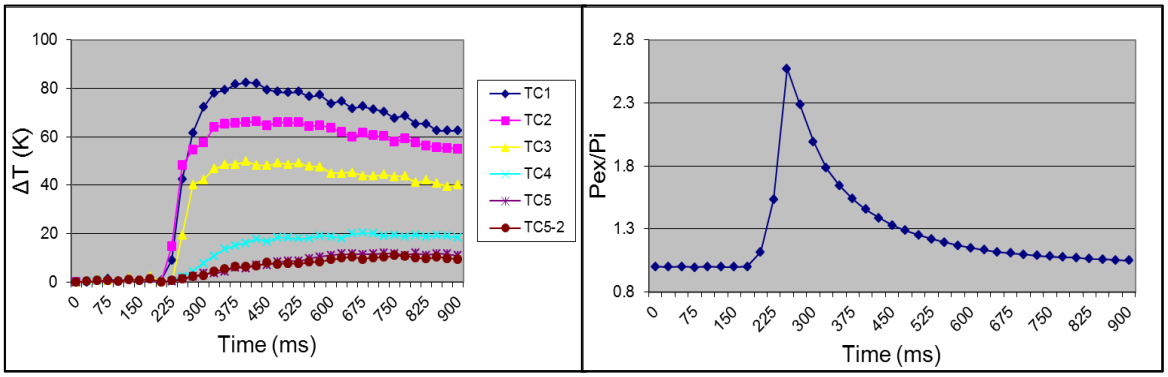

Figure 33 Temperature (left) and pressure (right) profiles for continuous flame propagation combustion (5% methane in air at 50 °C and 1 atm)

5) Violent flame propagation (Figure 34): temperature and pressure readings increase to the maximum in a very short duration of time (less than 100ms), maximum explosion pressure is at least 3 times of the initial pressure. This phenomenon rarely shows at the lower flammability limit.

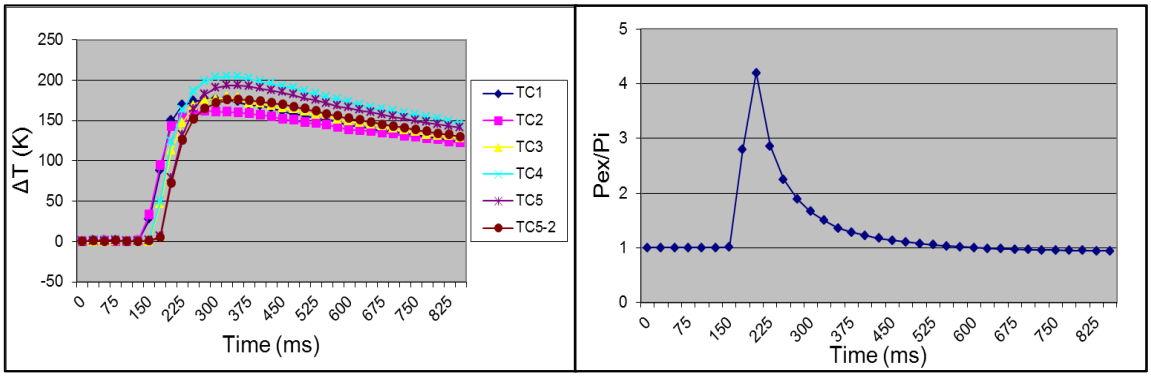

Figure 34 Temperature (left) and pressure (right) profiles for Violent flame propagation combustion (7% methane in air at ambient temperature and 1 atm)

Combustion behaviors can be easily distinguished for the lower flammability limit test, as fuel concentration increases, the combustion behavior will change from one to another. However, for upper flammability limit test, a 0.1% step change in the fuel concentration will change the combustion behavior from violent flame propagation to flash combustion. In UFL test, especially at higher initial pressure, due to non-uniform shape of the flame front developed during the combustion process, single thermocouple is not able to capture the exact location of flame front, which in turn generates more measurement error during the experiment. Therefore, the UFL measurement will generally require more repetitive tests for more accurate results.

It is worth mentioning that though the calculated flame temperature of methane was above 1,600K, the detected temperature rise was small compared to the calculated flame temperature. The main reason was due to the limited heat transfer between burning gas and the thermocouples. When the flame propagated upward, the contact time between burning gas and the tip of the thermocouple was typically less than 20ms, within this time length, the thermocouple could not receive a significant temperature rise without consistent heat supply. Also, at the flammability limit, the fuel involved in the combustion reaction only took a small portion of the total mass, the mass difference between the burning gas and metal thermocouple was diluting the energy generated from burning fuel. Therefore, the detected temperature rise from the experiment is much smaller compared to the calculated flame temperature. However, in this experiment, the main focus was to detect the temperature rise from combustion reaction to confirm the flammability of the gas mixture rather than on measuring temperature rise quantitatively. It was acceptable to use ΔT of 10°C to indicate the flame propagation.

4.2 Comparison of flammability limit criteria

Combustion behavior categorization mentioned above is a semi-quantitative method that was originally developed based on the flame propagation distance in a constant pressure system. However, this method which rely on human judgment to determine the exact combustion pattern, cannot distinguish the exact boundary between flammable and non-flammable zone. To quantitatively define the flammability limit, a more accurate and precise method is needed.

According to the US Bureau of Mines (USBM) flammability test [3], the flammable range for methane is 5-15%. This flammable range is defined based on the criterion of visual flame propagation for more than 75 cm in a 1.5 m long, 5 cm I.D. glass tube (constant pressure). If this flammability limit criterion is applied in this work, the experimental data indicates that even when the concentration is out of the flammable range, a considerable fraction of the fuel/air mixtures can still be burned (see Figure 35), which proves that the USBM flammability limit criterion may not be suitable for a constant volume cylindrical vessel. So it is critical to choose the suitable flammability limit for experimental measurement and define the corresponding combustion behavior.

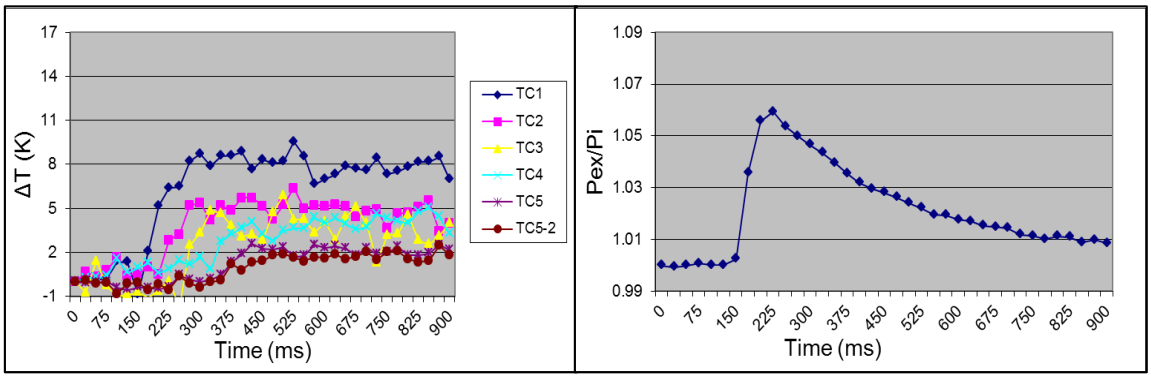

Figure 35 Temperature (left) and pressure (right) profiles for 16.6% methane combustion in air at ambient temperature and 1 atm)

To find the appropriate flammability criterion, three flammability limit criteria mentioned above are compared. EN-1839 (B) standard defines the flammability limit as a combustion reaction that can produce at least a 5% rise of the initial absolute pressure (Equation.14),

$$\frac{P_{ex}}{P_0} \geq 1.05 \qquad (14)$$

where P_{ex} is the maximum explosion pressure and P_0 is the initial pressure before ignition. ASTM-918 standard defines the flammability limit as a combustion reaction that can produce at least a 7% rise of the initial absolute pressure (Equation.15).

$$\frac{P_{ex}}{P_0} \geq 1.07 \qquad (15)$$

The last criterion, which defines the flammability limit as a flame that can propagate to the top of the vessel upon ignition, has also been used by Wong [23] and Zhao [8].

Table 4 Comparison of lower flammability limits of methane determined by different flammability criteria and combustion behavior (20 °C and 1atm)

	EN-1839 B (5%)	ASTM 918-83 (7%)	Flame propagation
Flame propagation distance (cm)	<20	50	100
ΔP (psi)	0.84 ±0.05	3.33 ±0.05	7.44 ±0.05
Lower Flammability limit (vol % in air)	4.70 ±0.05	4.75 ±0.05	4.9 ±0.1

Table 4 is an example for the comparison of the lower flammability limit determined using three criteria at the condition of 20 ℃ and 1 atm. Corresponding

combustion behavior for the LFL value determined using each criterion are also compared in the Figure 36, Figure 37 and Figure 38.

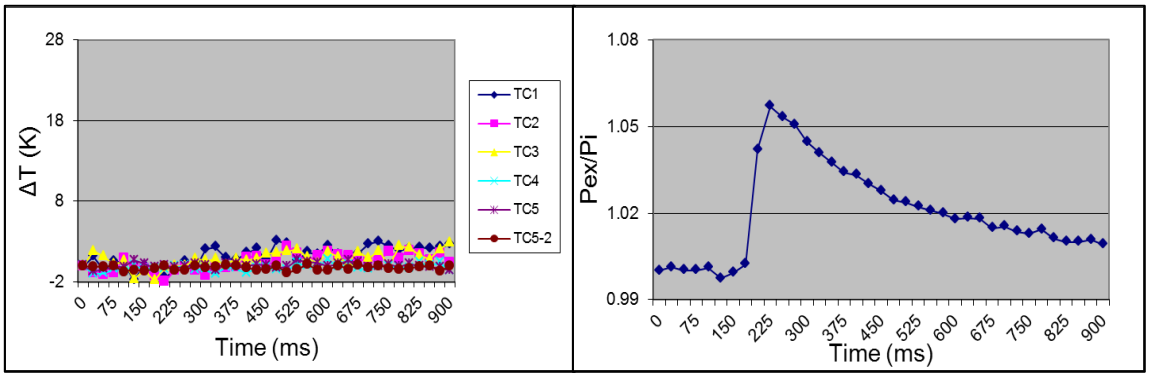

Figure 36 Temperature (left) and pressure (right) profiles for flammability limit using EN-1839 B criterion (4.7% methane combustion in air at ambient temperature and 1 atm)

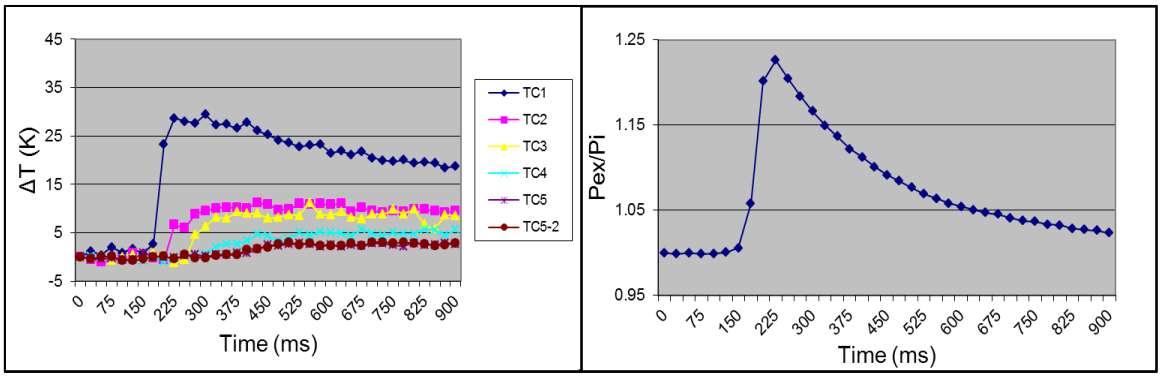

Figure 37 Temperature (left) and pressure (right) profiles for flammability limit using ASTM 918-83 criterion (4.8% methane combustion in air at ambient temperature and 1 atm)

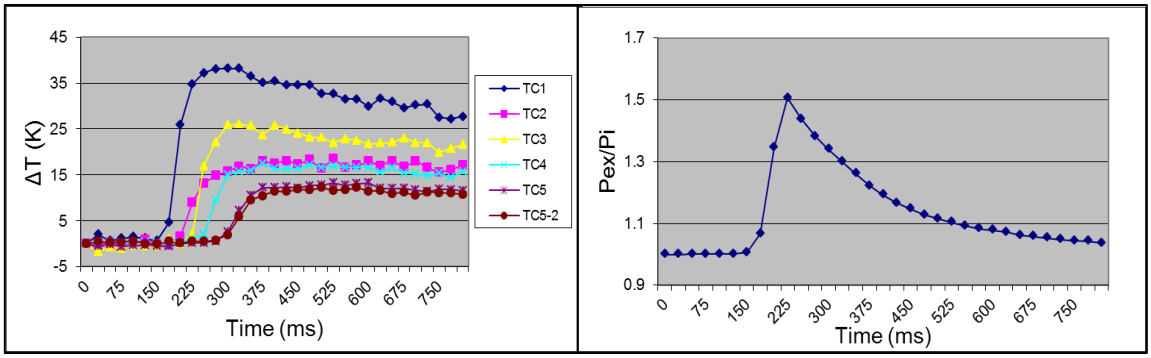

Figure 38 Temperature (left) and pressure (right) profiles for flammability limit using flame propagation criterion (4.9% methane combustion in air at ambient temperature and 1 atm)

As indicated in Figure 36 and Table 4, the European standard EN-1839 B has the smallest flame propagation distance, pressure rise, as well as the flammability concentration. The combustion behavior corresponding to this criterion falls into the category of flash combustion. While the flame propagation criterion has the largest propagation distance, pressure rise, and flammability concentration. The combustion behavior for flame propagation criterion is continuous flame propagation.

For better understanding of the criteria application on the flammability boundary, the upper flammability limit values with the initial condition as 100 ℃ and 2atm determined using three criteria are also compared in Table 5.

Table 5 Comparison of upper flammability limits of methane determined by different flammability criteria (100 °C and 2atm)

	EN 1839 B (5%)	ASTM 918-83 (7%)	Flame propagation
Flame propagation distance (cm)	<35	35	100
ΔP (psi)	1.49 ± 0.05	2.73 ± 0.05	111.89 ± 0.05
Upper Flammability limit (vol % in air)	18.8 ± 0.1	18.7 ± 0.1	18.2 ± 0.2

Based on the value of the lower flammability limit at ambient temperature and atmospheric pressure, the difference between each standard is relatively small (±0.2). However, for the upper flammability limit and the situation where the elevated conditions are applied, the difference becomes larger (±0.6).

Considering the elevated temperature or pressure may affect the flammability limit value, three flammability limit criteria are compared together at different initial conditions. The flammability limit values determined from each criterion are plotted versus temperature change and pressure change.

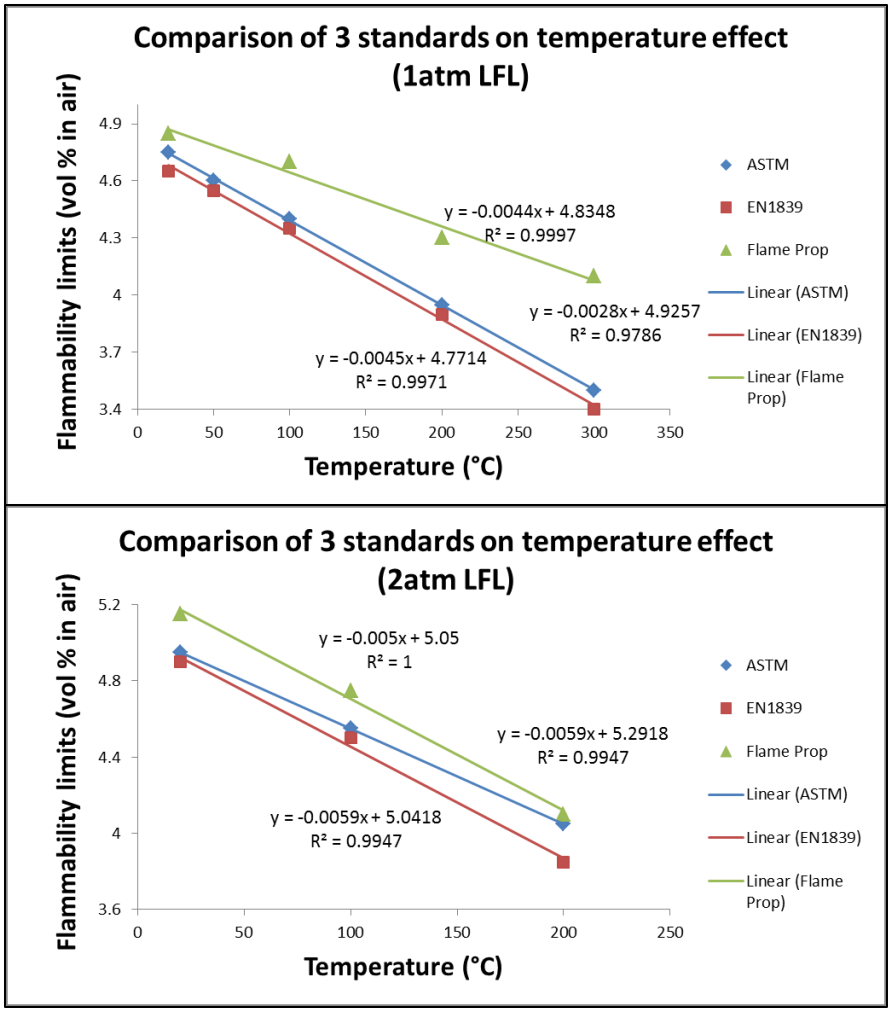

Figure 39 Comparison of 3 standards on temperature effect at LFL with initial pressure of 1 atm (upper) and 2 atm (lower)

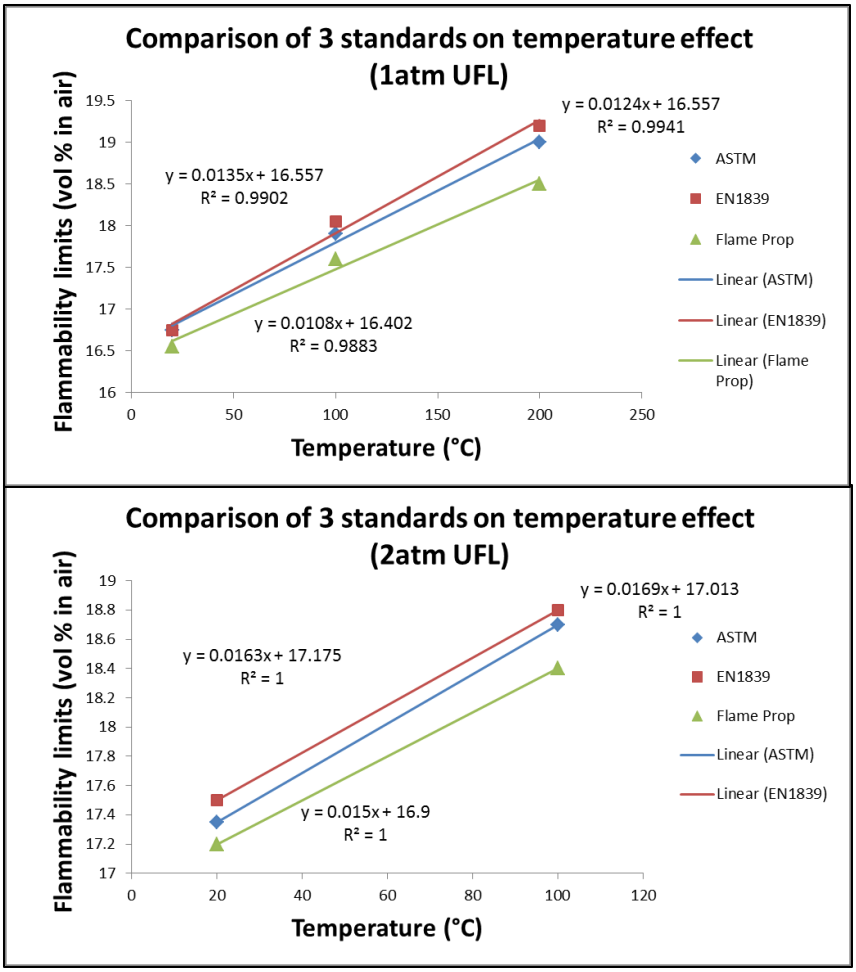

Figure 40 Comparison of 3 standards on temperature effect at UFL with initial pressure of 1 atm (upper) and 2 atm (lower)

As shown in Figure 39 and Figure 40, as temperature increases, the trend of increase in the flammability limit region is observed with all three flammability criteria. LFL decreases with increase in temperature whereas UFL increases with increase in temperature. At the initial condition of 1 atm, the differences between the flame propagation criterion and the pressure criterion become larger as temperature increases.

However, at the initial condition of 2 atm, the ASTM flammability value is consistently 5% smaller than flame propagation flammability value in LFL and 1% larger in UFL. The main reason for the difference in the trend between pressure criterion and flame propagation criterion is due to the difference in the equipment system. The flame propagation criterion is developed based on constant pressure system while the pressure criteria (ASTM and EN1839) are developed based on constant volume system. The temperature increment has less impact on the flame propagation since if the flame propagation distance is the same, same amount of fuel will be ignited for each test. While for pressure criteria, increase in the temperature will reduce the energy to heat up the unburned gas, which in turn reduces the amount of the fuel for combustion (i.e., lower fuel concentration).

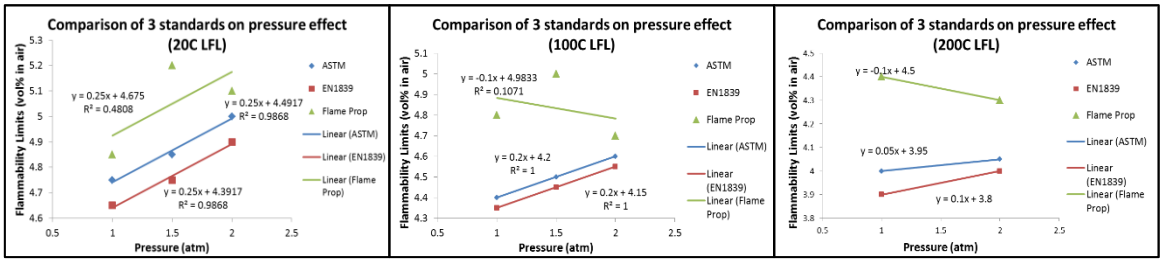

Figure 41 Comparison of 3 standards on pressure effect at LFL with initial temperature of 20 °C (left), 100 °C (middle) and 200 °C (right)

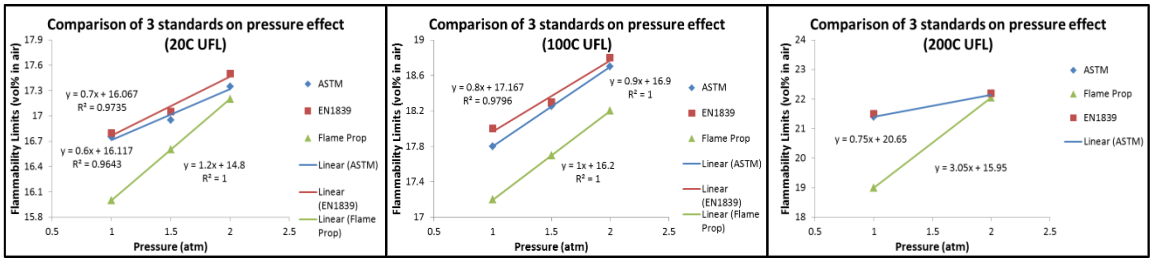

Figure 42 Comparison of 3 standards on pressure effect at UFL with initial temperature of 20 °C (left), 100 °C (middle) and 200 °C (right)

On the other hand, as pressure increases, the trend of increasing in the flammability limit is consistent in pressure criteria only (Figure 41 and Figure 42). Especially at the initial condition of elevated temperature, the flammability limit measured using flame propagation criterion does not form a clear trend, nor does the difference between the two criteria stay constant. Because the pressure tests are only conducted in a narrow range (less than 2atm), the data is not sufficient to prove any conclusion about pressure effect. Also for flame propagation determined flammability limit data, the accuracy is relatively low (error ±0.2%) and the margin between continuous flame propagation and violent flame propagation is not quantitatively defined. Therefore, larger pressure range is needed to validate the pressure effect on flame propagation criterion. Since the temperature effect and pressure effect are not very consistent for all three flammability criteria, it is suggested that there are other factors affecting the conversion between the pressure criterion and flame propagation criterion.

The combustion of methane, which is a violent and quick oxidizing reaction, follows the energy balance $\Delta H=\Delta U+\Delta PV$. Since the combustion reaction occurs in a

very short time frame, it can be assumed that there is no heat transfer to the surroundings (i.e., wall of the reactor), thus the combustion reaction is adiabatic to a certain extent. The energy released from the oxidizing of fuel is transformed into internal energy, which is represented as the increase of temperature, and volume expansion, which is represented as the increase of pressure. In this case, the maximum explosion pressure ratios are compared with the maximum temperature increment and the flame propagation distance so that a simplified conversion of the flame propagation criterion versus the pressure criterion can be calculated. However, one very important factor is that the temperature change will change the kinetics of the reaction [29]. With lower temperature and rich mixtures, the reaction kinetics become more complicated [30].

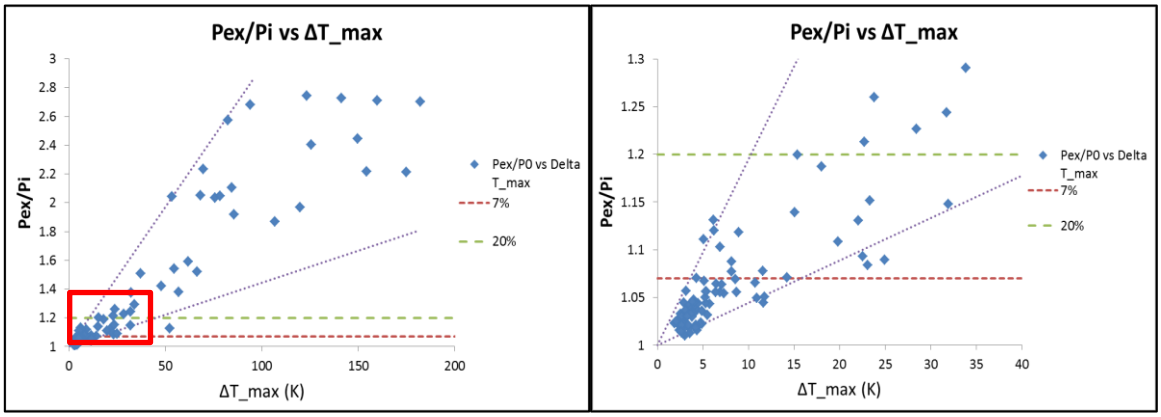

Figure 43 Maximum explosion pressure ratios vs. Maximum temperature increment. Right side is the enlarged area.

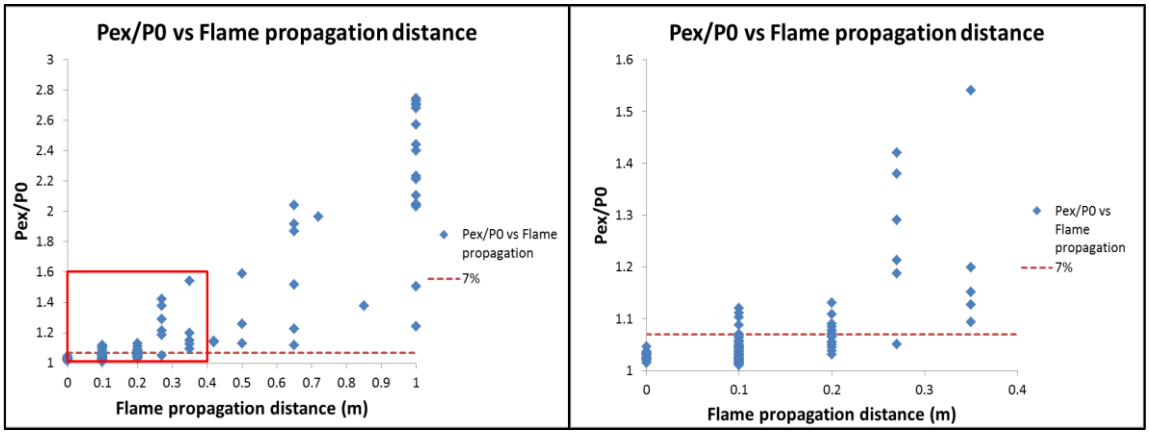

Figure 44 Maximum explosion pressure ratios vs. Flame propagation distance. Right side is the enlarged area.

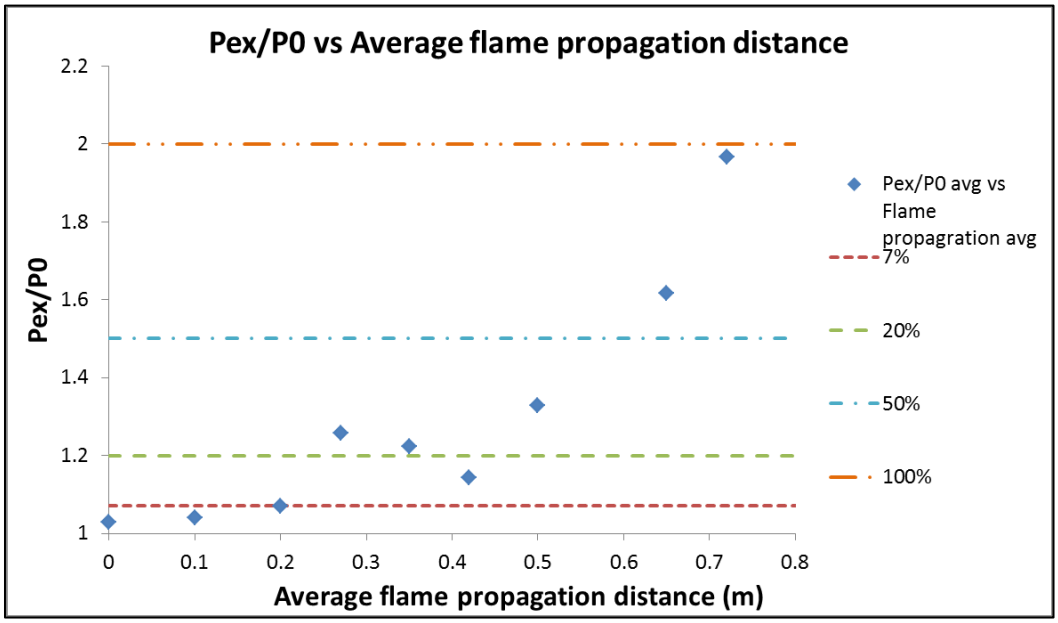

Figure 45 Maximum explosion pressure ratios vs. average flame propagation distance.

Figure 43 indicates that the maximum pressure ratio is not a linear function of the maximum temperature increment. However, it should be noted that for a fixed explosion pressure ratio value, the maximum temperature increment will lie within a certain range. For example, if 7% pressure increment criterion is used for flammability limit, then the maximum detected flame temperature rise from all of the thermocouples are between 3℃ to 16℃. On the other hand, Figure 44 shows that for a certain flame propagation distance, the maximum explosion ratio varies, especially when the flame propagation distance is larger. Due to instrument capability, it is very difficult to precisely identify the exact position where the flame fades away (i.e., flame can distinguish between two thermocouples). So as shown in Figure 45, maximum explosion ratio plotted versus the average flame propagation distance, and if 7% pressure increment criterion is used for flammability limit definition, the typical flame propagation distance is around 20cm in the flame tube that we used for the experiment.

4.3 Define the flammability limit

Based on the data summary and analysis, both pressure criteria and flame propagation criterion are suitable for the flammability limit experimental measurement. However, the flame propagation criterion involves probabilistic uncertainty due to random errors in the propagation distance measurement and flame turbulence, especially at the upper flammability limit where the flame is developing slowly and asymmetrically after the ignition, the sensors may not be able to capture the flame propagation

accurately. Thus, if the flame propagation criterion is to be used, multiple experiments with the same composition need to be executed to minimize the error.

In conclusion, 7% pressure criterion is a conservative standard which can be applied for the flammability limit measurement on the non-standard vessel. In this work, the data for flammability limit are mainly determined based on pressure increment. However, since the combustion process is taking place in a cylindrical chamber, there is possibility for the cool flame phenomenon and pre-deflagration to detonation situation. Therefore, the situation, where the pressure increment is less than 7% of the initial pressure with a flame propagation distance larger than 20cm is also considered as flammable. To accurately measure the flammability limit using flame propagation criterion, one group test of flash combustion or continuous combustion and another group test of non-propagation must be identified. For non-ASTM standard equipment, it is recommended to have both temperature and pressure data recorded to validate the flammability results.

5. FLAMMABILITY LIMITS OF PURE LIGHT HYDROCARBON[2]

With the determined criterion, the experimental measurement for the flammability limit starts with pure fuel component including methane (the entire flammable range), propane and ethylene. The test are conducted at the initial condition of temperature from ambient to maximum 300 ℃ and pressure up to 2 atm. In this section, detailed measurement results are presented and compared with theoretical predictions. Further analysis including the apparatus effect, temperature effect and initial pressure effect are provided for the discussion of the possible reasons behind differences between experimental results and predictions.

5.1 Experimental results of flammability limit

For each test initial condition, the LFL and UFL are measured as shown in Table 3. For gas mixture preparation, the pressure loading error can be controlled within ±0.02 psi (1.36×10^{-3}bar), which will result in the error of concentration of ±0.02 vol% for single test. Repetitive experiment at the maximum concentration of non-flammable zone and minimum concentration of flammable zone will minimize the measurement error of the flammability limit boundary to ±0.05 for LFL test and ±0.1 for UFL test. This measurement error is consistent for all of the data represented in this work. Table 6,

[2] Reprinted with permission from "Application of flammability limit criteria on non-ASTM standard equipment" by Gan, N., Bukur, D. & Mannan, M.S., 2018. J Therm Anal Calorim (2018), P1-14, https://doi-org.ezproxy.library.tamu.edu/10.1007/s10973-018-7413-6 Copyright 2018 Springer International Publishing.

Table 7 and Table 8 are the summary of the experimental measured flammability limit for methane, propane and ethylene, respectively.

Table 6 Experimental measured flammability limit (vol%) of methane

Methane CH_4	Pressure (atm)	Temperature (℃)				
		20	50	100	200	300
LFL	1	4.75 ±0.05	4.6 ±0.05	4.4 ±0.05	3.95 ±0.05	3.5 ±0.05
	1.5	4.85 ±0.05	-	4.5 ±0.05	-	-
	2	4.95 ±0.05	-	4.55 ±0.05	4.05 ±0.05	
UFL	1	16.75 ±0.1	-	17.9 ±0.1	19 ±0.1	21.4 ±0.1
	1.5	16.95 ±0.1	-	18.25 ±0.1	-	-
	2	17.35 ±0.1	-	18.7 ±0.1	19.3 ±0.1	22.15 ±0.1

Table 7 Experimental measured flammability limit (vol%) of propane

Propane C_3H_8	Pressure (atm)	Temperature (℃)		
		20	100	200
LFL	1	1.95 ±0.05	1.85 ±0.05	1.65 ±0.05
	2	2.05 ±0.05	1.9 ±0.05	1.65 ±0.05
UFL	1	11.2 ±0.1	11.9 ±0.1	12.6 ±0.1
	2	11.8 ±0.1	12.9 ±0.1	15.3 ±0.1

Table 8 Experimental measured flammability limit (vol%) of ethylene

Ethylene C_2H_4	Pressure (atm)	Temperature (℃)		
		20	100	200
LFL	1	2.65 ±0.05	2.35 ±0.05	2.25 ±0.05
	2	2.71 ±0.05	2.45 ±0.05	2.3 ±0.05
UFL	1	34.1 ±0.1	35.2 ±0.1	39.2 ±0.1
	2	36.9 ±0.1	38.35 ±0.1	40.85 ±0.1

It is observed through the experiments that for pure propane and pure ethylene UFL test, the fuel concentration range to distinguish gas mixtures from flammable to non-flammable is very narrow (i.e., usually the fuel concentration difference between flammable zone and non-flammable zone are within 0.2 vol%). Contrary to the LFL test results, in UFL experiment the maximum Pex/P_0 ratio does not decrease linearly as the fuel concentration increases. Once the fuel concentration enters the non-flammable zone, the maximum explosion pressure drops from at least 2 times of the initial pressure to less than 1.07 times of the initial pressure, while the combustion behavior changes from violent flame propagation to non-propagation without any transition.

One special phenomenon observed during the experiment is that for UFL test at the concentration close to the flammability limit, flame may not be detected at early propagation stage (i.e., temperature rise at the flame front cannot be detected by 1^{st} or 2^{nd} thermocouple but by 4^{th} or 5^{th} thermocouple). Also for some of the UFL tests, the

ignition delay time (time between the ignitor is fired and the first detection of temperature rise) is significantly larger than in other tests. It is suspected that this situation is caused by the cool flame phenomenon. Moreover in the UFL test when the fuel concentration is close to the flammability limit boundary, the probability of flame propagation (success combustion /ignition) may decrease. This is especially true for tests at elevated pressure, where the probability of successful combustion changes from 80% (4 successful ignitions out of 5 tests) to 20% (1 successful ignition out of 5 tests).

5.2 Apparatus effect on the flammability limit

Typically, for flammability tests, 20L spherical vessel would be selected [5]. Since the vessel used in this work is a cylindrical vessel, the apparatus effect need to be taken into consideration. In previous flammability test studies, cylindrical vessels were used at German Federal Institute for Materials Research and Testing (BAM) 6L[18], and Warsaw University of Technology (WUT) 40L[18]. However, in this work, the cylindrical vessel used are not like any of the vessel mentioned above since the vessel has large length vs. diameter ratio (L/D = 10) which constrain the energy released from the oxidation reaction in one direction and allows the researcher to study the flame propagation process better. In another previous apparatus effect study, Takahashi [20] investigated the effect of vessel size and shape on the flammability limit of gases. It was found that for a test vessel with a small diameter, the quench effect is the major parameter that determines the flammability limits. For a vessel with a small height, the hot gas accumulation underneath the ceiling and the unburnt gas heating during flame

propagation would change the flammability limit value. In this study, the vessel diameter is 10cm, which is larger than the 76mm in the ASTM standard [9], therefore these effects should be minimized. For better understanding of the vessel shape effect, the maximum explosion pressure of methane at atmospheric pressure measured in this work is compared with previous literature results which were measured using 20L spherical vessel.

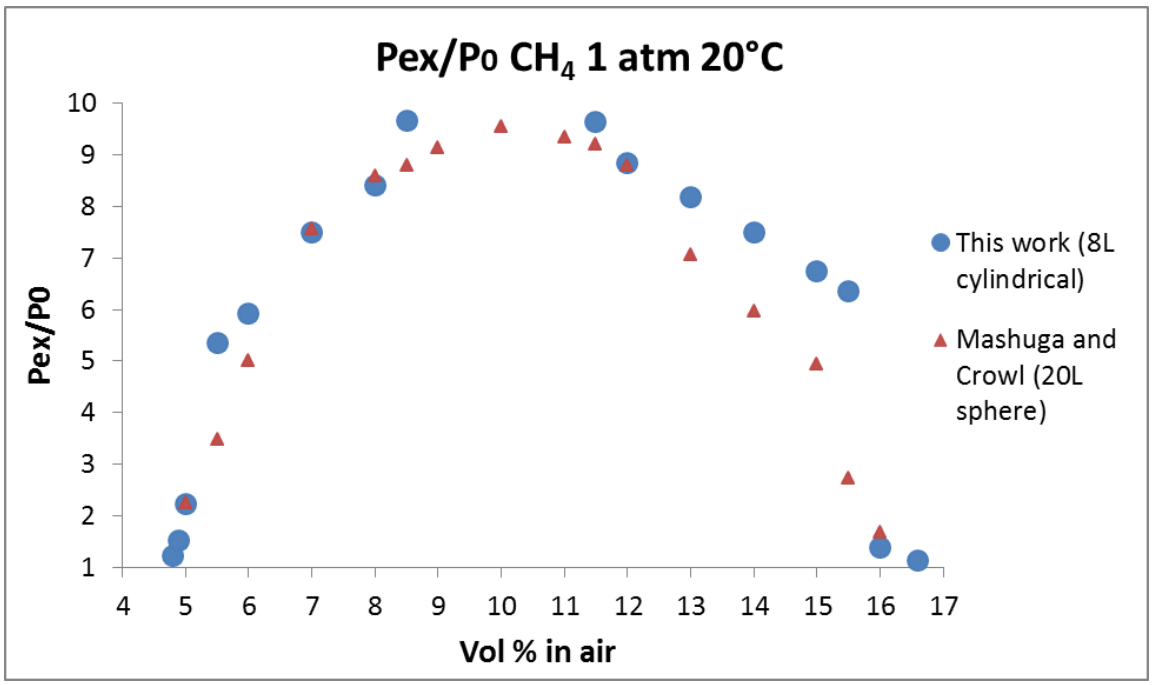

Figure 46 Maximum explosion pressure ratio of methane vs fuel concentration (1atm, ambient temperature)

In Figure 46, the maximum explosion pressure ratio is plotted vs the methane concentration. Experimental data are compared with results reported by Mashuga [5]

using a 20L sphere. It is found that when the concentration of methane (8-12 vol%) is close to the stoichiometric ratio (9.5 vol% of methane), the maximum explosion pressure values are similar. But when the concentration is away from the stoichiometric ratio and getting close towards the flammability limits (i.e., 5-7 vol% or 13-15.5 vol%), the cylindrical vessel generates higher explosion pressure. However, once the concentration of methane reaches exactly flammability limit boundary (below 5.5% or above 15.5%), the maximum explosion pressure is the same again.

The explanation for this phenomenon is that when the concentration is close to the stoichiometric ratio, a majority of the fuel is completely oxidized in the combustion reaction. When the concentration is getting away from the stoichiometric ratio, the cylindrical vessel tends to generate higher explosion pressure because of the buoyancy effect, which makes it easier for the flame to propagate upward. If a spherical vessel is used, only the upper part of the fuel is ignited and it is difficult for the flame to propagate horizontally and downwards. However, once the concentration of methane reaches flammability limit boundary, only the portion closest to the ignition source is ignited. Typically, the fire ball generated from the center of ignition sources usually fades away before it can reach the side of the reactor, in this way, both cylindrical vessel and spherical vessel would generate similar explosion pressures.

When the methane concentration is close to the stoichiometric ratio (8%-11%), the flame propagation speed is significantly increased compared with the flame propagation speed at flammability limit. Also during the combustion, the reaction makes noises. The explanation for the noise is still unknown but it is considered as an early

indication of flame speed change, and this phenomenon is named as pre-DDT (pre-deflagration to detonation transition).

For methane, the flammability limit range measured using the cylindrical vessel is 4.75%-16.75%, which is larger than the flammability limit measured using the 20L spherical vessel range 4.85%-16.14% [5]. Comparison between of measured flammability limit in this study and literature values for several gases, is shown in Figure 47.

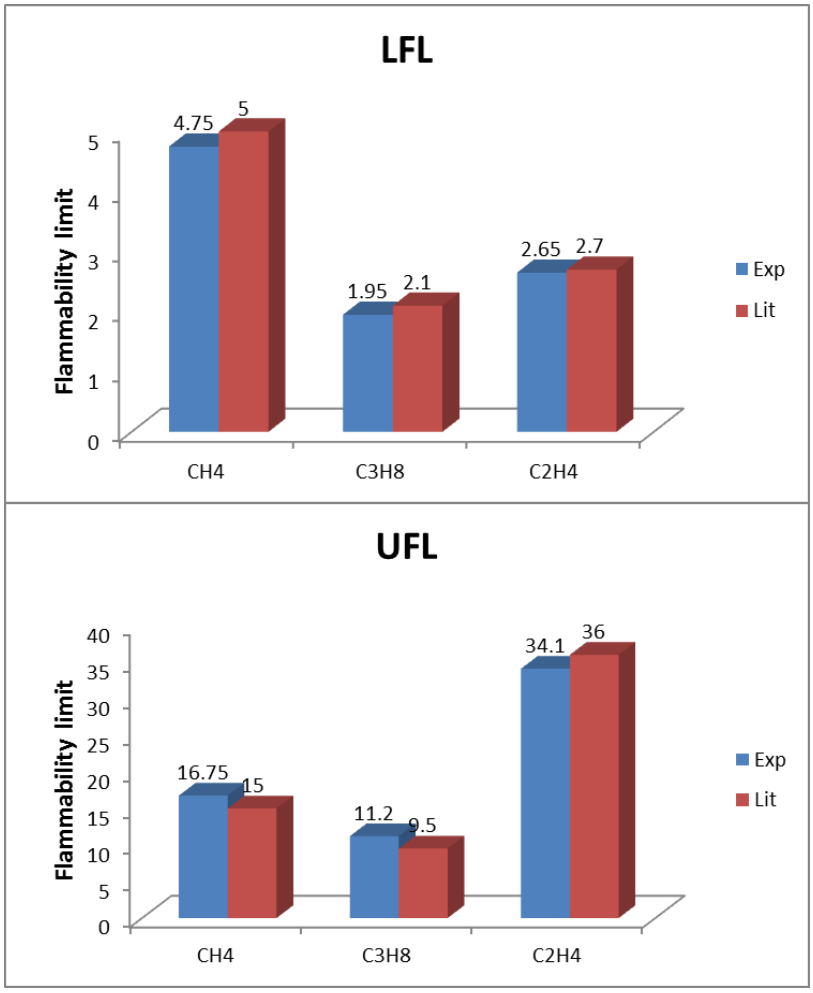

Figure 47 Comparison of flammability limit value measured using 20L sphere [5] (red) and the cylindrical vessel in this work (blue)

As shown in Figure 47, all of the experimentally measured LFL values are smaller than the literature value. For LFL test in the cylindrical vessel, due to buoyance effect, the burned gas, which has smaller density will tend to diffuse upward and make the heat transfer between burned gas and unburned gas easier compared with the flame propagation in horizontal direction or downwards. Since in the LFL test fuel is limiting

component, fuel will be completely oxidized to carbon dioxide and water. Therefore, the upward propagation requires less energy to heat up unburned gas (i.e., less fuel need to be ignited). However, for UFL test, the experimental measured values are not consistent for all three gas species. It is true that in UFL test, the buoyancy effect will still behave similarly as in the LFL test. But since in UFL test, oxygen is the limiting component, less energy consumption means less oxygen is needed, which in turn means more fuel can be added in the test. Therefore for methane and propane UFL test, the experimentally measured values are larger than the values reported using spherical vessel. However, in the UFL test, the reaction mechanism not only involves the oxidation of fuel component, but also the decomposition of fuel. The decompositions of the C-C bond, C-H bond and C=C double bond are endothermic reaction. For the reaction of methane, the majority of the energy released from the chain reaction (the combination of C and O or H and O is exothermic reaction) is used for the further decomposition of O_2 and C-H bond. Similarly for propane, the majority of the energy released from the chain reaction is used for further decomposition of O_2, C-C bond and C-H bond. Compared with the decomposition of ethylene, the breaking of C=C double bond requires less energy. At the same time, the decomposition of ethylene generates more hydrogen, which resulted in the elevation of pressure. Since the flammability criterion is mainly dependent on the pressure increment, with enough decomposition of ethylene, it can generate same results as oxidation reaction. In terms of the geometry, since the decomposition of ethylene requires certain temperature and pressure, the cylindrical vessel, which constrains the reaction energy in one direction, is easier than

the spherical vessel to generate the condition needed for decomposition. Therefore, the experimentally measured ethylene flammability limit would be lower than the reported value from spherical vessel. It is expected that other unsaturated light hydrocarbons like propylene and acetylene would behave similarly as ethylene while other saturated light hydrocarbons like ethane and butane would behave similarly as methane.

In summary, the geometry and the apparatus shape have effect on measured flammability limit value. The geometry will have consistent effect on the LFL measurement as long as the apparatus can constrain the flame propagation to a certain extent. Typically, smaller vessel (such as 5L vessel) will generate lower LFL compared with larger vessel (such as $1m^3$ vessel) and cylindrical vessel generates wider flammability range than a spherical vessel for saturated light hydrocarbons. While the UFL test results are not simply influenced by the geometry, but also by the reaction mechanism and this will have effect on experimentally measured values.

5.3 Temperature effect on pure component

Previous literature [3] suggests that an increase in temperature usually widens the flammable range. It is suggested that for LFL the limit value varies linearly with temperature. Our experimental data, as shown in Figure 48, indicate that for all initial pressures, the flammability limit (both LFL and UFL) of methane, propane and ethylene varies linearly as the initial temperature increases, which is in agreement with the previous study[31, 32].

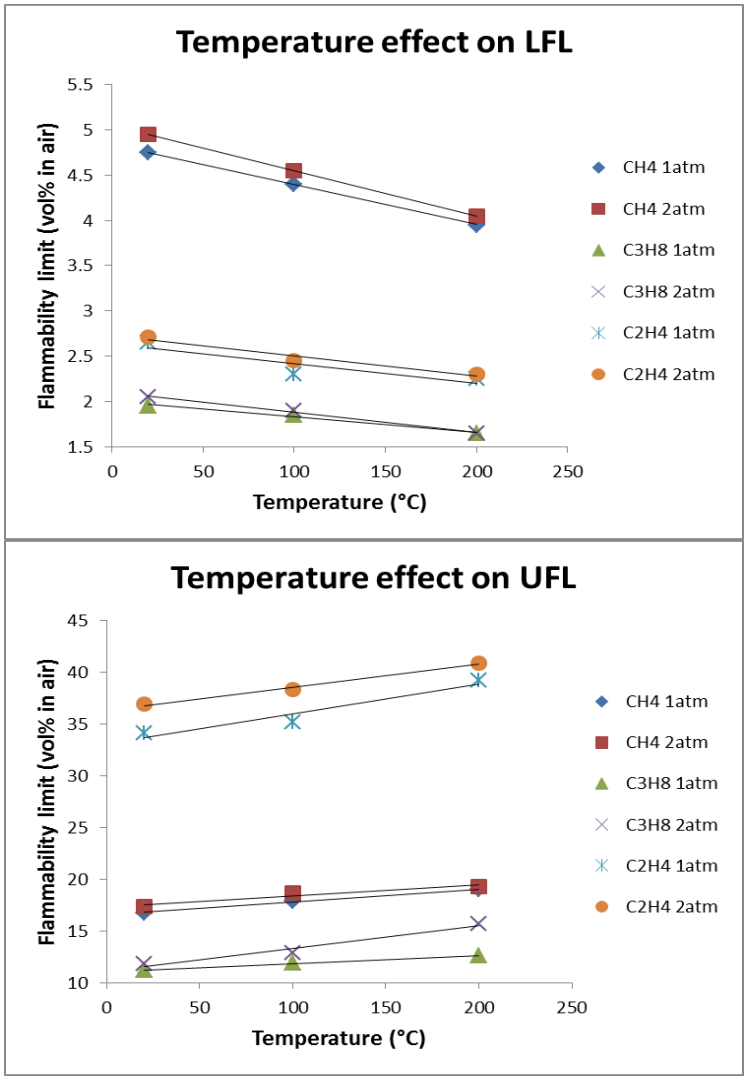

Figure 48 Linear temperature effect on flammability limit of methane, propane and ethylene

According to the White criterion that the flame temperature is constant [11], the lower limit dependence on temperature should intersect with the temperature axis at 1,225 ℃. However, our experiments indicate that the intersect temperatures of methane (1atm), methane (2atm), propane (1atm), propane (2atm), ethylene (1atm) and ethylene

(2atm) are 1099 ℃, 1010 ℃, 1174 ℃, 957 ℃, 1204 ℃ and 1239 ℃, respectively (see Figure 49 & Figure 50). All of the extrapolated flame temperatures are lower than the prediction, especially for the calculated flame temperature of methane, which suggests that using LFL dependence on the temperature may not be a suitable method to calculate the flame temperature.

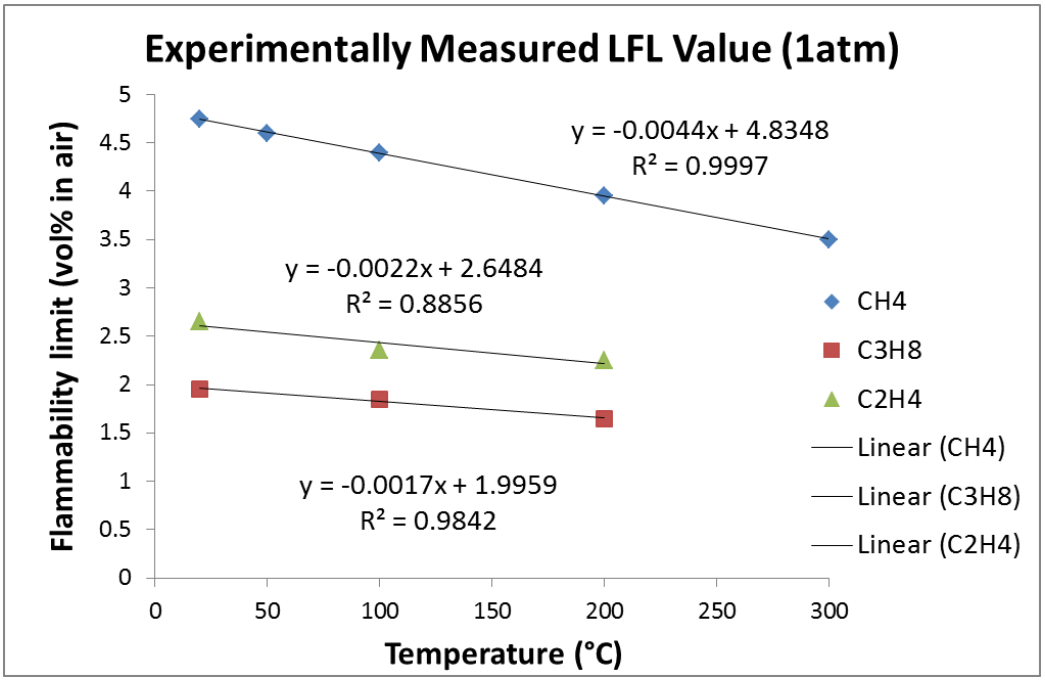

Figure 49 Experimentally measured LFL value for methane, propane and ethylene at 1atm and their corresponding best linear fitting for the temperature dependence

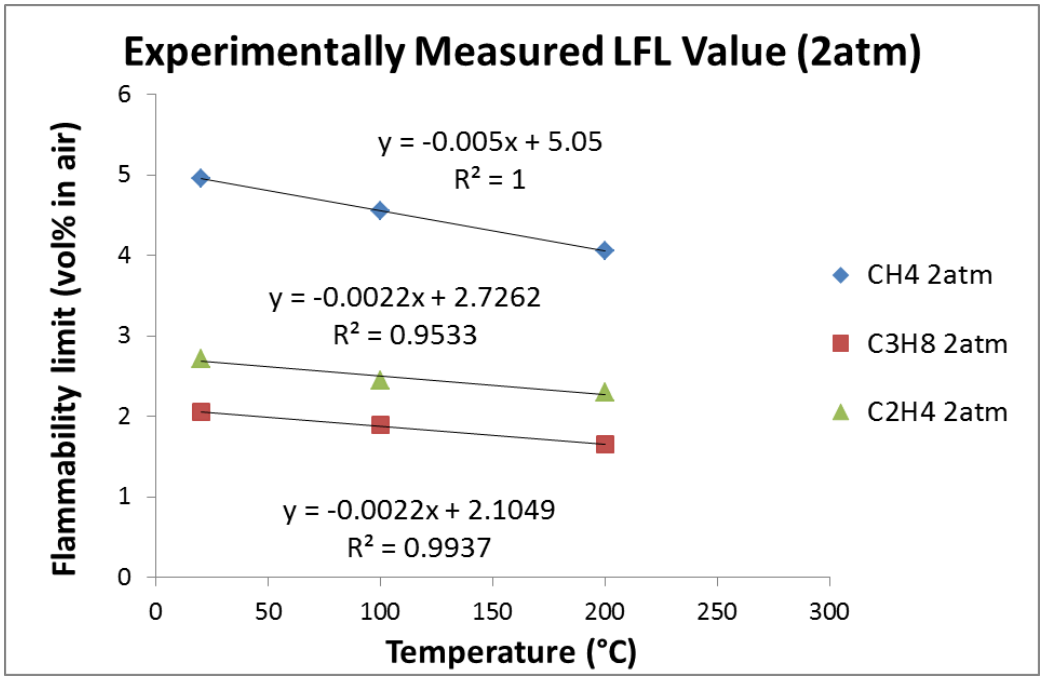

Figure 50 Experimentally measured LFL value for methane, propane and ethylene at 2atm and their corresponding best linear fitting for the temperature dependence

The linearity of the flammability limit dependence on temperature can be fitted through the equation [6] as (Equation. 16):

$$\frac{FL\,(T)}{FL\,(T_0)} = 1 + c \times (T - T_0)\ (16)$$

in which T is the initial temperature, T_0 is the reference temperature, and c is constants to be determined from the least squares fit of the experimental data points. Zabetakis [33] suggested the correlation for calculation of lower flammability limit at higher temperature utilizing LFL value at 25 ℃ as the modified Burgess-Wheeler Law (Equation.3 & Equation.4):

$$LFL_T = LFL_{25°C} - \frac{\alpha}{\Delta H_c}(T - 25°C)\ (3)$$

$$UFL_T = UFL_{25°C} + \frac{\alpha}{\Delta H_c}(T - 25°C) \quad (4)$$

where ΔHc is the net heat combustion (kcal/mol) for flammable gas and T is the temperature of gas mixtures in ℃ and α is a constant as 0.75. To see if the modified Burgess-Wheeler Law also fit for our experimental data, the measured flammability limit value and their best linear fitting are plotted and compared with the modified Burgess Wheeler law in Figure 51 to Figure 58.

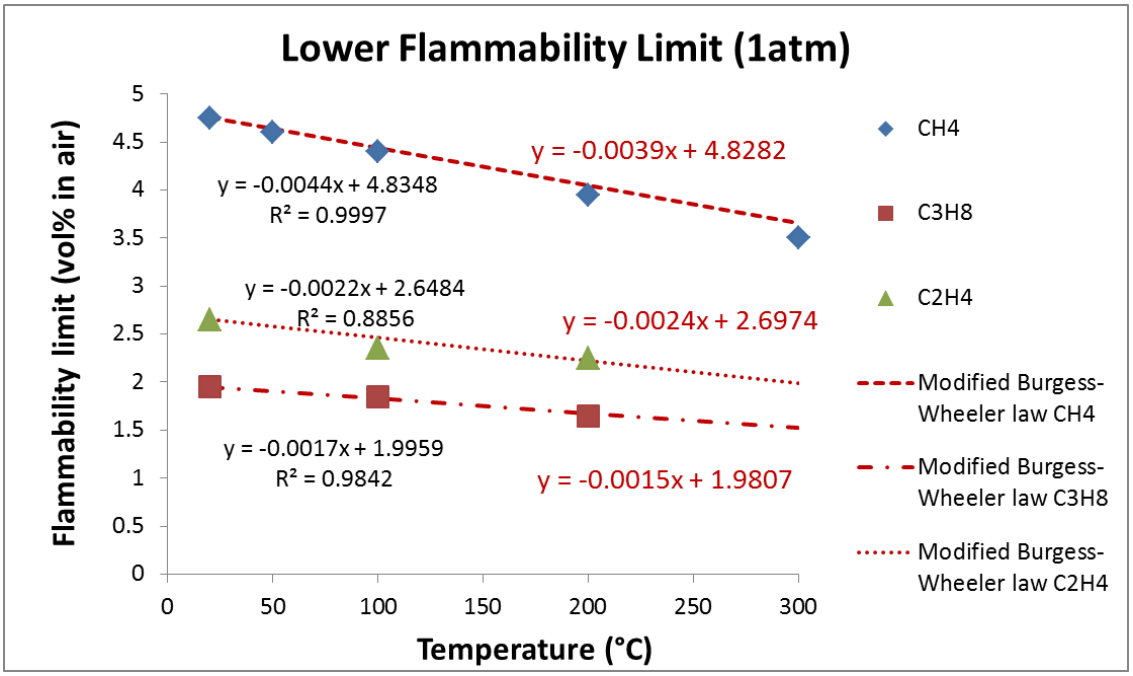

Figure 51 Comparison of experimentally measured LFL of methane, propane, ethylene at 1atm and their best linear fitting vs. the predicted LFL using modified Burgess Wheeler law

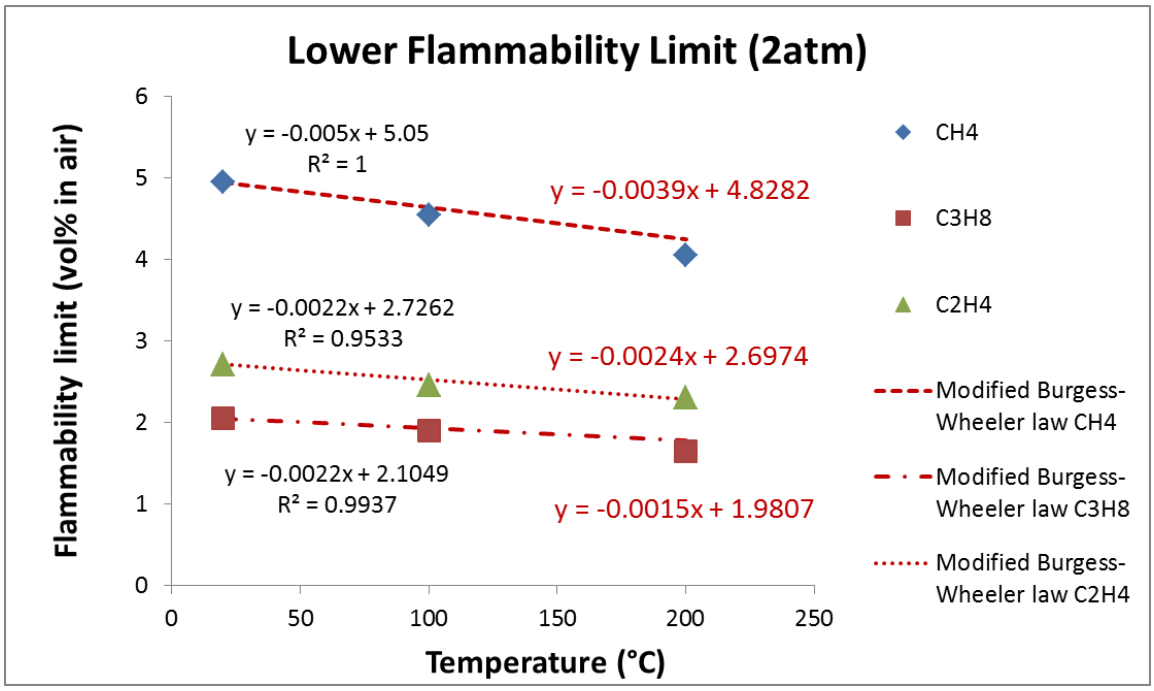

Figure 52 Comparison of experimentally measured LFL of methane, propane, ethylene at 2atm and their best linear fitting vs. the predicted LFL using modified Burgess Wheeler law

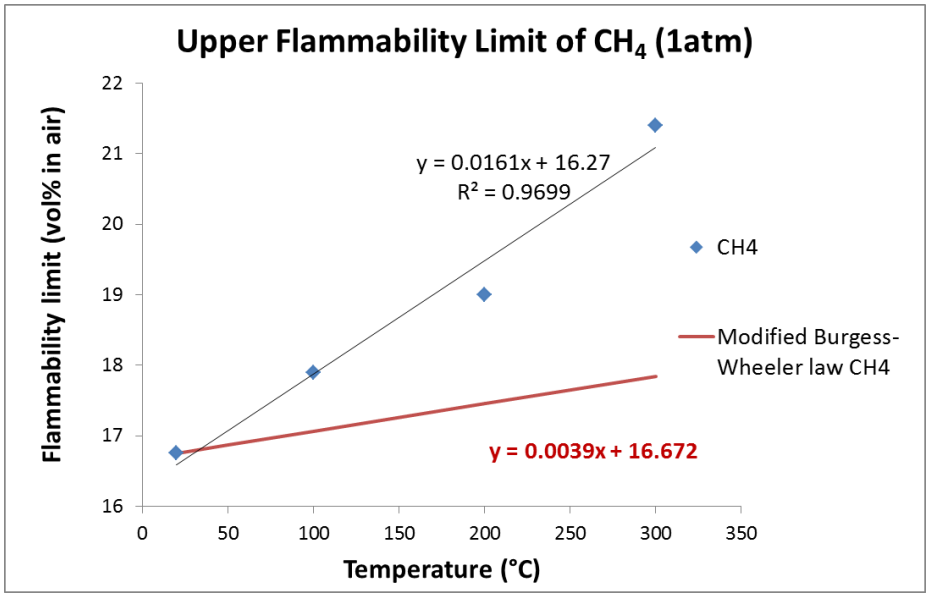

Figure 53 Comparison of experimentally measured methane UFL at 1atm and its best linear fitting vs. the predicted UFL using modified Burgess Wheeler law

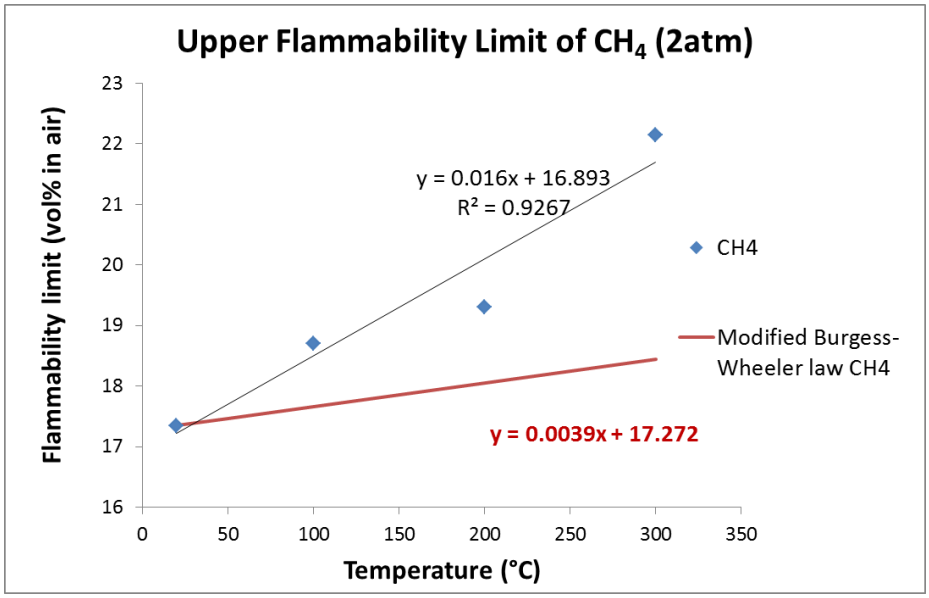

Figure 54 Comparison of experimentally measured methane UFL at 2atm and its best linear fitting vs. the predicted UFL using modified Burgess Wheeler law

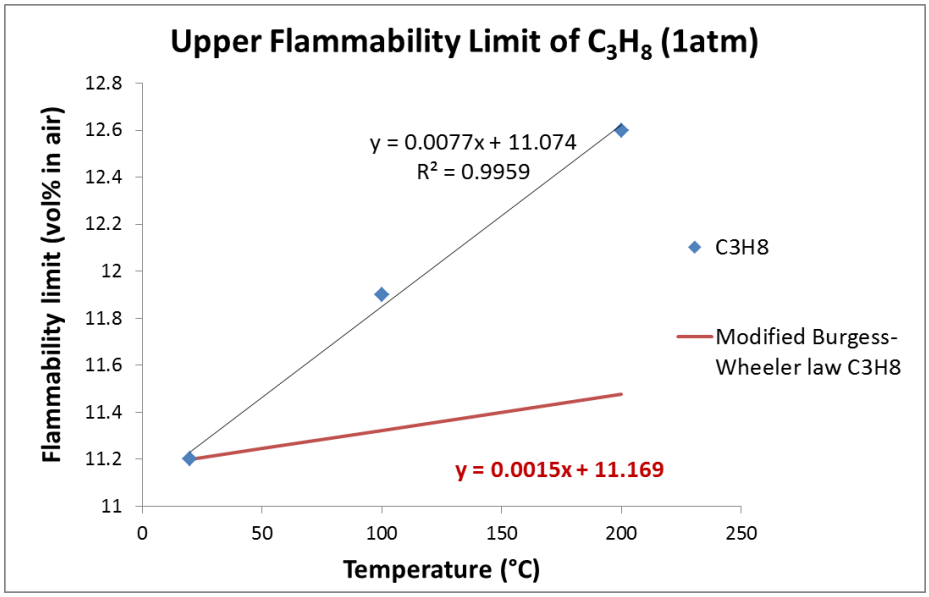

Figure 55 Comparison of experimentally measured propane UFL at 1atm and its best linear fitting vs. the predicted UFL using modified Burgess Wheeler law

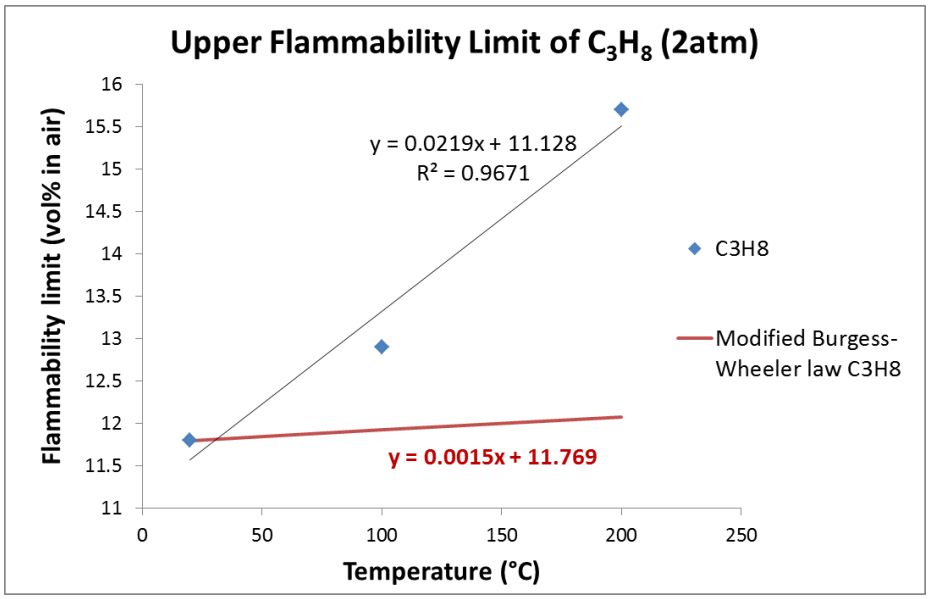

Figure 56 Comparison of experimentally measured propane UFL at 2atm and its best linear fitting vs. the predicted UFL using modified Burgess Wheeler law

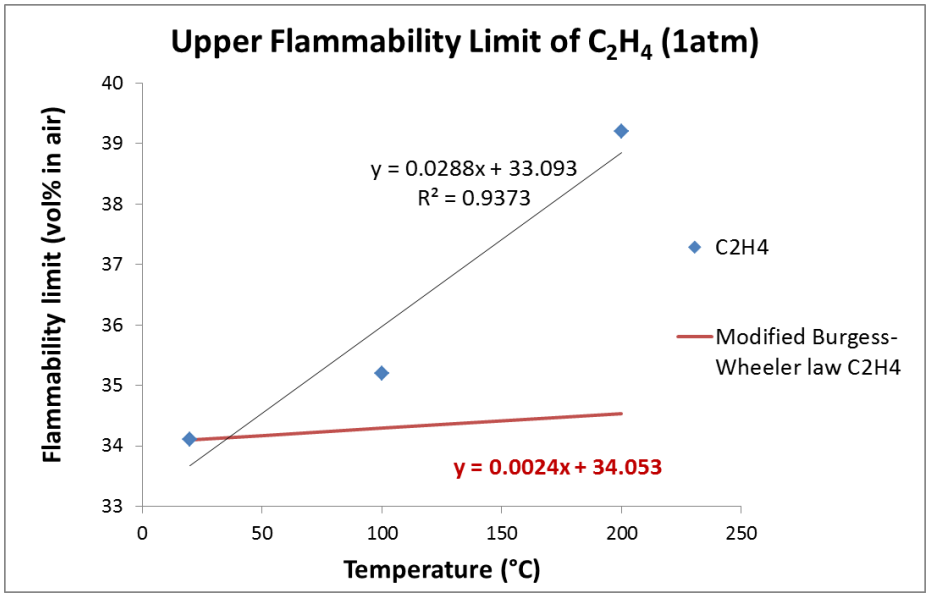

Figure 57 Comparison of experimentally measured ethylene UFL at 1atm and its best linear fitting vs. the predicted UFL using modified Burgess Wheeler law

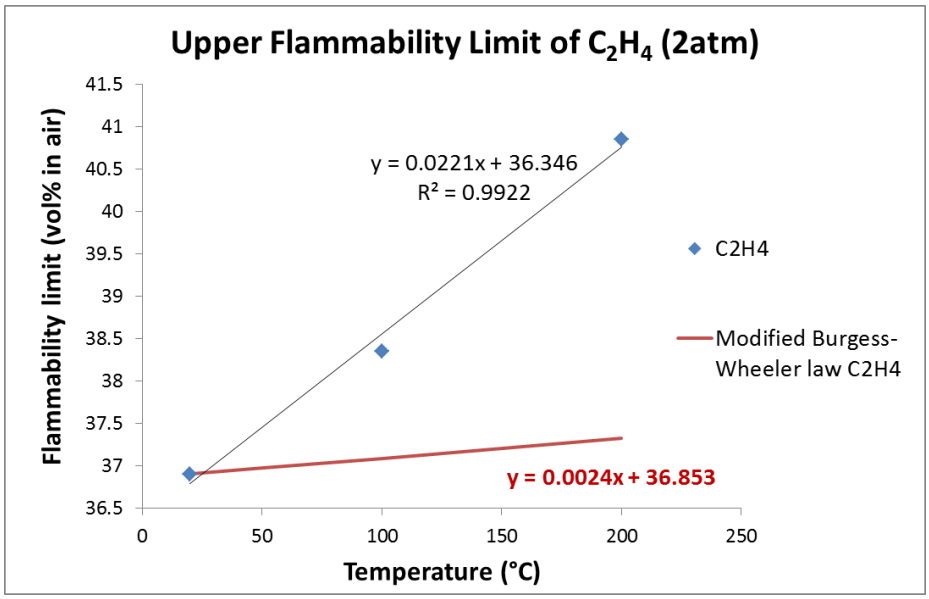

Figure 58 Comparison of experimentally measured ethylene UFL at 2atm and its best linear fitting vs. the predicted UFL using modified Burgess Wheeler law

As shown in Figure 51 and Figure 52, the best linear fitting of lower flammability experimental data are close to the modified Burgess Wheeler law and the difference between the experimental data and predictions are in a fairly acceptable range (±0.2 vol%). However, as shown in Figure 53 to Figure 58, the differences between the experimentally measured UFL value and predictions are significant for all three gas species. It is clear that for the flammability limit at elevated temperature, the modified Burgess Wheeler Law can give a fairly accurate prediction of lower flammability but will inevitably underestimate the upper flammability limit for pure component.

To find the appropriate coefficient c and α that can be used for the prediction of fuel flammability limit at elevated temperatures, experimental data are also fitted into the temperature dependence equation and the modified template of Burgess and Wheeler law as presented in Table 9 and Table 10.

Table 9 Parameters and coefficient to fit the straight line based on temperature dependence of pure substance LFL

Gas Species	Pressure (atm)	LFL (vol%)	c (×100 ℃$^{-1}$)	R^2	α
CH_4	1	4.75	-0.094	0.999	0.85
	2	4.95	-0.101	0.999	0.96
C_3H_8	1	1.95	-0.086	0.984	0.82
	2	2.05	-0.109	0.994	1.09
C_2H_4	1	2.65	-0.082	0.886	0.69
	2	2.71	-0.083	0.953	0.71

Table 10 Parameters and coefficient to fit the straight line based on temperature dependence of pure substance UFL

Gas Species	Pressure (atm)	UFL (vol%)	c (×100 ℃$^{-1}$)	R^2	α
CH_4	1	16.75	0.096	0.969	3.08
	2	17.35	0.0923	0.927	2.96
C_3H_8	1	11.2	0.0692	0.996	3.79
	2	11.8	0.1858	0.967	10.17
C_2H_4	1	34.1	0.0845	0.937	9.11
	2	36.9	0.0598	0.992	9.95

As indicated in Table 9 and Table 10, coefficient α calculated from fitted LFL lines are close to the value measured by Zabetakis (0.75) [3] while the values calculated from fitted UFL lines are not of the same magnitude. The main reason for the difference between coefficients α calculated from LFL and UFL is that the modified Burgess and Wheeler law are determined based on the net heat of combustion of the gases, which uses the assumption of complete oxidation of the gas. However, in the combustion process, complete oxidation would only occur during the LFL test. While in the UFL test, insufficient oxygen quantity, soot formation and decomposition of the gases would lead to incomplete combustion. Therefore, the modified Burgess and Wheeler law is not the perfect tool for the estimation of UFL dependence in temperature.

In all, for temperature dependence, it is confirmed that both LFL and UFL varies linearly with temperature rise. Temperature dependence coefficient c and calculated coefficient α are compared with previous literature which proves that the modified Burgess and Wheeler law only works with lower flammability limit and the temperature dependence coefficient is not a constant. The experimental data indicate that for temperature dependence of pure component, value of α also depends on the gas species and the test initial pressure.

5.4 Pressure effect on pure component

For pressure effect, generally it is understood that moderate changes in pressure do not affect the lower limits, but the upper limit increases significantly as the initial

pressure increases [6]. However, our experimental data show that as the initial pressure increases, both LFL and UFL increase. (Figure 59 to Figure 61)

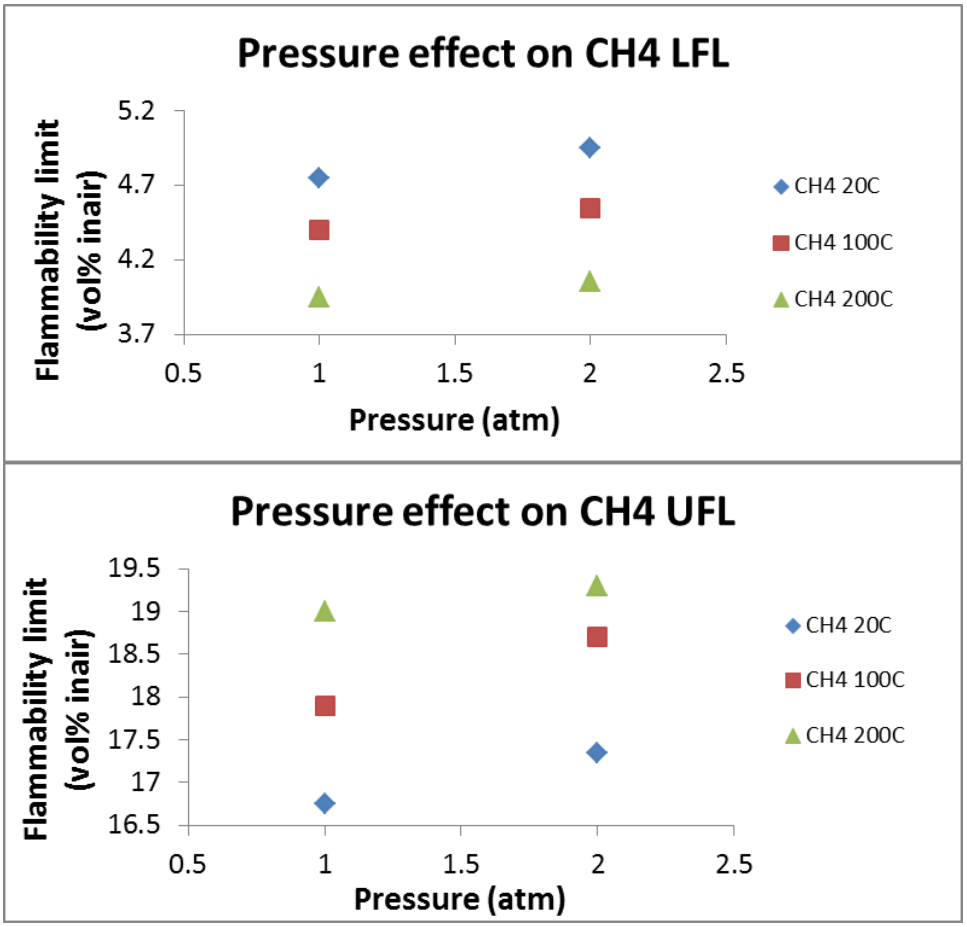

Figure 59 Methane flammability limit vs. pressure

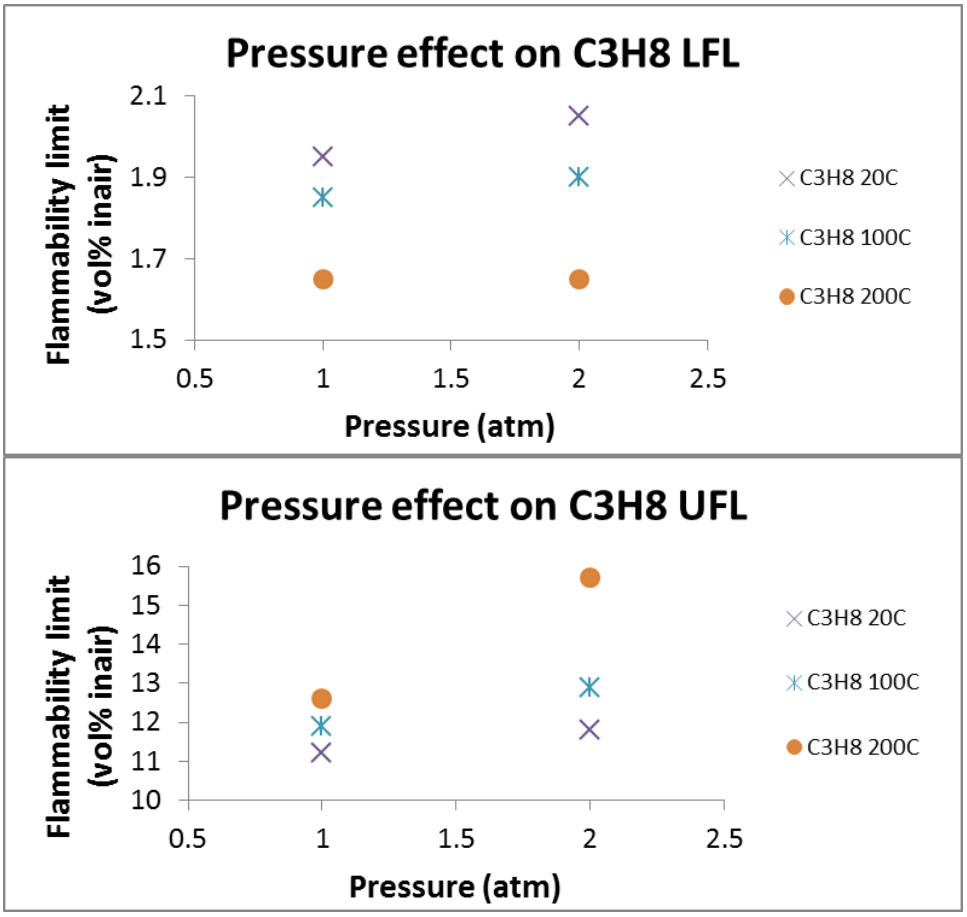

Figure 60 Propane flammability limit vs. pressure

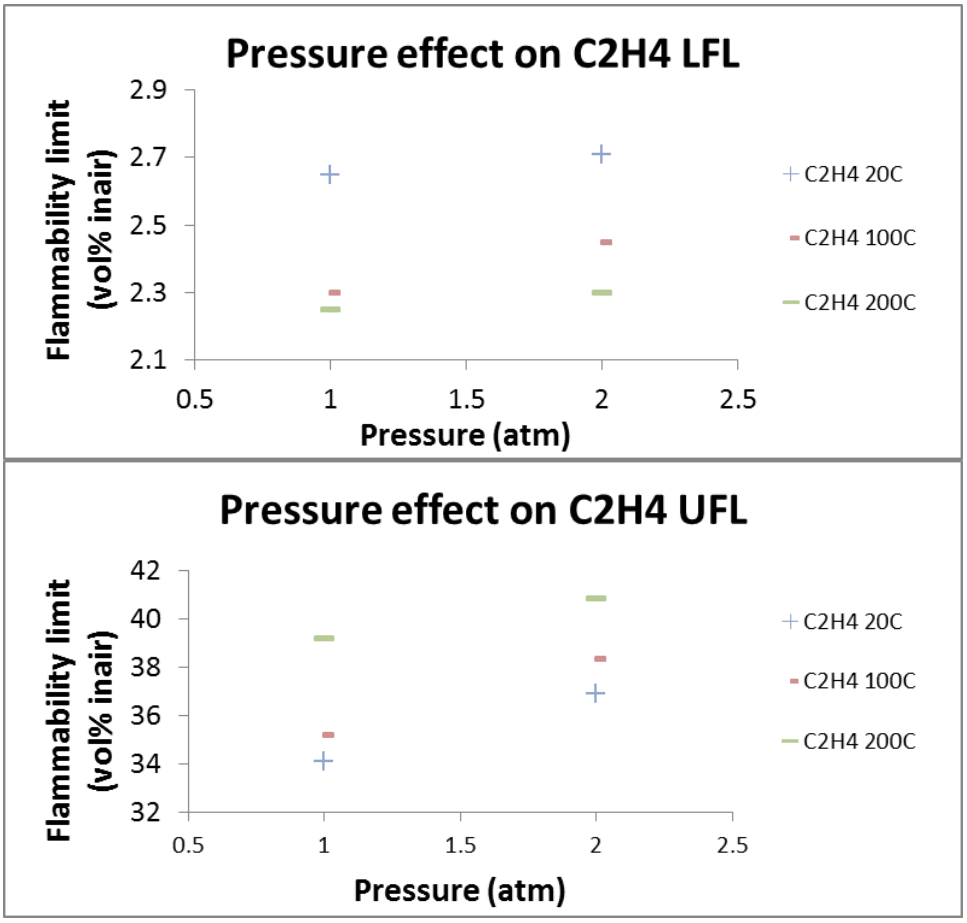

Figure 61 Ethylene flammability limit vs. pressure

Zabetakis [3] suggested an empirical expression for the upper limit, which shows that it varies linearly with the logarithm of the initial pressure, as shown in Equation 5,

$$UFL_P = UFL + 20.6(logP + 1) \quad (5)$$

where P is the pressure in megapascals absolute, UFL is the upper flammable limit for fuel in air at 1atm. Comparing with our experimental data, the predicted values are significantly higher (Figure 62).

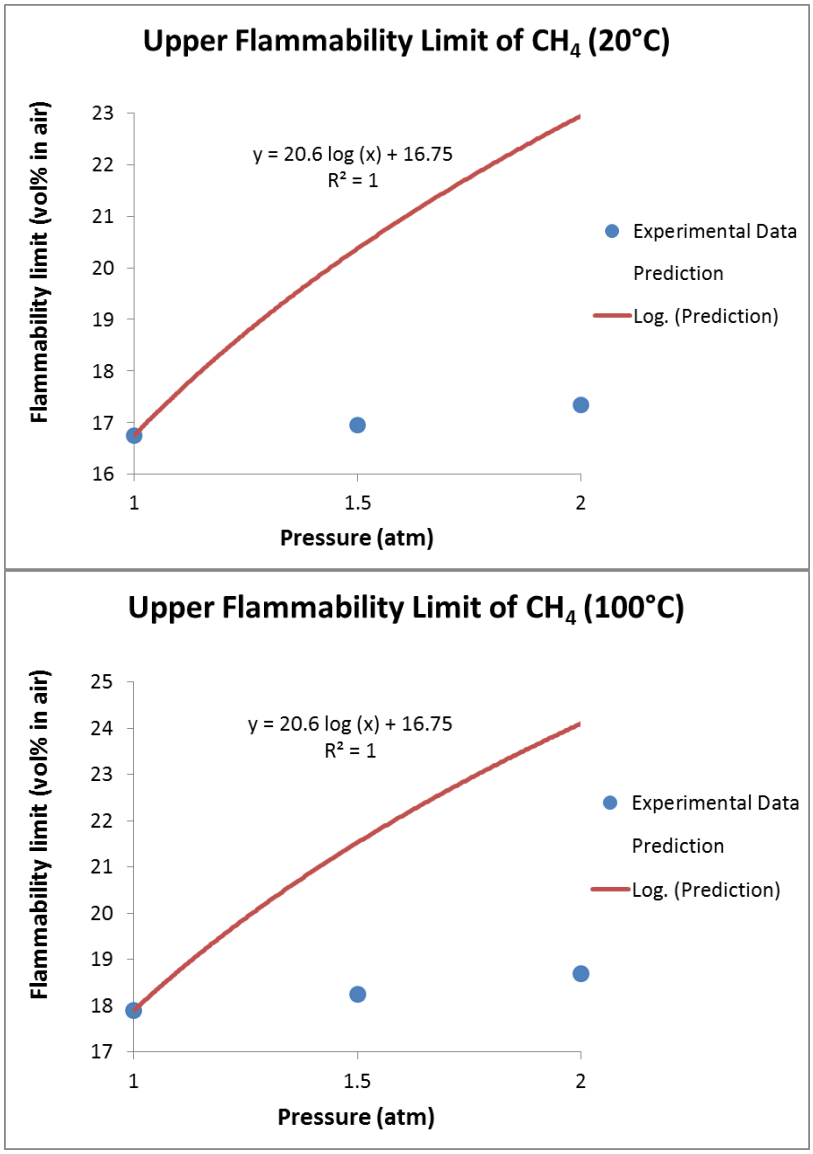

Figure 62 Comparison of methane experimental measured flammability with literature elevated pressure prediction

Though the empirical expression cannot be used to fit our experimental data, Figure 63 to Figure 65 show that the upper flammability limits are still directly

proportional to the logarithm of the initial pressure and the empirical relation can be extended to lower flammability limit estimation but with a different coefficient.

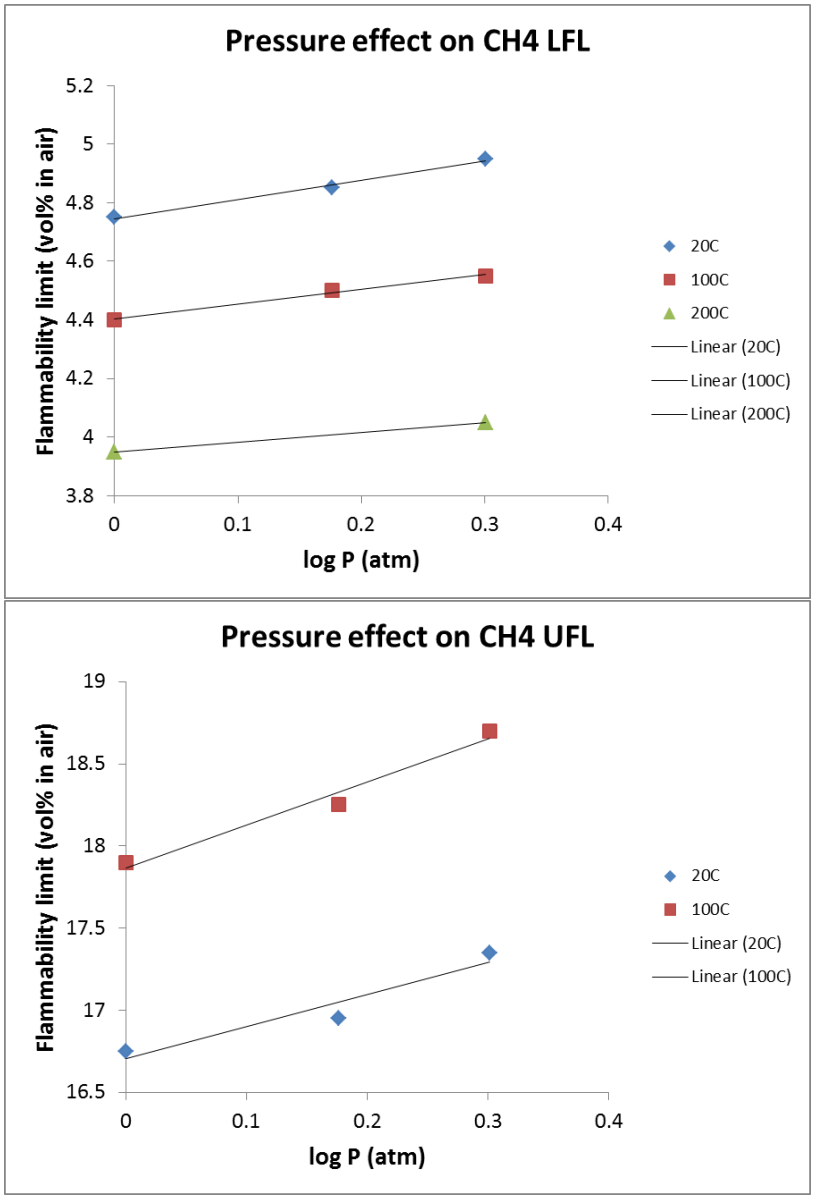

Figure 63 Flammability limits of methane vs. logarithm of the initial pressure

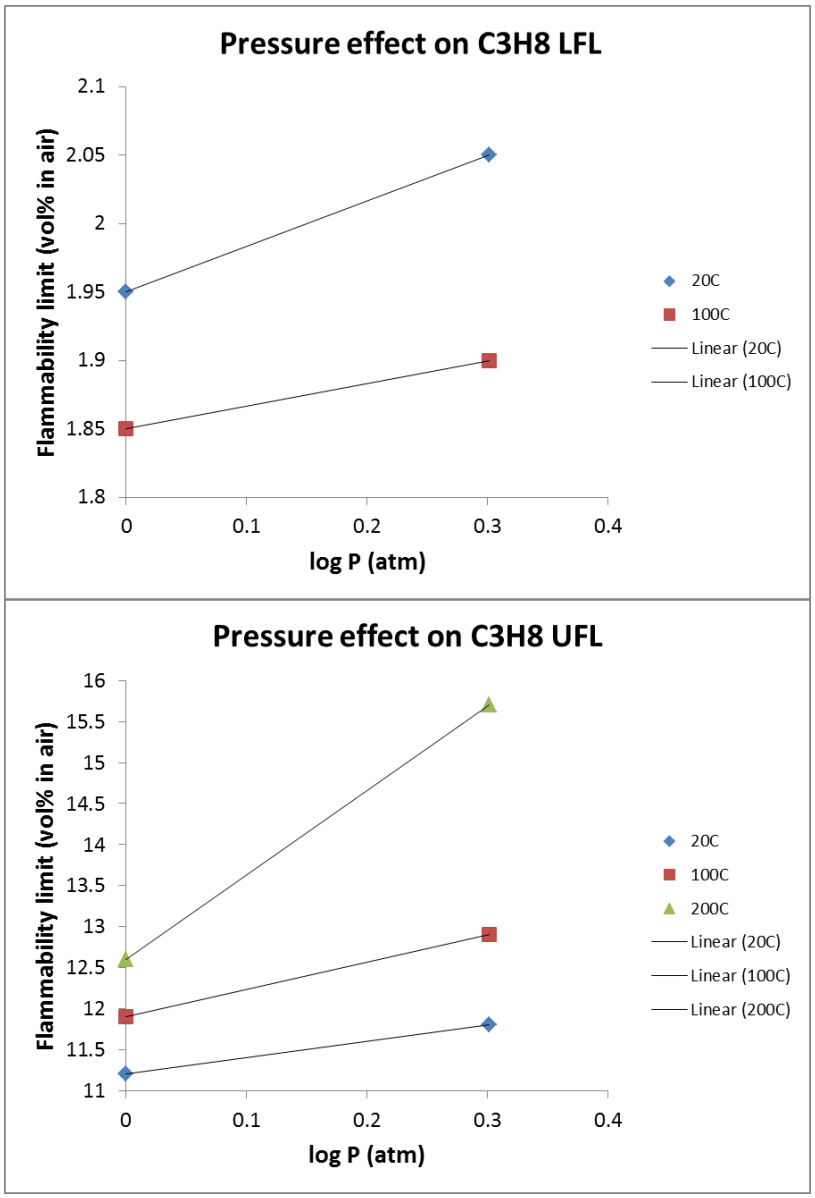

Figure 64 Flammability limits of propane vs. logarithm of the initial pressure

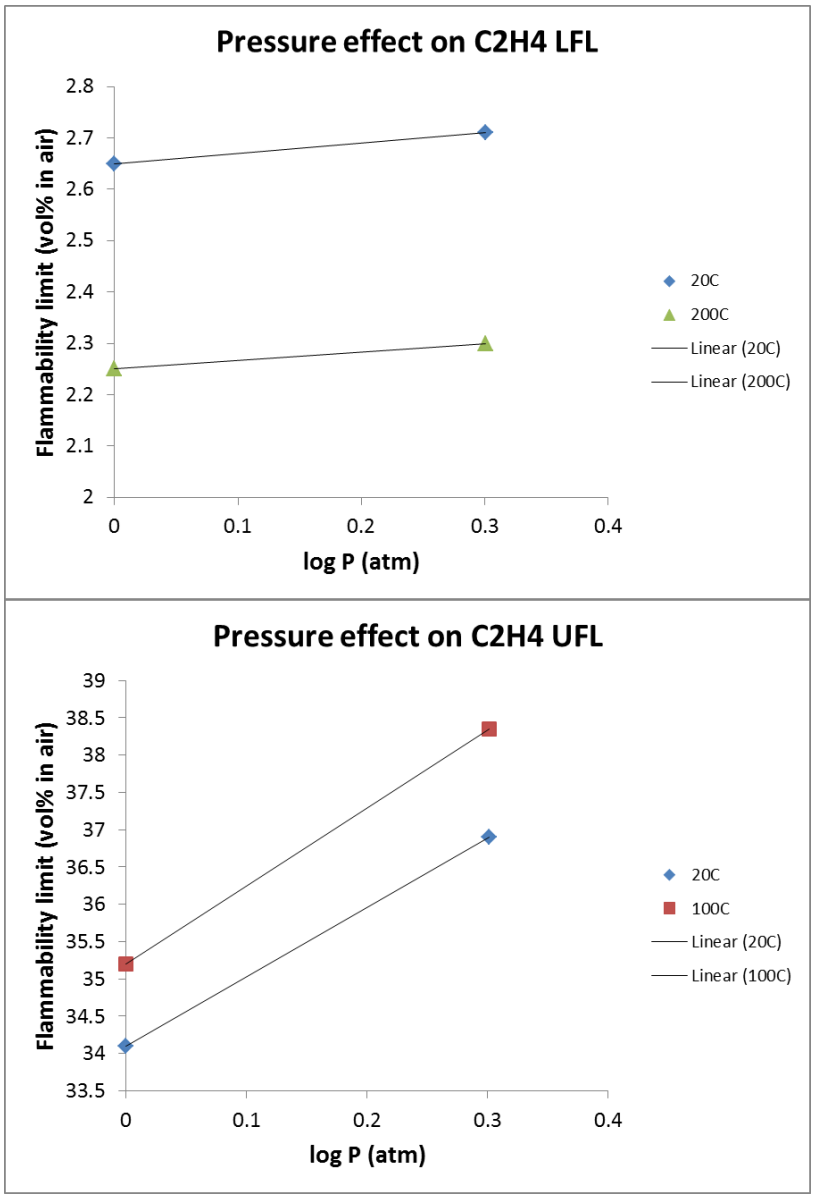

Figure 65 Flammability limits of ethylene vs. logarithm of the initial pressure

The coefficient of the flammability limit dependence on pressure, which is a function of temperature, also depends on the fuel species. The pressure effect on flammability limit can be rewritten as (Equation 17):

$$FL_P = \beta \times \log P + FL \quad (17)$$

where P is the pressure in atm, FL is the flammable limit for fuel in air at 1atm and β is the pressure dependence coefficient. As indicated in Figure 66, Figure 67 and Figure 68, the pressure dependence coefficient that can be used to estimate the pressure effect on the fuel is a function of temperature.

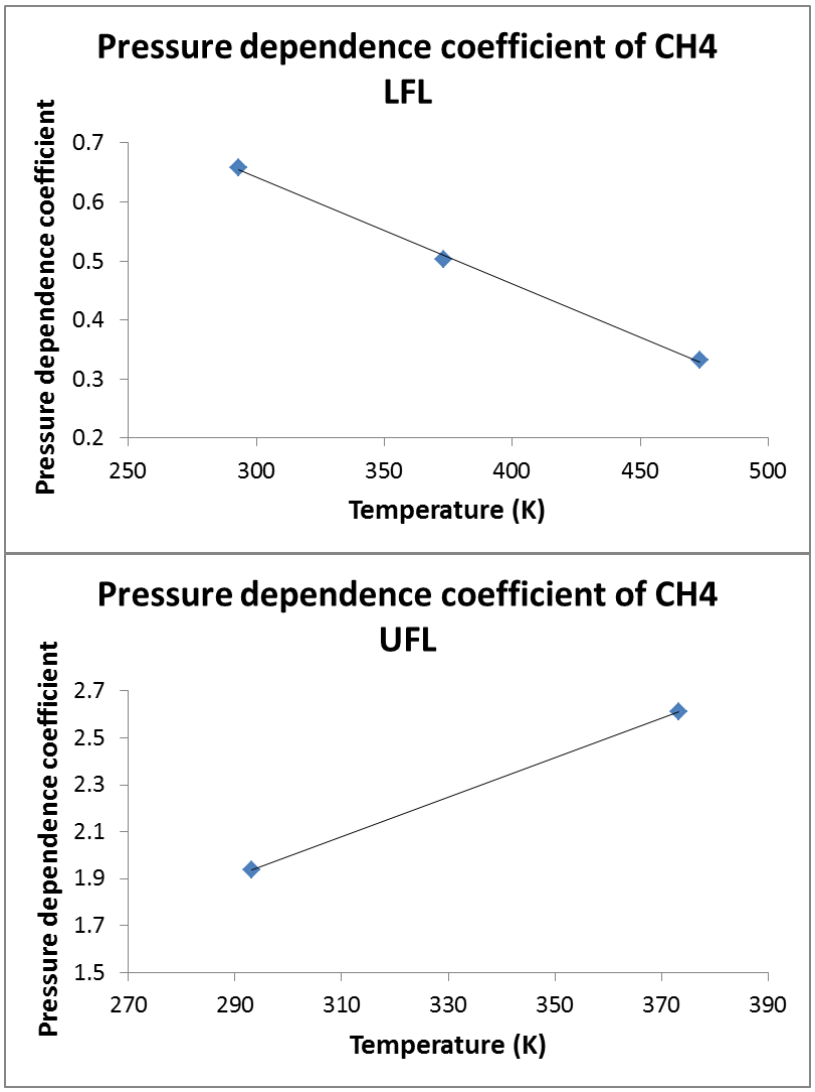

Figure 66 Methane pressure dependence coefficient vs. Temperature

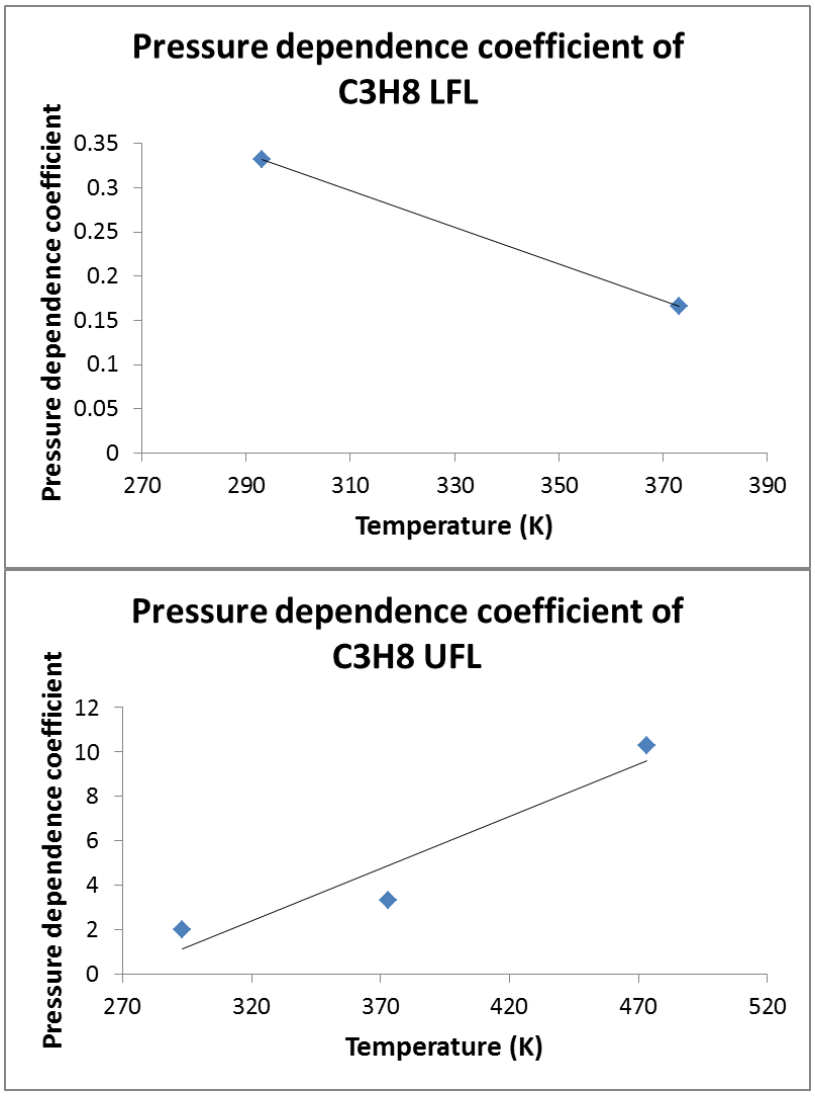

Figure 67 Propane pressure dependence coefficient vs. Temperature

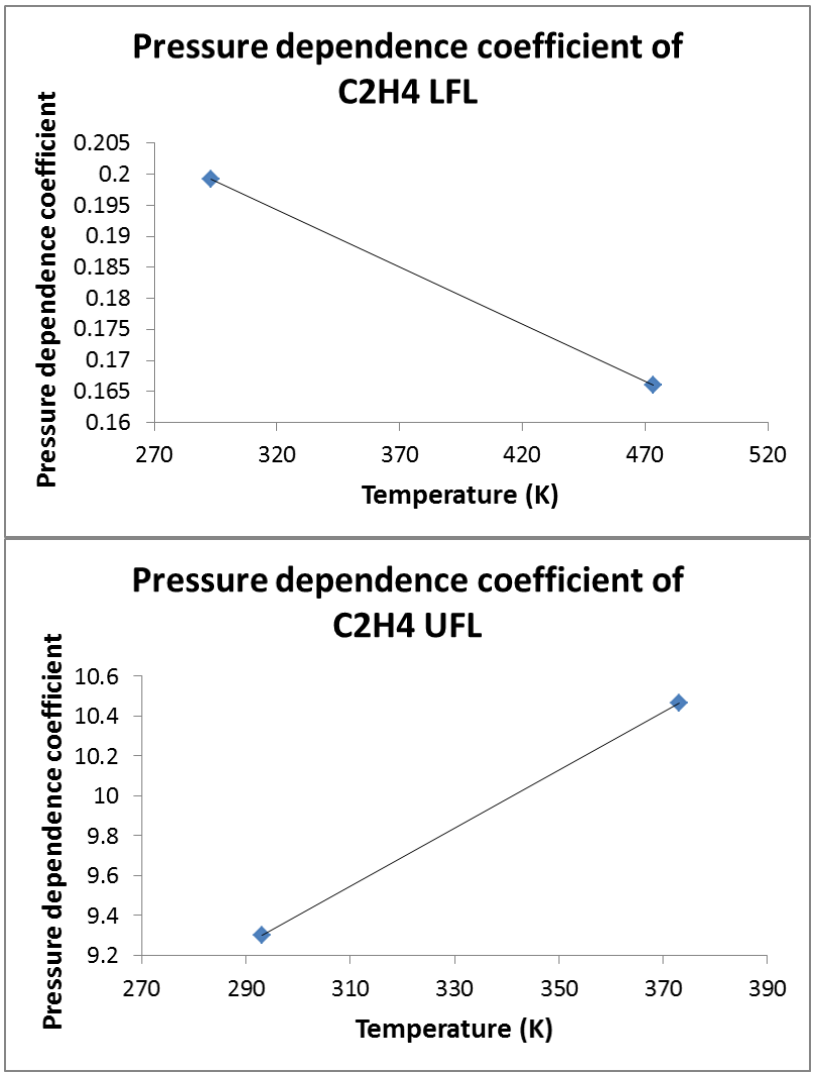

Figure 68 Ethylene pressure dependence coefficient vs. Temperature

5.5 Prediction of pure component flammability limit at elevated condition

With the investigation of temperature effect, pressure effect on each gas species, the flammability limit of fuel at elevated conditions can be estimated using standard condition (20 ℃, 1atm) flammable limit value through equation 18:

$$FL(T,P) = \beta \times \log P + FL(T, 1atm) \quad (18)$$

where T is temperature in °C, β is a function of temperature (Equation 19):

$$\beta = b \times (T + 273.15) + d \quad (19)$$

and the coefficient b and coefficient d is a best fitted number based on pressure dependence coefficient relation with temperature as shown in Table 11.

Table 11 Coefficient for elevated condition flammable limit calculation

Gas Species	Type	Standard FL (vol%)	c (×100 ℃$^{-1}$)	b	d
CH_4	LFL	4.75	-0.094	-0.0018	1.1838
	UFL	16.75	0.096	0.0085	-0.5428
C_3H_8	LFL	1.95	-0.086	-0.0021	0.9409
	UFL	11.2	0.0692	0.0471	-12.687
C_2H_4	LFL	2.65	-0.082	-0.002	0.2534
	UFL	34.1	0.0845	0.0145	5.0412

After taking the temperature effect into consideration, the final equation can be written as (Equation 20):

$$FL\ (T, P) = \beta \times \log P + FL(T_0, P_0) \times [1 + c \times (T - T_0)] \quad (20)$$

where the $FL(T_0,P_0)$ is the flammability limit of fuel at standard condition (20 ℃, 1atm). Comparing the predicted flammable limit with experimental data, the prediction method can give estimation with error less than 3% (Table 12). The yield percentage in Table 12

refers to the percentage difference between experimental measured results and predictions using equation 20.

However, equations 18, 19, 20 and the coefficient in Table 11 are calculated according to the temperature effect and pressure effect study in this work. Therefore, the correlations between flammability limit at elevated conditions and flammability limit at normal condition only work for methane, propane and ethylene with limited reaction condition (temperature: ambient to 300 ℃, pressure: 1~2atm), but may not be suitable for other light hydrocarbons. Also, the usage of equation 18 and equation 20 requires at least experimental measured results of light hydrocarbons at normal conditions.

Table 12 Comparison of experimental data and predictions of fuel flammability at elevated conditions

Conditions			Predicted FL	Experimental Data	Yield percentage (%)
Fuel species	P (atm)	T (℃)			
CH4 LFL	1	20	4.75	4.75	0
	1	50	4.62	4.6	0.35
	1	100	4.39	4.4	0.16
	1	200	3.95	3.95	0.09
	1	300	3.5	3.5	0.01
	1.5	20	4.87	4.85	0.32
	1.5	100	4.48	4.5	0.38
	2	20	4.95	4.95	0.05
	2	100	4.55	4.55	0.07
	2	200	4.05	4.05	0.09
CH4 UFL	1	20	16.75	16.75	0
	1	100	18.04	17.9	0.76
	1	200	19.64	19	3.39
	1	300	21.25	21.4	0.69
	1.5	20	17.09	16.95	0.84

Table 12 Continued

Conditions			Predicted FL	Experimental Data	Yield percentage (%)
Fuel species	P (atm)	T (℃)			
CH4 UFL	1.5	100	18.5	18.25	1.37
	2	20	17.34	17.35	0.08
	2	100	18.83	18.7	0.68
	2	300	22.56	22.15	1.83
C3H8 LFL	1	20	1.95	1.95	0
	1	100	1.82	1.85	1.85
	1	200	1.65	1.65	0.11
	2	20	2.05	2.05	0.1
	2	100	1.86	1.9	1.94
	2	200	1.63	1.65	1.07
C3H8 UFL	1	20	11.2	11.2	0
	1	100	11.82	11.9	0.672
	1	200	12.6	12.6	0.04
	2	20	11.54	11.8	2.23
	2	100	13.29	12.9	3.04
	2	200	15.48	15.7	1.37

Table 12 Continued

Conditions			Predicted FL	Experimental Data	Yield percentage (%)
Fuel species	P (atm)	T (℃)			
C2H4 LFL	1	20	2.65	2.65	0
	1	100	2.48	2.35	5.37
	1	200	2.26	2.25	0.39
	2	20	2.71	2.71	0.05
	2	100	2.53	2.45	3.26
	2	200	2.31	2.3	0.29
C2H4 UFL	1	20	34.1	34.1	0
	1	100	35.99	35.2	2.24
	1	200	38.35	39.2	2.17
	2	20	36.9	36.9	0.01
	2	100	39.13	38.35	2.04
	2	200	41.93	40.85	2.64

6. FLAMMABILITY LIMITS OF BINARY MIXTURES

As stated in the introduction part, one of the primary objectives of this research is to measure the flammability limits of hydrocarbon mixtures and compare the experimental value with predictions from estimation methods such as Le Chatelier's rule so that mixture rules can be validated at elevated conditions. With the determined quantitative flammability criterion, the flammability experiments have been extended to binary mixtures of methane (CH_4), propane (C_3H_8) and ethylene (C_2H_4). These gas species are selected as the samples of saturated and unsaturated light hydrocarbons and due to their unique molecules structures, the combustion process of these gases could possibly involve the breaking of C-H bond, C-C bond and C=C bond. Mixture ratios of each two gases are controlled as 30:70, 50:50 and 80:20 to represent the flammability limit of binary hydrocarbon mixtures. The initial test conditions are selected as 1atm/20 ℃, 2atm/20 ℃, 1atm/200 ℃, and 2atm/200 °C to show the flammability properties at normal condition, increased pressure, increased temperature and elevated condition.

6.1 Experimental results of binary mixtures

The experimental flammability limit of mixture 1 (methane and propane), mixture 2 (methane and ethylene), mixture 3 (propane and ethylene) are plotted in Figure 69-92 and compared with predictions of Le Chatelier's rule. Measurement error of the flammability limit is ±0.05 for LFL test and ±0.1 for UFL test (not shown in the figures).

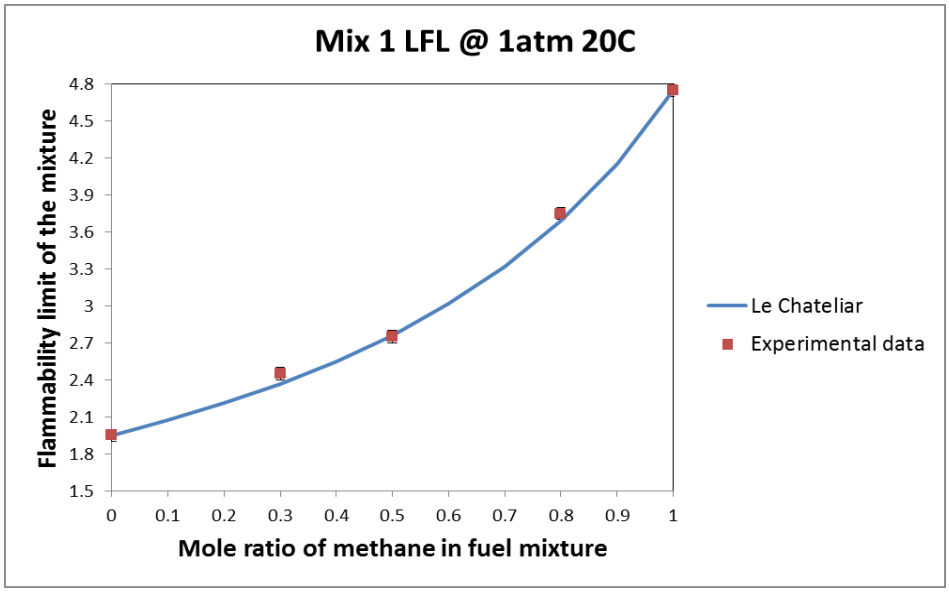

Figure 69 Lower flammability limit of methane (30%, 50%, 80%) and propane mixture at 1atm 20 °C

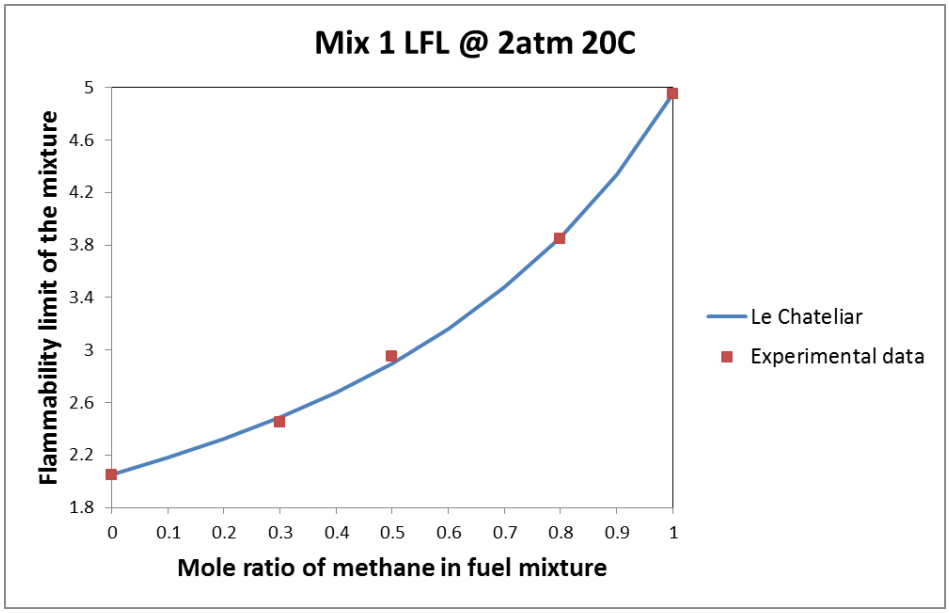

Figure 70 Lower flammability limit of methane (30%, 50%, 80%) and propane mixture at 2atm 20 °C

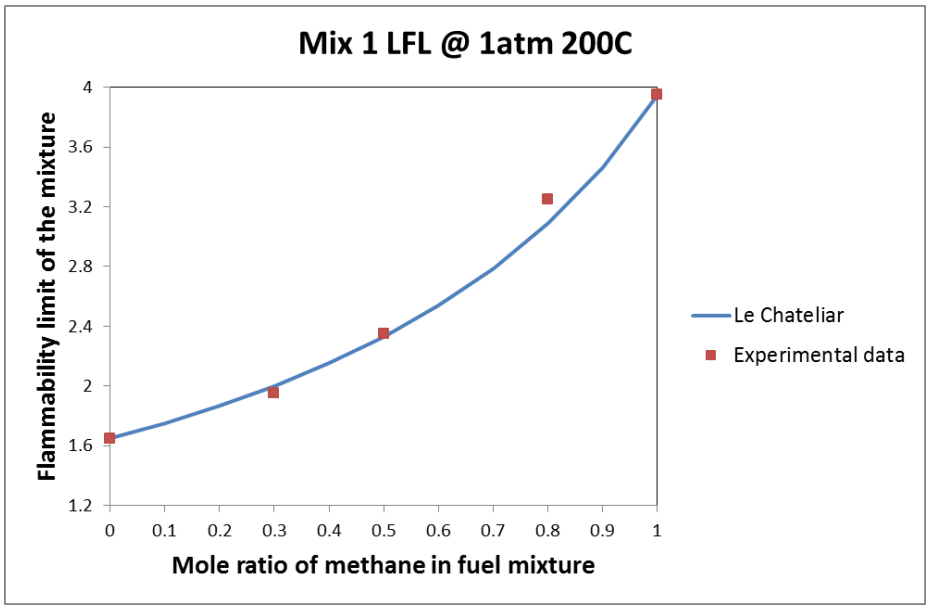

Figure 71 Lower flammability limit of methane (30%, 50%, 80%) and propane mixture at 1atm 200 °C

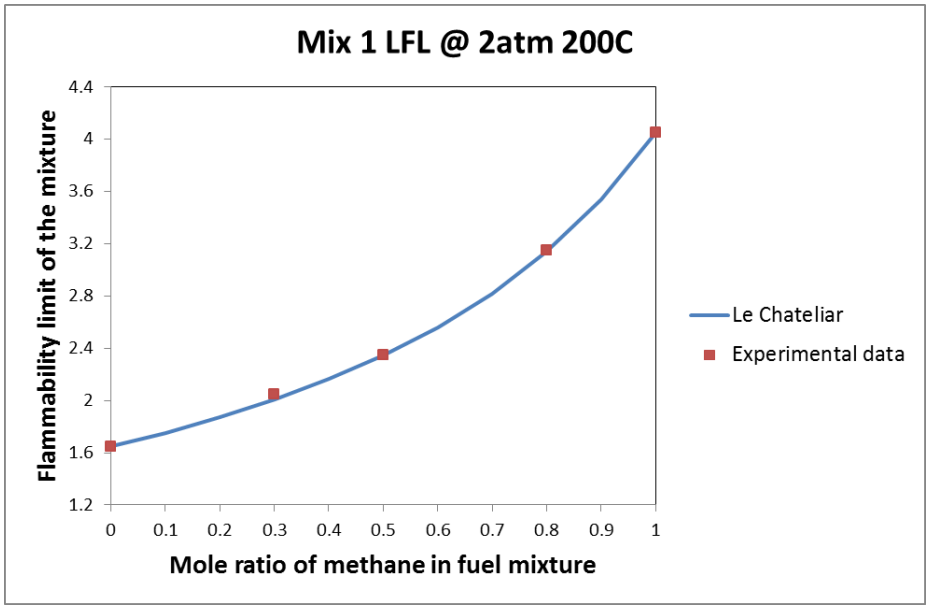

Figure 72 Lower flammability limit of methane (30%, 50%, 80%) and propane mixture at 2atm 200 °C

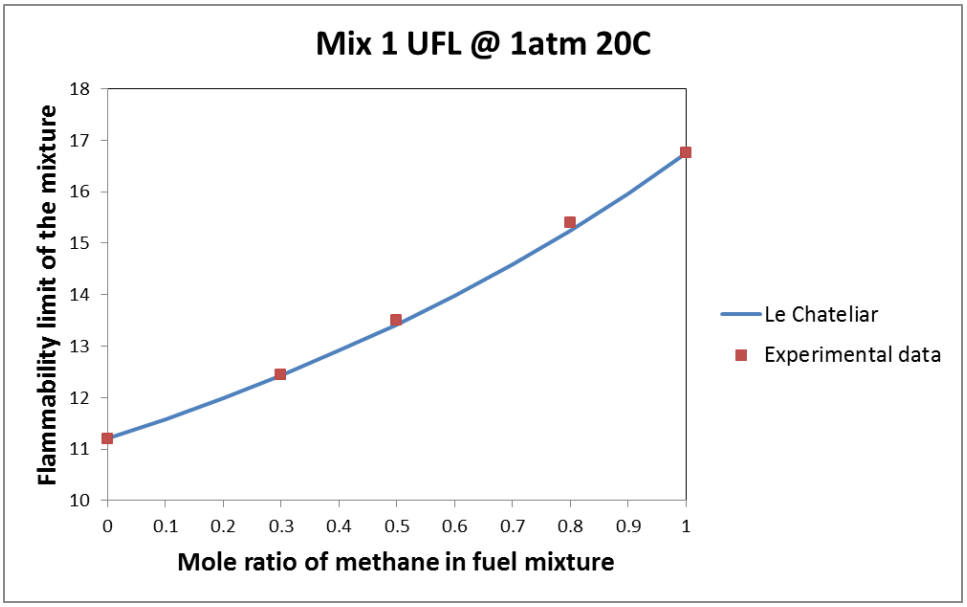

Figure 73 Upper flammability limit of methane (30%, 50%, 80%) and propane mixture at 1atm 20 °C

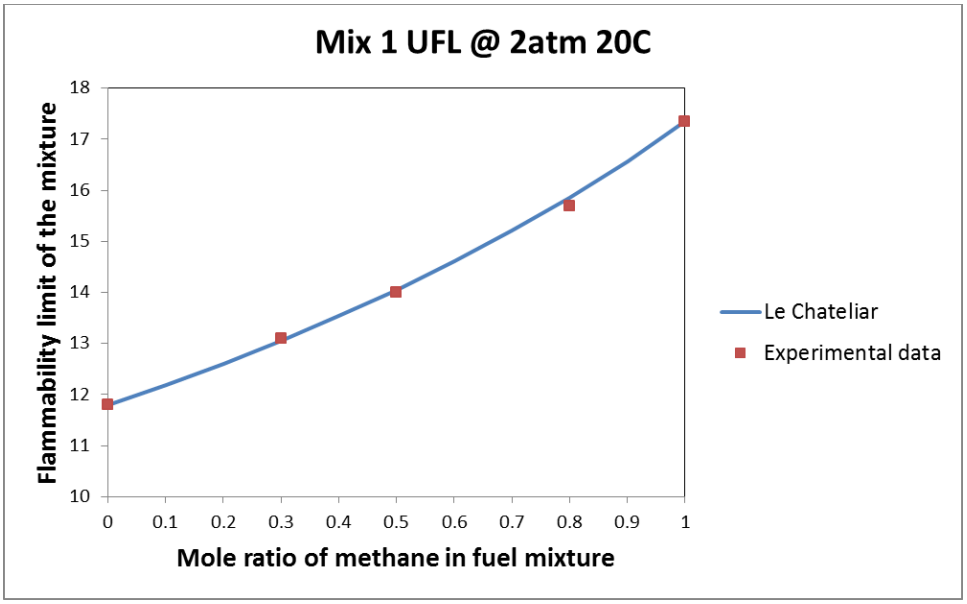

Figure 74 Upper flammability limit of methane (30%, 50%, 80%) and propane mixture at 2atm 20 °C

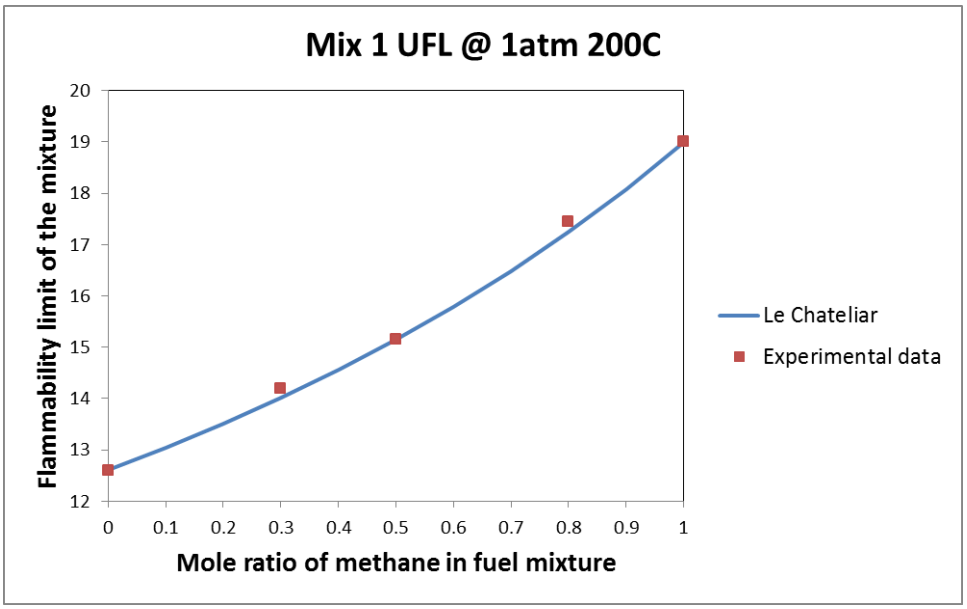

Figure 75 Upper flammability limit of methane (30%, 50%, 80%) and propane mixture at 1atm 200 °C

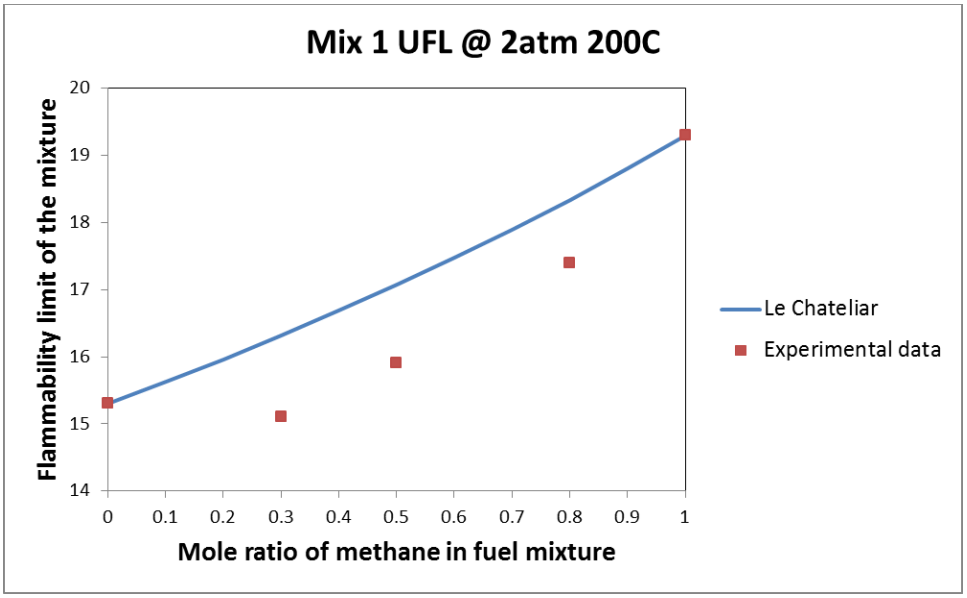

Figure 76 Upper flammability limit of methane (30%, 50%, 80%) and propane mixture at 2atm 200 °C

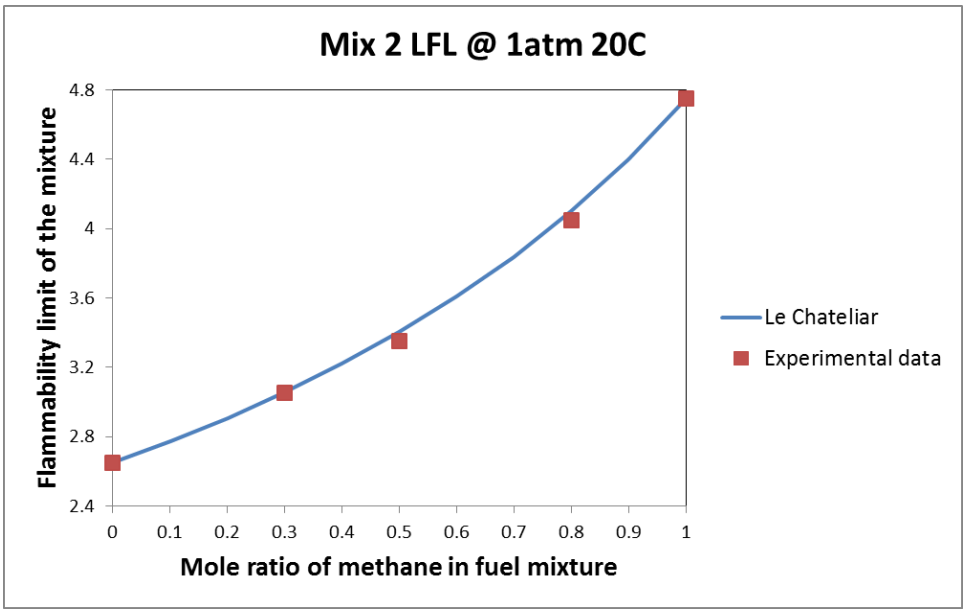

Figure 77 Lower flammability limit of methane (30%, 50%, 80%) and ethylene mixture at 1atm 20 °C

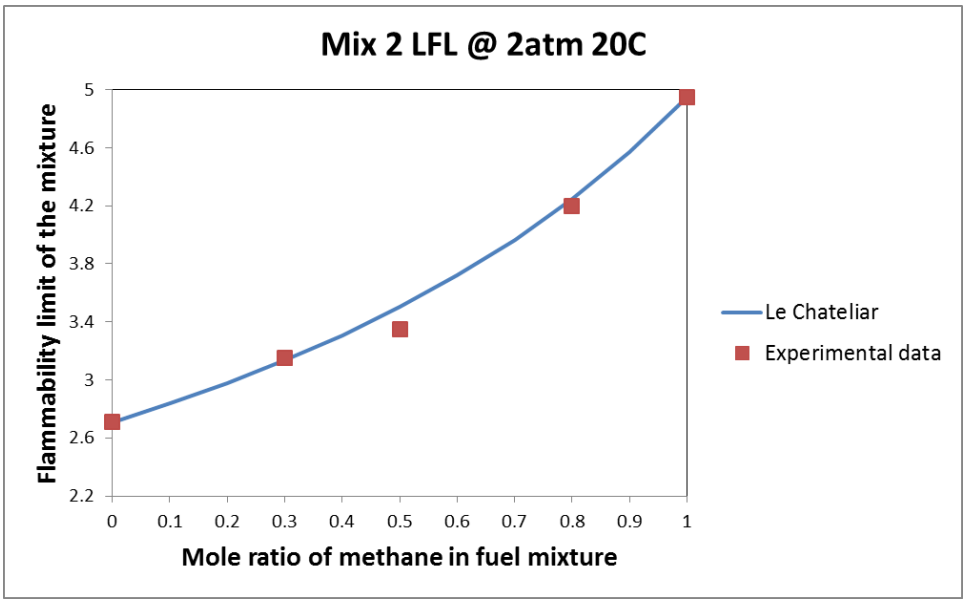

Figure 78 Lower flammability limit of methane (30%, 50%, 80%) and ethylene mixture at 2atm 20 °C

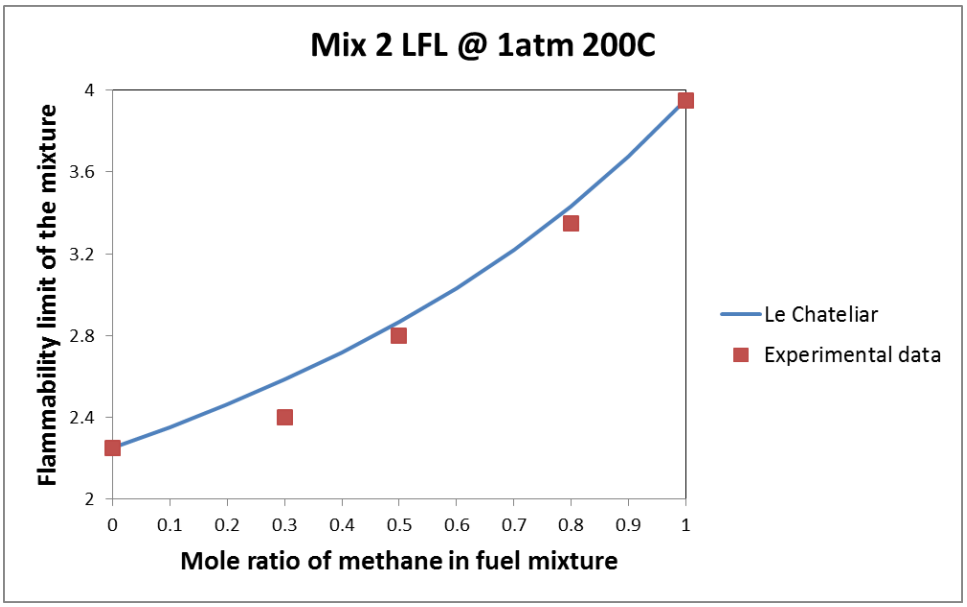

Figure 79 Lower flammability limit of methane (30%, 50%, 80%) and ethylene mixture at 1atm 200 °C

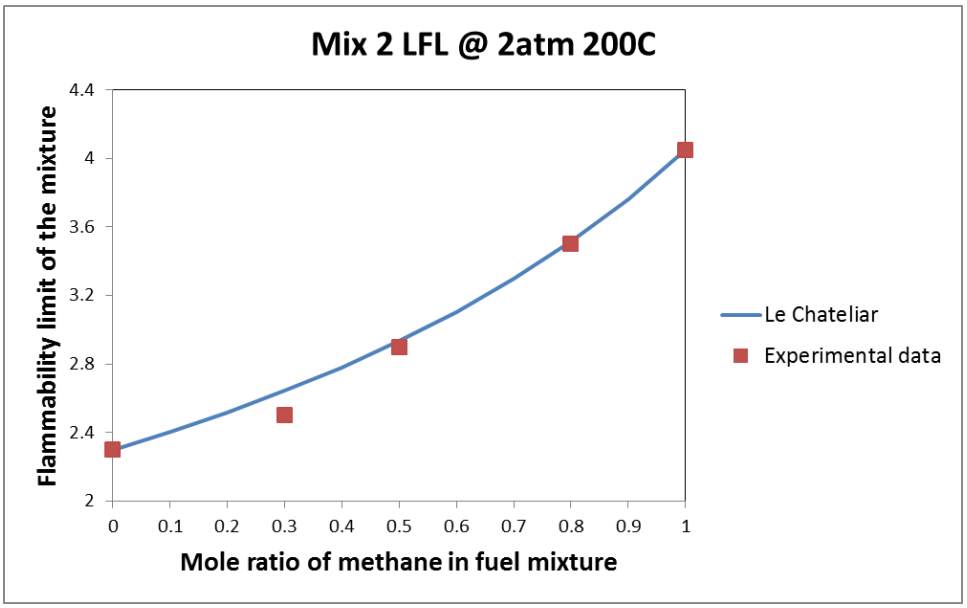

Figure 80 Lower flammability limit of methane (30%, 50%, 80%) and ethylene mixture at 2atm 200 °C

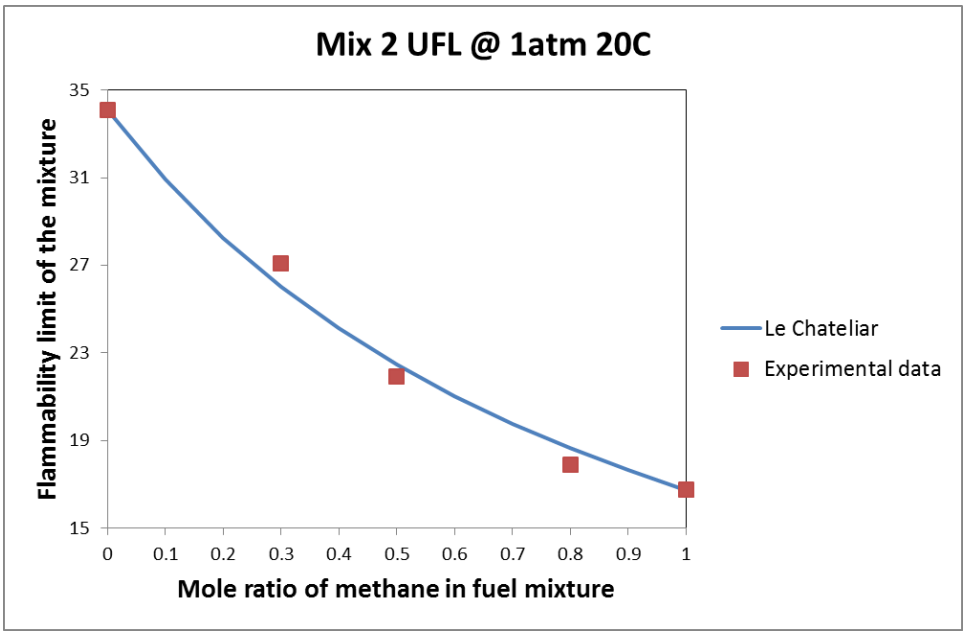

Figure 81 Upper flammability limit of methane (30%, 50%, 80%) and ethylene mixture at 1atm 20 °C

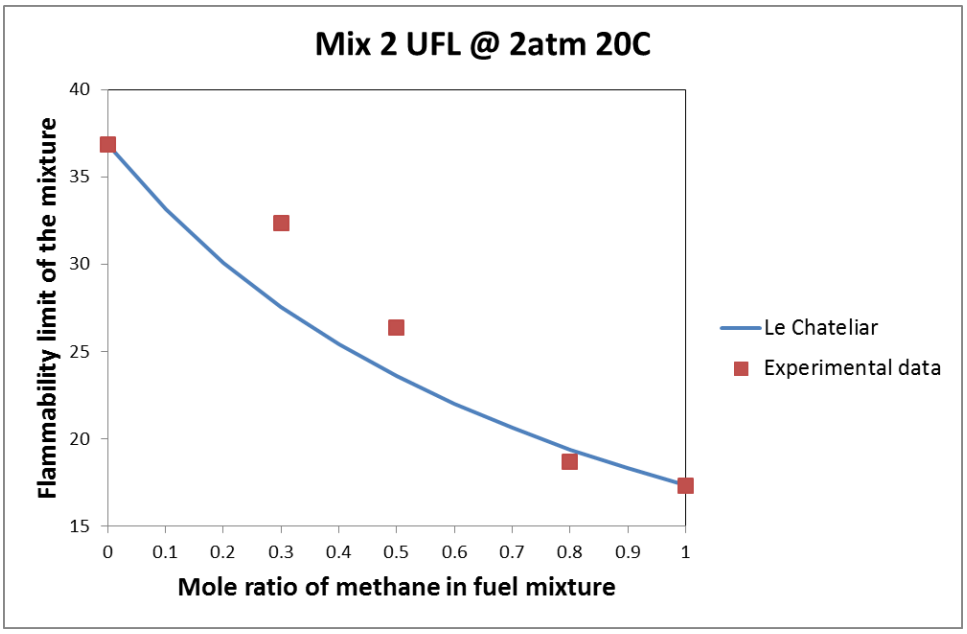

Figure 82 Upper flammability limit of methane (30%, 50%, 80%) and ethylene mixture at 2atm 20 °C

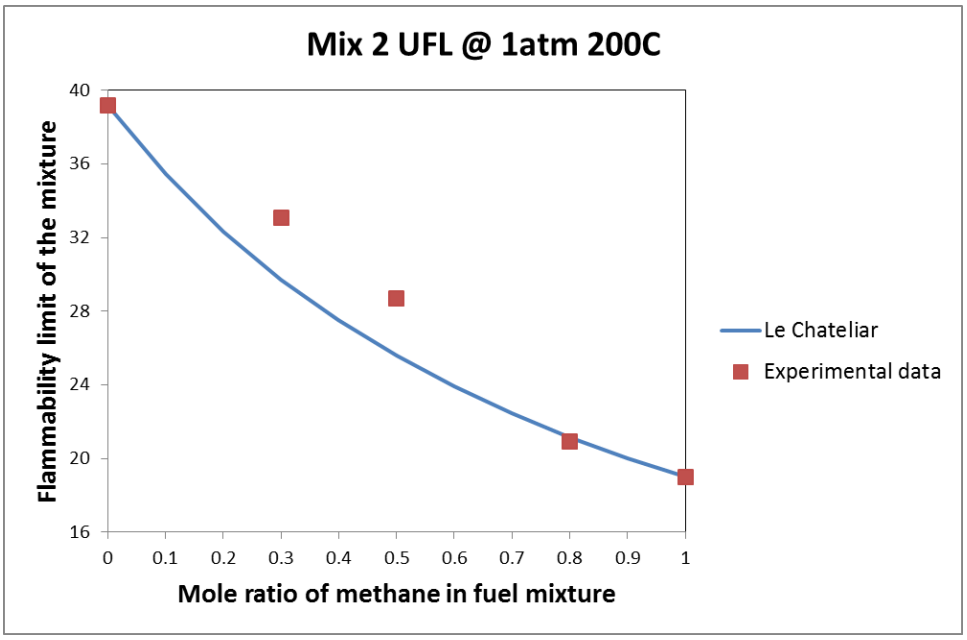

Figure 83 Upper flammability limit of methane (30%, 50%, 80%) and ethylene mixture at 1atm 200 °C

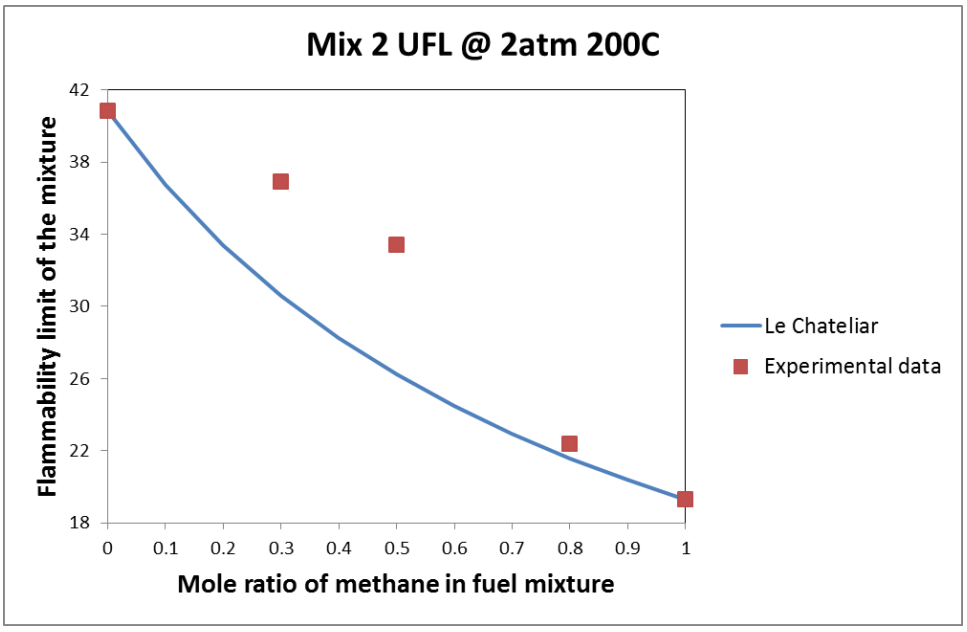

Figure 84 Upper flammability limit of methane (30%, 50%, 80%) and ethylene mixture at 2atm 200 °C

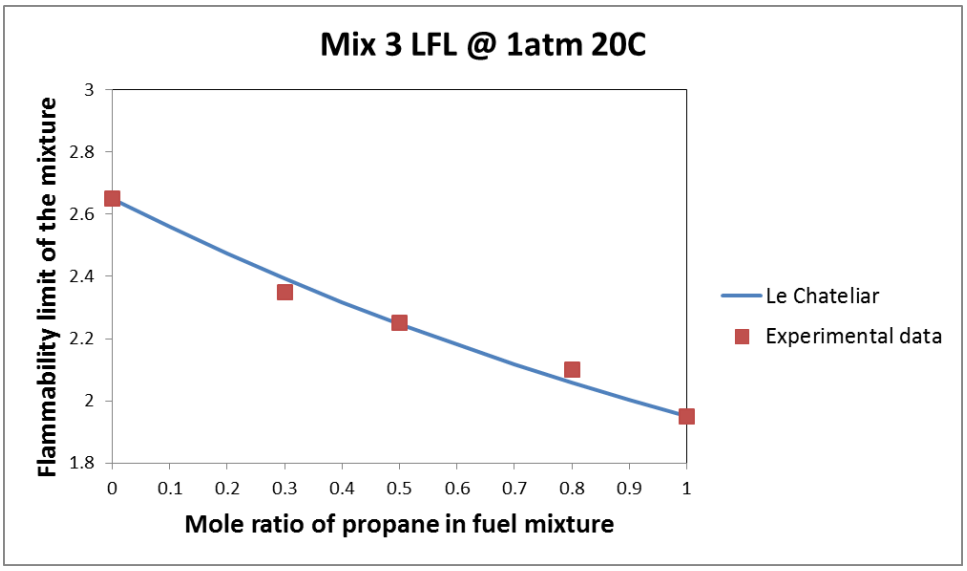

Figure 85 Lower flammability limit of propane (30%, 50%, 80%) and ethylene mixture at 1atm 20 °C

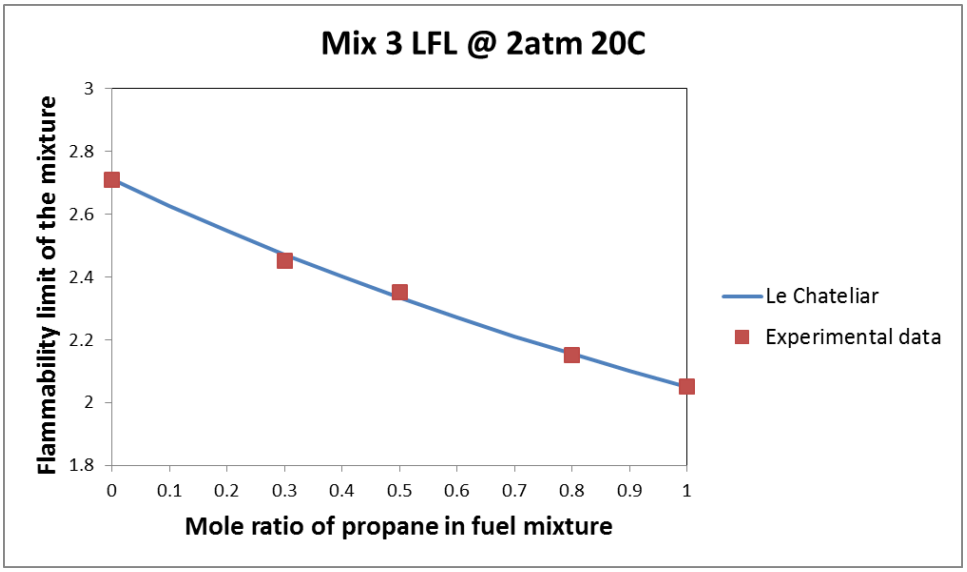

Figure 86 Lower flammability limit of propane (30%, 50%, 80%) and ethylene mixture at 2atm 20 °C

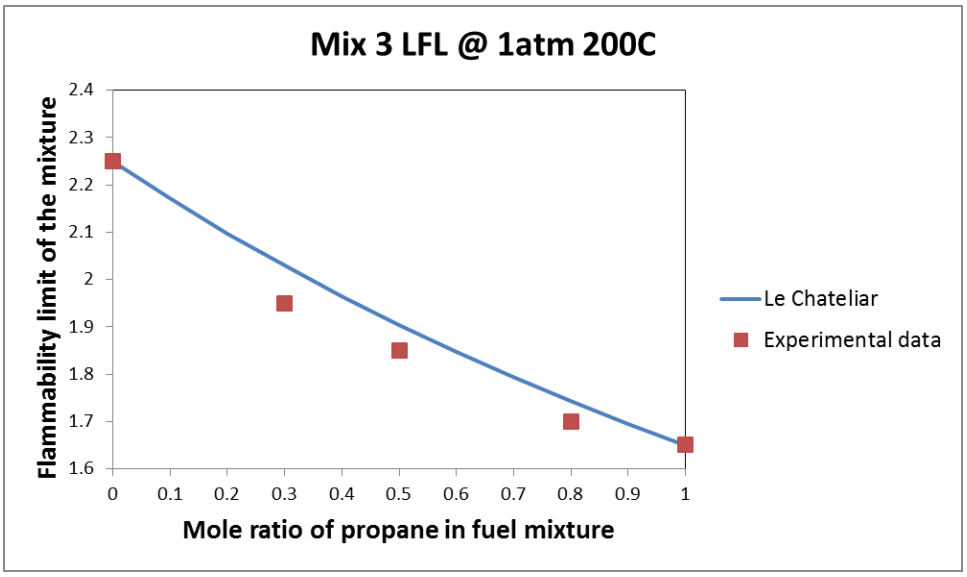

Figure 87 Lower flammability limit of propane (30%, 50%, 80%) and ethylene mixture at 1atm 200 °C

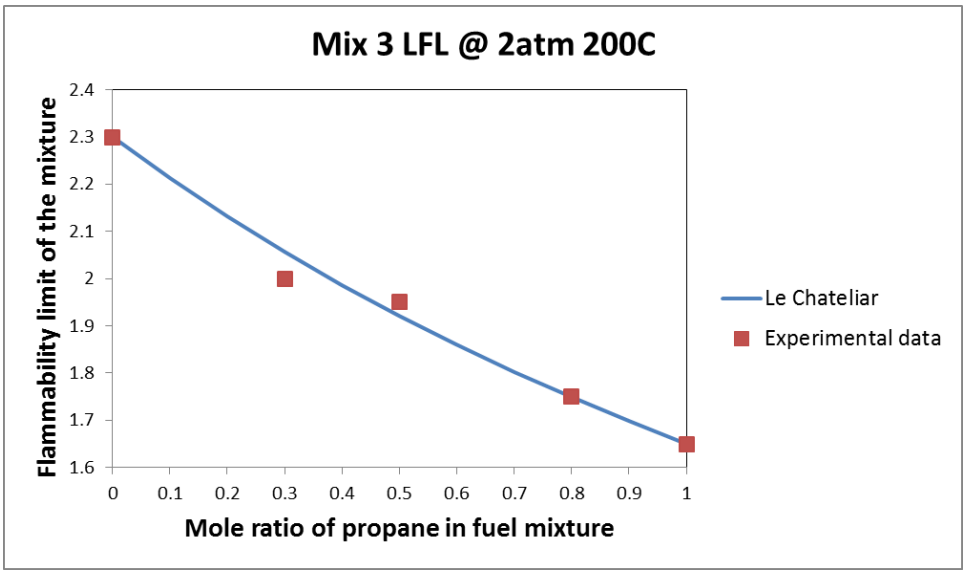

Figure 88 Lower flammability limit of propane (30%, 50%, 80%) and ethylene mixture at 2atm 200 °C

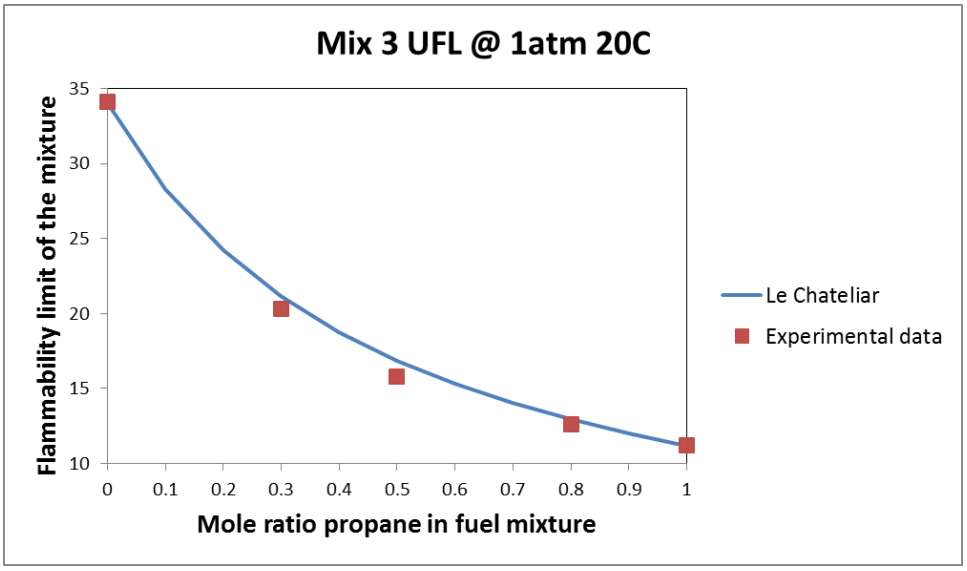

Figure 89 Upper flammability limit of propane (30%, 50%, 80%) and ethylene mixture at 1atm 20 °C

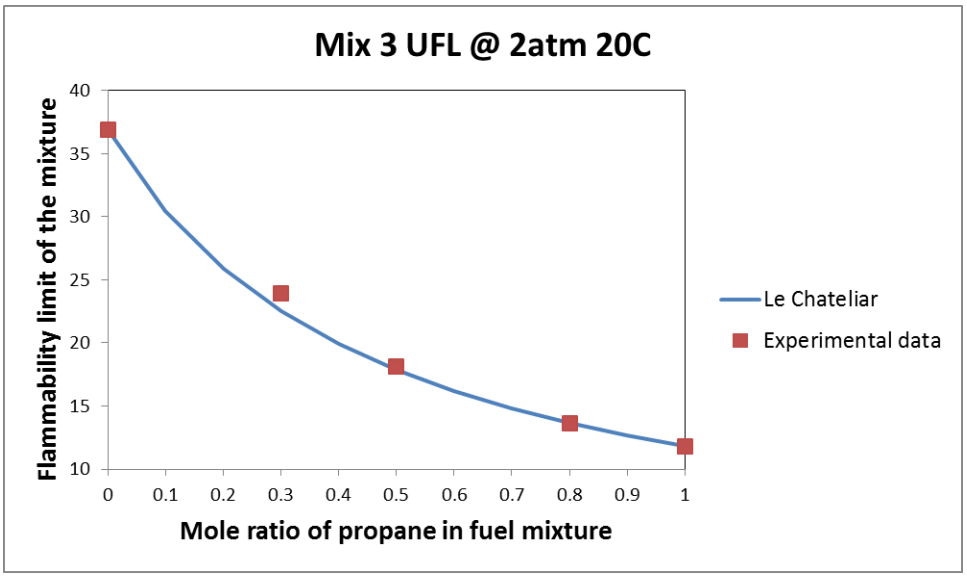

Figure 90 Upper flammability limit of propane (30%, 50%, 80%) and ethylene mixture at 2atm 20 °C

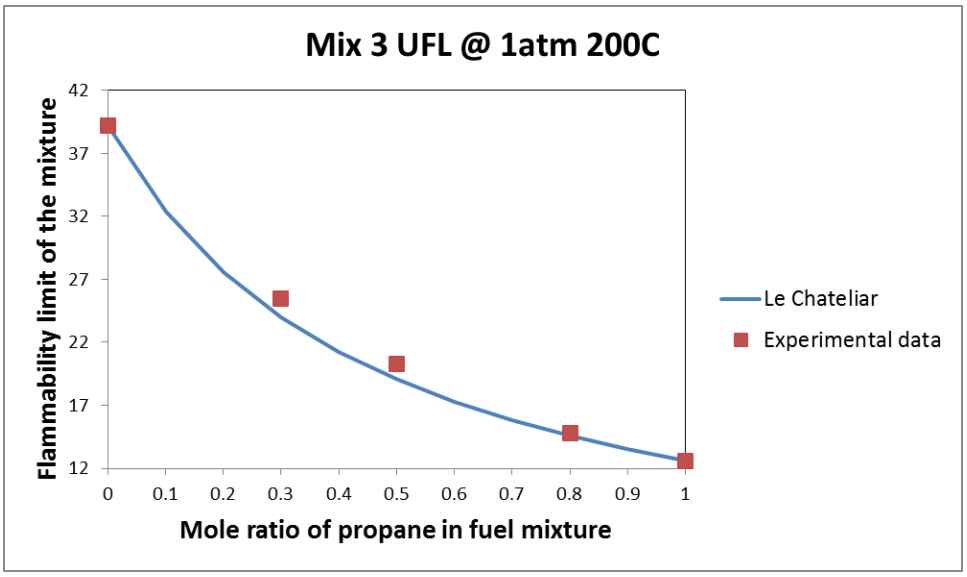

Figure 91 Upper flammability limit of propane (30%, 50%, 80%) and ethylene mixture at 1atm 200 °C

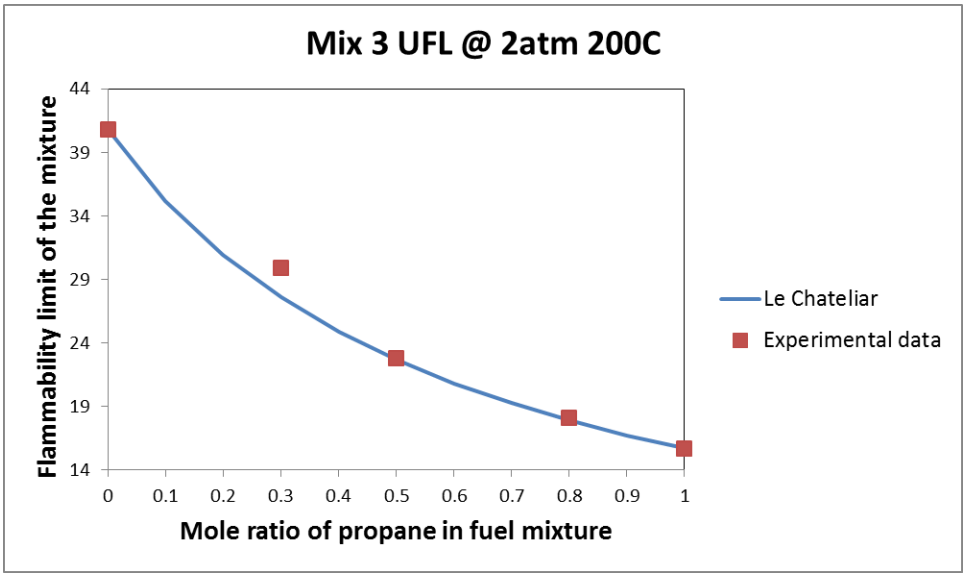

Figure 92 Upper flammability limit of propane (30%, 50%, 80%) and ethylene mixture at 2atm 200 °C

As shown in the Figure 69-76, the experimental results of methane and propane flammability limits agree with predictions from Le Chatelier's rule very well except at the condition of 2atm 200 ℃. The main reason for the big difference between data and predictions in Figure 76 is related to the uncertainty of the flammability limit of pure propane at this test condition. At the upper flammability limit of propane at 2atm/200 ℃, the flame behavior becomes very unstable. Unlike observations from other propane and ethylene UFL test, the fuel concentration range to distinguish gas mixtures from flammable to non-flammable is wide at this circumstance (the fuel concentration difference between flammable zone and non-flammable zone are within ±1.0 vol%). Since the flammability limit criterion is primarily determined on the pressure increment, it is suspected that for the propane UFL test at elevated condition, the decomposition of propane, which consumes the heat and forms hydrogen gas, instead of oxidation reaction, fulfills the pressure increment without flame propagation. To precisely quantify the UFL value, extra tests are conducted for each concentration step (0.1vol%). Though 10 identical tests are performed for each concentration, the probability of ignition cannot be guaranteed as zero. However, since the probability of ignition is already lower than 10%, 15.3% is considered as the UFL for pure propane at 2atm/200C.

For methane and ethylene mixtures, the flammable ranges of the mixture at any conditions are wider than the predictions (LFL data lower than LFL predictions, UFL data higher than UFL predictions), especially when methane is lean in the mixture or

half of the mixture concentration. This phenomenon is more significant in the UFL test results.

For propane and ethylene mixtures, the LFL experimental data agree with predictions from Le Chatelier's Rule fairly well except at the condition of 1atm/200°C where the experiment data are all lower than predictions. While for the UFL results, the prediction values tend to be lower than the experimental data.

In all, the Le Chatelier's rule works fairly well for the prediction of lower flammability limit of binary mixtures at all conditions. While at UFL predictions, Le Chatelier's rule is less reliable at elevated conditions as shown in Table 13.

Table 13 Flammability limits of binary mixtures and comparison with predictions using Le Chatelier's Rule

Mix I	Species 1	Species 2	Experimental data					Le Chatelier's Rule			Difference Percentage		
	CH4	C3H8	CH4 percentage										
	T (℃)	P (atm)	0	30%	50%	80%	100%	30%	50%	80%	30%	50%	80%
LFL	20	1	1.95	2.45	2.75	3.75	4.75	2.37	2.76	3.69	-3.3	0.5	-1.6
	20	2	2.05	2.45	2.95	3.85	4.95	2.49	2.90	3.86	1.5	-1.7	0.2
	200	1	1.65	1.95	2.35	3.25	3.95	2.00	2.33	3.09	2.5	-0.9	-5.0
	200	2	1.65	2.05	2.35	3.15	4.05	2.01	2.34	3.14	-2.1	-0.2	-0.4
UFL	20	1	11.2	12.45	13.5	15.4	16.75	12.44	13.42	15.24	-0.1	-0.6	-1.0
	20	2	11.8	13.1	14	15.7	17.35	13.05	14.05	15.86	-0.4	0.3	1.0
	200	1	12.6	14.2	15.15	17.45	19	14.02	15.15	17.25	-1.3	0.0	-1.2
	200	2	15.3	15.1	15.9	17.4	19.3	16.31	17.07	18.34	8.0	7.4	5.4

Table 13 Continued

Mix II	Species 1	Species 2	Experimental data					Le Chatelier's Rule			Difference Percentage		
	CH4	C2H4	CH4 percentage										
	T (℃)	P (atm)	0	30%	50%	80%	100%	30%	50%	80%	30%	50%	80%
LFL	20	1	2.65	3.05	3.35	4.05	4.75	3.06	3.40	4.10	0.2	1.6	1.2
	20	2	2.71	3.15	3.35	4.2	4.95	3.14	3.50	4.25	-0.5	4.6	1.1
	200	1	2.25	2.4	2.8	3.35	3.95	2.58	2.87	3.43	7.6	2.4	2.4
	200	2	2.3	2.5	2.9	3.5	4.05	2.64	2.93	3.52	5.7	1.2	0.4
UFL	20	1	34.1	27.1	21.9	17.9	16.75	26.02	22.47	18.65	-4.0	2.6	4.2
	20	2	36.9	32.4	26.4	18.7	17.35	27.58	23.60	19.41	-14.9	-10.6	3.8
	200	1	39.2	33.1	28.7	20.9	19	29.72	25.59	21.18	-10.2	-10.8	1.4
	200	2	40.85	36.9	33.4	22.4	19.3	30.60	26.21	21.58	-17.1	-21.5	-3.7

Table 13 Continued

Mix III	Species 1	Species 2	Experimental data					Le Chatelier's Rule			Difference Percentage		
	C3H8	C2H4	C3H8 percentage										
	T (℃)	P (atm)	0	30%	50%	80%	100%	30%	50%	80%	30%	50%	80%
LFL	20	1	2.65	2.35	2.25	2.1	1.95	2.39	2.25	2.06	1.8	-0.1	-2.0
	20	2	2.71	2.45	2.35	2.15	2.05	2.47	2.33	2.15	0.9	-0.7	0.2
	200	1	2.25	1.95	1.85	1.7	1.65	2.03	1.90	1.74	4.0	2.9	2.5
	200	2	2.3	2	1.95	1.75	1.65	2.06	1.92	1.75	2.8	-1.5	-0.1
UFL	20	1	34.1	20.3	15.8	12.6	11.2	21.14	16.86	12.94	4.1	6.7	2.7
	20	2	36.9	23.9	18.1	13.6	11.8	22.53	17.88	13.66	-5.8	-1.2	0.4
	200	1	39.2	25.5	20.3	14.8	12.6	24.00	19.07	14.58	-5.9	-6.1	-1.5
	200	2	40.85	29.9	22.8	18.1	15.3	27.22	22.26	17.49	-9.0	-2.4	-3.4

6.2 Temperature dependence of mixtures

As indicated in Section 5.3, our experimental data proves that flammability limit of pure light hydrocarbons varies linearly as the temperature increases and the linearity of the flammability limit dependence on temperature can be fitted [34] through the equation 16,

$$\frac{FL\,(T)}{FL\,(T_0)} = 1 + c \times (T - T_0) \quad (16)$$

Similarly, the flammability temperature dependence of mixtures can also be calculated using the same equation. To better understand the temperature effect on the gas mixtures, the coefficient c for all three binary mixtures are compared in Table 14-15 and Figure 93-95.

Table 14 Coefficient c (x100 °C-1) value for methane and propane mixture

Mix I	**Species 1**	**CH_4**	**Species 2**	**C_3H_8**	
	P (atm)	**CH_4 percentage**			
		0	**30%**	**50%**	**80%**	**100%**
LFL	1	-0.086	-0.113	-0.081	-0.074	-0.094
	2	-0.109	-0.091	-0.113	-0.101	-0.101
UFL	1	0.069	0.078	0.068	0.074	0.096
	2	0.186	0.085	0.075	0.060	0.092

Table 15 Coefficient c (x100 °C-1) value for methane and ethylene mixture

Mix II	Species 1	CH_4	Species 2	C_2H_4	
	P (atm)	CH_4 percentage			
		0	30%	50%	80%	100%
LFL	1	-0.082	-0.118	-0.091	-0.096	-0.094
	2	-0.083	-0.115	-0.075	-0.093	-0.101
UFL	1	0.085	0.123	0.173	0.093	0.096
	2	0.060	0.077	0.147	0.110	0.092

Table 16 Coefficient c (x100 °C-1) value for propane and ethylene mixture

Mix III	Species 1	C_3H_8	Species 2	C_2H_4	
	P (atm)	C_3H_8 percentage			
		0	30%	50%	80%	100%
LFL	1	-0.082	-0.095	-0.099	-0.106	-0.086
	2	-0.083	-0.102	-0.095	-0.103	-0.109
UFL	1	0.085	0.142	0.158	0.097	0.069
	2	0.060	0.140	0.144	0.184	0.186

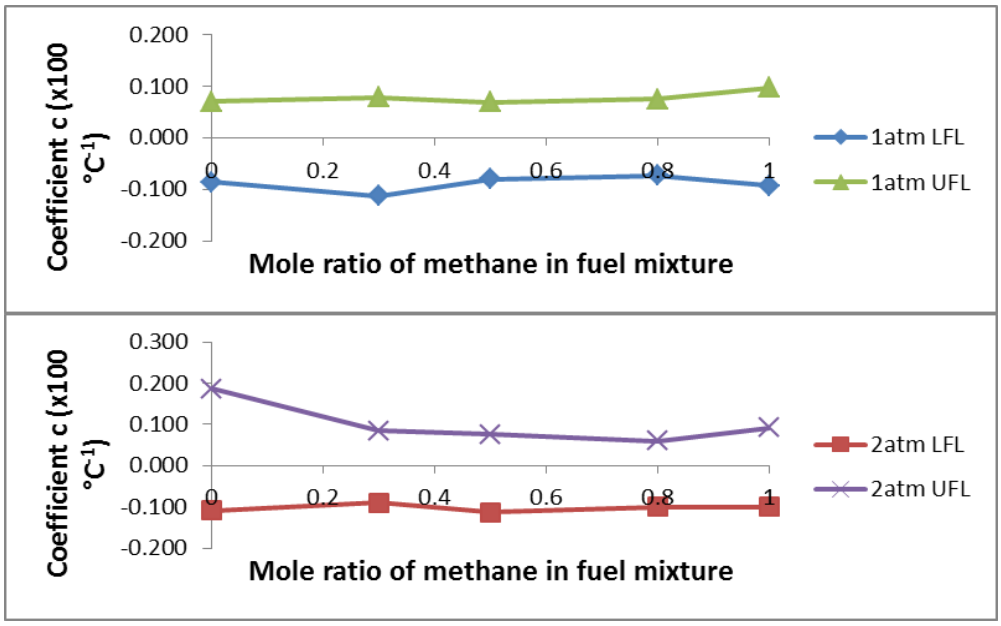

Figure 93 Coefficient c (x100 °C-1) value for methane and propane mixture vs. methane mole ratio. A) upper, 1atm; B) lower, 2atm

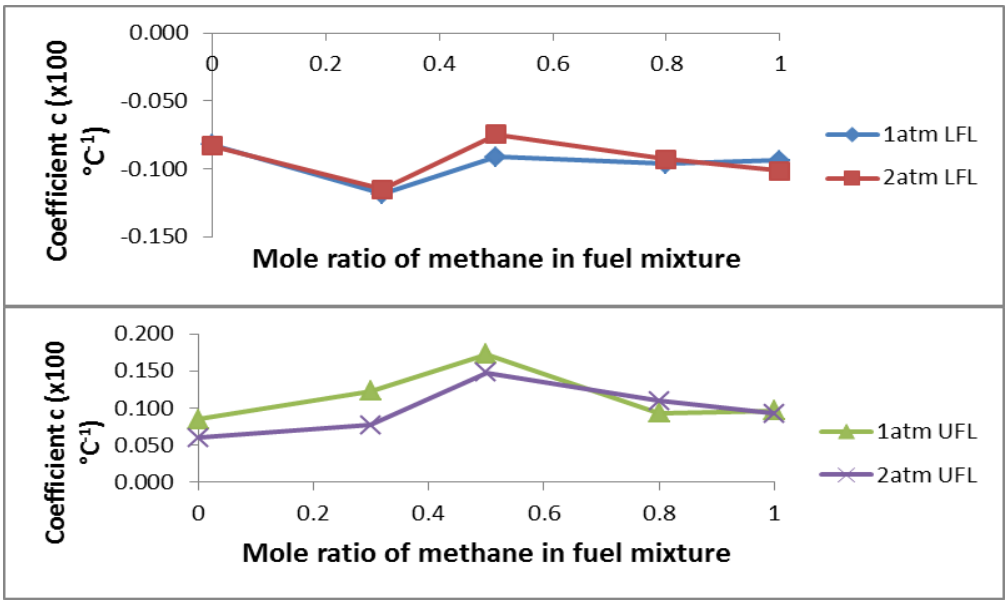

Figure 94 Coefficient c (x100 °C-1) value for methane and ethylene mixture vs. methane mole ratio. A) upper, LFL; B) lower, UFL

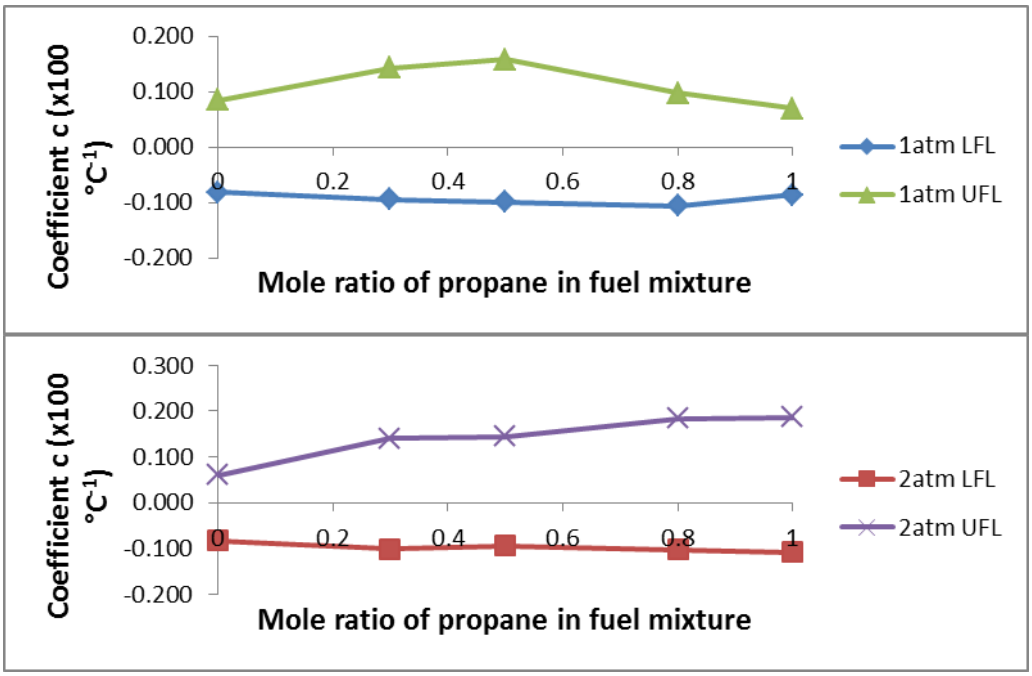

Figure 95 Coefficient c (x100 °C-1) value for propane and ethylene mixture vs. propane mole ratio. A) upper, 1atm; B) lower, 2atm

The data in Table 14-15 indicate that in general, increasing the pressure will not greatly impact the flammability temperature dependence of the gas mixtures. For methane and propane mixtures, Figure 93 proves that increase of the methane ratio in the mixtures will have the symmetrical effect on both LFL and UFL (increase on the LFL temperature dependence and decrease on the UFL temperature dependence). But increasing the methane mole ratio will cause different effect on either LFL or UFL when the initial pressure is different. On the contrary, for methane and ethylene mixtures (Figure 94), even the initial pressures of the gas mixture are different, increasing the methane mole ratio will have the same effect on the flammability temperature dependence and the coefficients are maximized when methane takes half of the fuel

mixture. For propane and ethylene mixtures, the temperature dependence coefficients behave similarly as the methane/propane mixtures. In all, the lower flammability limit temperature dependence coefficient is not significantly impacted by the fuel gas mixing ratio compared with the upper flammability limit temperature dependence coefficients.

6.3 Reaction pathway analysis

Combustion reaction at upper flammability limit becomes more complex as shown in Figure 76, especially for the fuel mixtures at elevated conditions. Using a simple reaction mechanism assumption for the prediction of the flammability limit could cause significant overestimation or underestimation. Without knowing the detailed reaction mechanism, the difference between the experimental data and predictions from estimation methods cannot be easily explained. Therefore, a proper CFD combustion simulation program is needed for better understanding of the fuel oxidation kinetics. Modern chemical reaction program, ANSYS CHEMKIN is a joint software program that is designed to couple detailed chemistry with third-party CFD codes [35]. The software introduces more accurate chemistry into reacting, fluid flow simulation and it has the capabilities to calculate kinetics and transport problems simultaneously. In this section, the combustion simulation results of pure light hydrocarbons and binary light hydrocarbons are studied for better understanding of the reaction and how some reactions dominate the reaction heat release and affect the flammability of gas mixtures.

6.3.1 Simulation conditions

In theory, flammability limit is the concentration of the fuel that has the capability to provide heat from burned gas to unburned gas as a chain reaction. With the exception of the initial stage of the combustion, where the burning of the gas is caused by hot glowing metal (sparks from ignitor), the steady phase of the combustion, which is also recognized as the continuous flame propagation, needs a heat transfer from oxidation or reaction of the burning fuel to the unreacted gas. In reality, when the flame is developed in the reaction vessel and propagates further, it also involves the compression of unburned gas, heat loss to the surroundings (reaction vessel, thermocouples, etc.), frictions between the flame front and the wall, and turbulence. However, our goal of using the ANSYS CHEMKIN [35] software is to study the reaction mechanism rather than rebuild the entire combustion process, therefore, the simulation in this work will be simplified as homogenous gas phase combustion in a 8L closed chamber (same as the experimental apparatus) and the entire reaction process is restricted to spontaneous ignition of fuel at constant volume.

The fuel and reaction condition selected for this study is limited to UFL and include pure methane at 2atm/1600K, pure propane at 2atm/1200K, pure ethylene at 1atm/1200K, methane and propane mixture (50% methane) at 2atm/1200K, methane and ethylene (30% methane) at 1atm/1200K, propane and ethylene (30% propane) at 1atm/1200K. Though these reaction temperatures are lower than adiabatic flame temperatures, they are high enough to generate flame without causing decomposition of fuel gases (for example, propane will decompose without oxidation reaction at 1,600K)

in a very short period of time (less than 10ms), which is considered as immediate ignition.

The chemistry set (kinetics file and thermodynamics file) used in this study mainly include 3 types: GRI-Mech 3.0 [36], Propane/Air combustion [37] and Ethylene/Air combustion [38]. The GRI-Mech 3.0 is a well-validated reaction mechanism developed by the Gas Research Institute. In this reaction mechanism, the gas-phase kinetics input file contains 5 elements, C, H, O, N and Ar, 53 chemical species, and 325 reactions. The reaction mechanism is primarily used for studying the combustion of methane and smaller species such as hydrogen. In this study, GRI-Mech 3.0 is used for pure methane and all mixture studies. The Propane/Air combustion mechanism is developed by the Center for Energy Research (CER), University of California, San Diego. It consists of 46 species and 235 reactions. The elements constituting the species are N, H, C, O, Ar, and He. All reactions are reversible, and some of the reactions include pressure-dependencies on the rate constant. In this work, Propane/Air mechanism is used for pure propane study. The ethylene-air combustion mechanism of Appel [38] is provided by the software package and this reaction mechanism consists of 101 species and 543 reactions. In this study, the ethylene/air combustion mechanism is used for pure ethylene simulation only.

6.3.2 Reaction pathway of pure hydrocarbons

The combustion simulation in air starts with methane at condition of 2atm, 1,600K and 19vol%. As shown in Figure 96, the temperature of the gas mixtures will

increase to the maximum value of 2,800K in 0.4ms, which indicates that immediate ignition has taken place. Also Figure 97 confirms that an increment of 2atm in the combustion process has happened. In Figure 98, for the first 0.35ms, the mole fraction of CH4 is decreasing and the mole fractions of CO, CO2 and H2O are increasing. However, after 0.35ms, the mole fraction of water starts to decrease, which suggests that other reaction takes place. For the research purpose of this study, it is important to focus on the reaction pathway and steps that generate heat and propagate flame, therefore, the reaction scope will be limited to the time where the reaction is able to produce a heat rise of 100K from initial temperature.

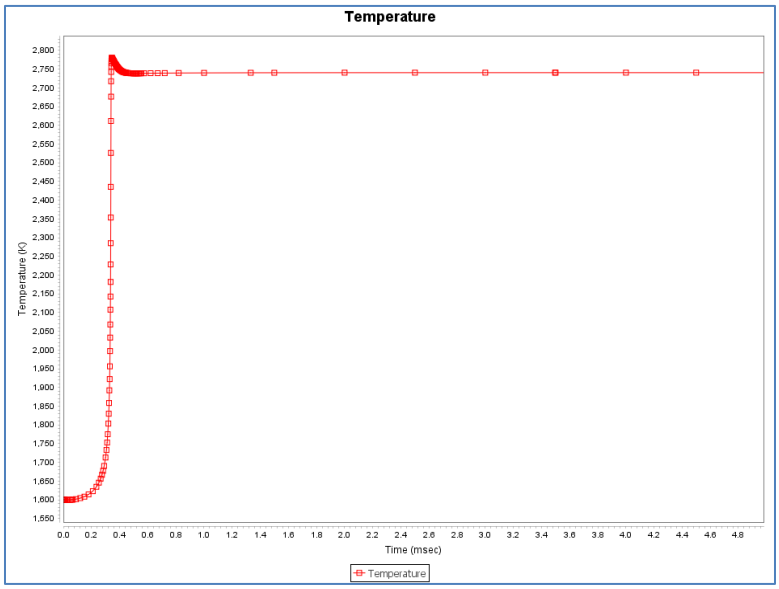

Figure 96 Temperature simulation profile of methane at 2atm, 1600K, 19vol% fuel

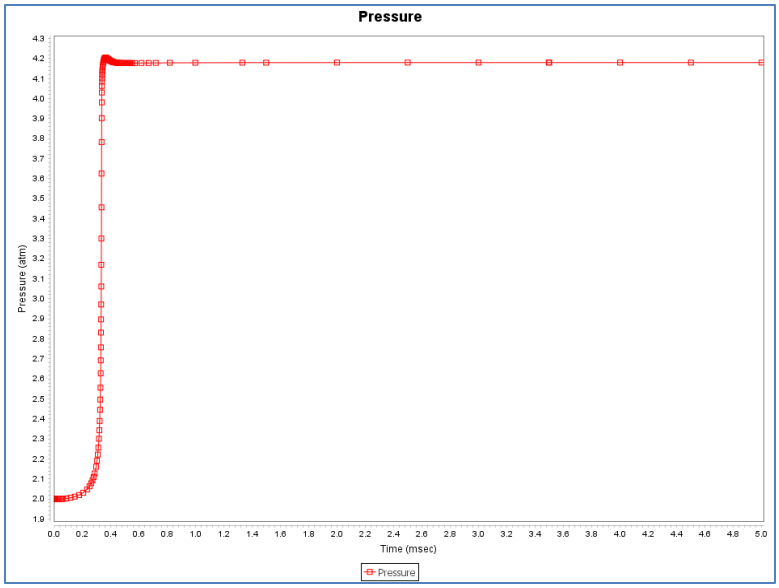

Figure 97 Pressure simulation profile of methane at 2atm, 1600K, 19vol% fuel

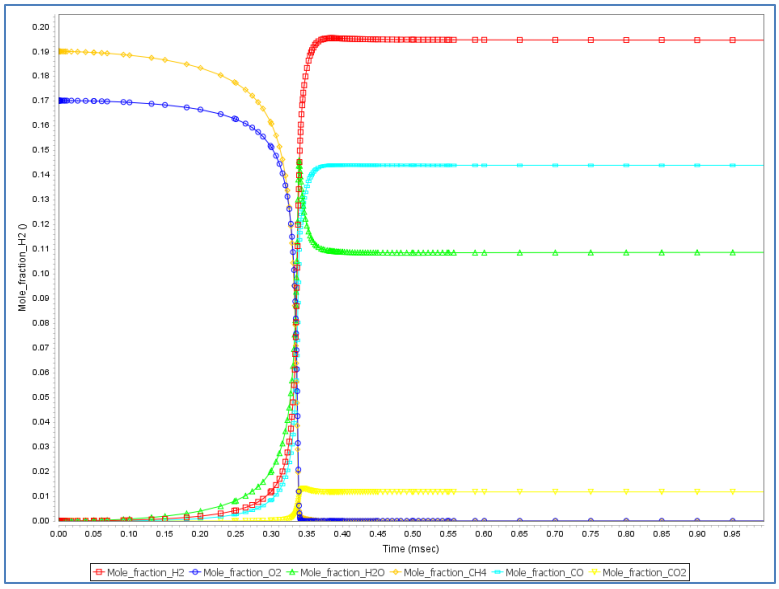

Figure 98 Mole fraction of major reactants and products profile of methane at 2atm, 1600K, 19vol% fuel

At the time when the gas reaches 1,700K, the total reaction pathway is shown in Figure 99. For entire reaction network, more than 20 chemical species are involved. But in this figure, only 10 of the selected chemical species that may involve carbon oxidation or hydrogen oxidation reaction are chosen. The relative sizing of the connecting pathways is related to the relative contribution of that pathway to the net rate of production of the species. Path widths with minimum rate of production corresponding to a line thickness of one, and the maximum rate of production scaled to the largest allowed line thickness. Intermediate line thicknesses are determined on a log scale. Since the reaction condition is set as UFL combustion for methane, the major reaction will be represented based on starting species as CH4 and ending species as CO. and the chain reaction for methane include: CH4→ CH3→ CH3O→CH2O→ HCO→CO. For each of the reaction (i.e., CH4→ CH3), different reaction pathway may happen, for example, for CH4→ CH3, possible reactions include: OH+CH4->CH3+H2O, H+CH4-> CH3+H2, CH4+HCO->CH3+CH2O, CH4+O->OH+CH3, CH4+HO2->CH3+H2O2, etc. Since the entire reaction network, which includes more than 50 reactions, is very complex for the study of the reaction pathway, for all of the reaction pathway analysis study in this section, the reaction pathway is simplified to the chain reaction with the starting species as fuel (CH4, C3H8, C2H4 or binary mixtures) and ending species as CO and H2O. Possible reaction for CH4 is also shown in the upper part of Figure 100. All of the reactions shown in upper picture of Figure 100 are reversible reactions, however, the forward and backward bars in the picture indicate if the rate of production is positive or negative (i.e. for reaction OH+CH4 => CH3+H2O, production bar is on the left side, this

reaction will consume CH4 and generate CH3). The absolute rate of production and normalized sensitivity of CH4 is shown in Figure 100. The normalized sensitivities used here are calculated based on the heat of formation for each reaction, as well as of its impact on the total heat generation. If the sensitivity coefficient for this reaction is positive, it is indicating that increasing the rate of this production will lead to a higher temperature (more heat production). In contrast, if the sensitivity coefficient for the reaction is large and negative, it is indicating that increasing the rate of this reaction will lead to a lower temperature (less heat production). So if the normalized sensitivity bar is on the right side in the lower part of Figure 100, it is suggesting that this reaction is an endothermic reaction. If the normalized sensitivity bar is on the left side in the lower part of Figure 100, it is suggesting that this reaction is an exothermic reaction. Since the simulation is based on steady phase combustion, the parameter limiting the flame propagation is the heat transfer between burned gas and unburned gas. It is critical to understand which reaction will contribute more to heat generation. According to the simulation results, the top 3 reactions that contribute to the temperature rise in the combustion process are: $CH3 + O2 \rightarrow O + CH3O$, $H + O2 \rightarrow O + OH$, and $H + CH4 \rightarrow CH3 + H2$. So it can be concluded that in the methane UFL test, the major steps that contribute to the flame propagation include the oxidation of CH3, decomposition of O2 and decomposition of methane to form H2.

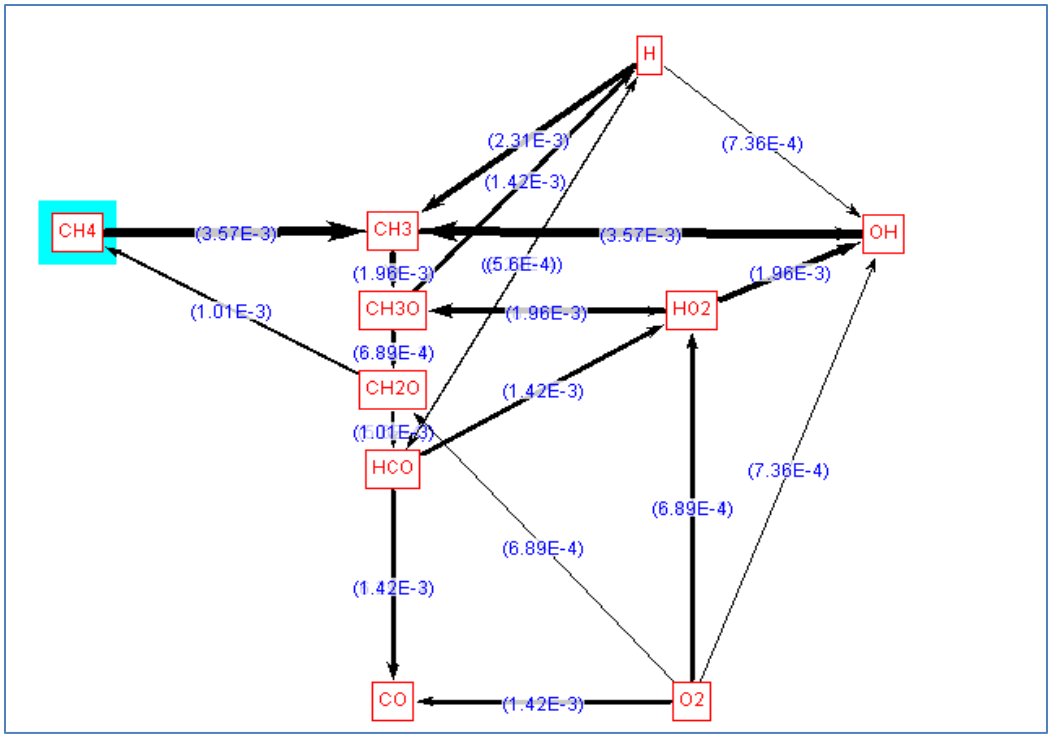

Figure 99 Reaction pathway of methane at 1700K, 2atm

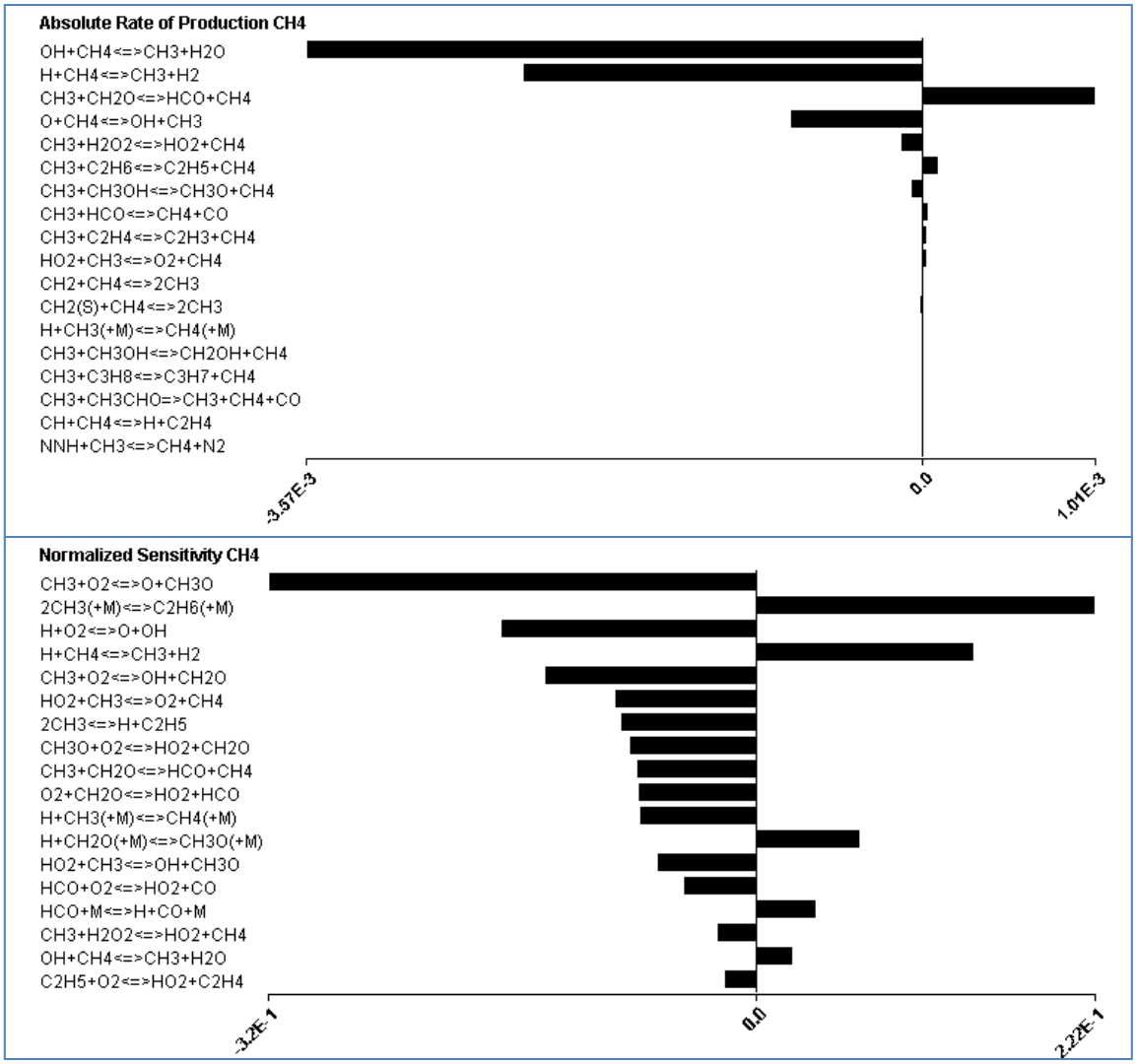

Figure 100 Absolute rate of production (upper) and normalized sensitivity (lower) of CH_4 at 1700K, 2atm

The combustion simulation of propane in air is set at the condition of 2atm, 1,200K and 15vol%. The temperature of propane/air mixture reaches the maximum value of 1,920K in 1.5ms, as presented in Figure 101, which indicates that propane is ignited immediately. In Figure 103, for the first 1.4ms, the mole fraction of C3H8 and

O2 is decreasing rapidly, while the mole fraction of H2, CO, CO2 and H2O is increasing. However, after 1.4ms, though C3H8 is depleted, the mole fraction of H2 is still increasing, and the pressure of the gas mixture is still slowly increasing (Figure 102), which suggests that other reaction takes place. Since in this study, the primary focus is to find the reaction pathway and steps that generate heat and propagate flame, therefore, the reaction scope will be limited to the time when reaction reaches 1300K.

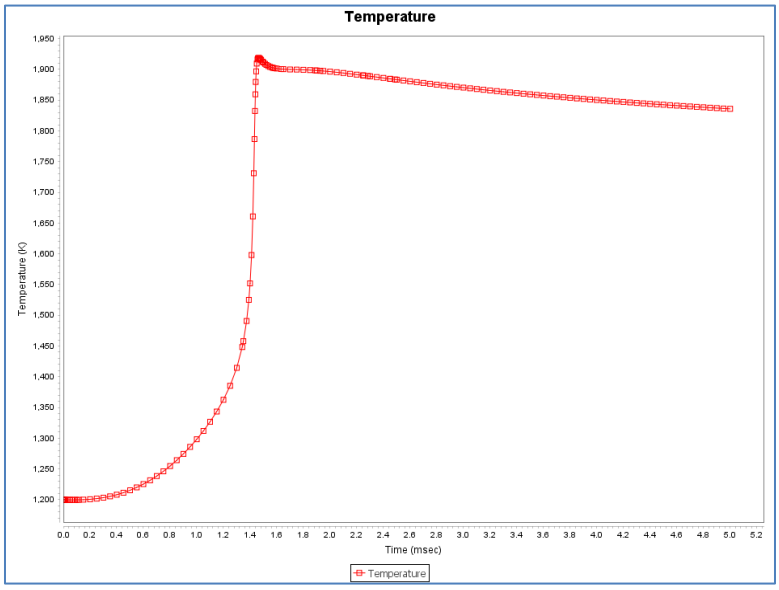

Figure 101 Temperature simulation profile of propane at 2atm, 1200K, 15vol% fuel

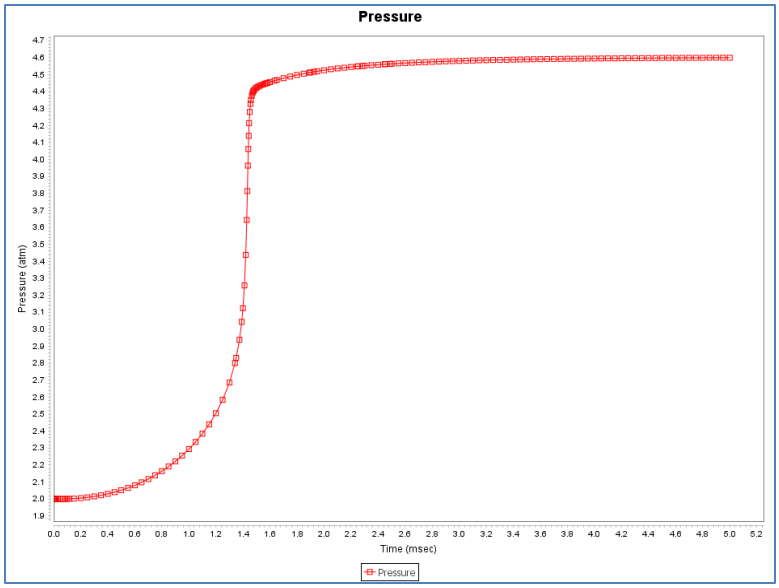

Figure 102 Pressure simulation profile of propane at 2atm, 1200K, 15vol% fuel

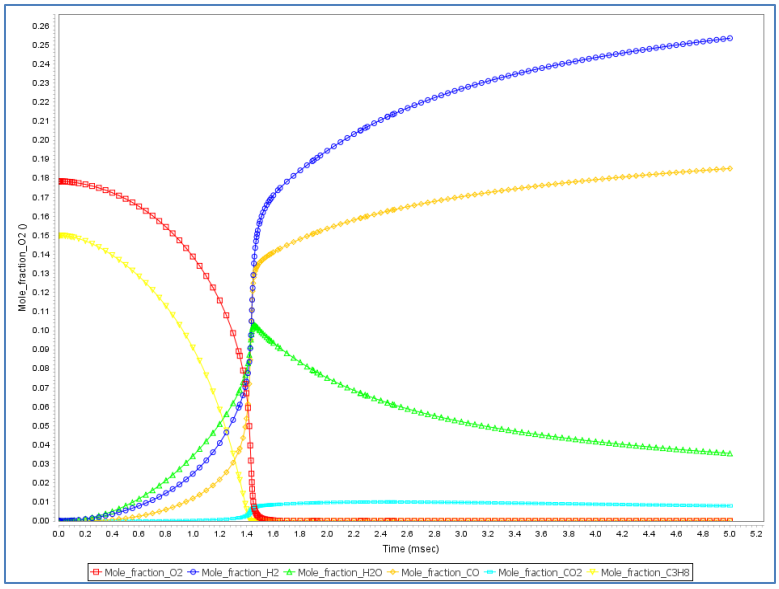

Figure 103 Mole fraction of major reactants and products profile of propane at 2atm, 1200K, 15vol% fuel

Similar to the reaction pathway study of methane, the reaction chain will be limited to the case that C3H8 is set as starting species, while CO is set as ending species. The total reaction pathway of propane combustion at UFL is shown in Figure 104. The pathway picture clearly shows that when the gas temperature reaches 1,300K, a lot of decomposition reaction is happening and shorter carbon chain products such as CO, CH4, C2H4, and C2H6 are formed. The absolute rate of production and normalized sensitivity of C3H8 is shown in Figure 105. As indicated in the normalized sensitivity chart, the top 3 reactions that contribute to the temperature rise in the combustion process are: $CH3 + O2 \rightarrow CH2O + OH$, $C3H5 + HO2 \rightarrow OH + C2H3 + CH2O$, $I - C3H7 + O2 \rightarrow C3H6 + HO2$. Therefore, it can be concluded that in the propane UFL test, the major reactions that limit heat transfer are the oxidation of CH3 and the decomposition of C3H5 and C3H7.

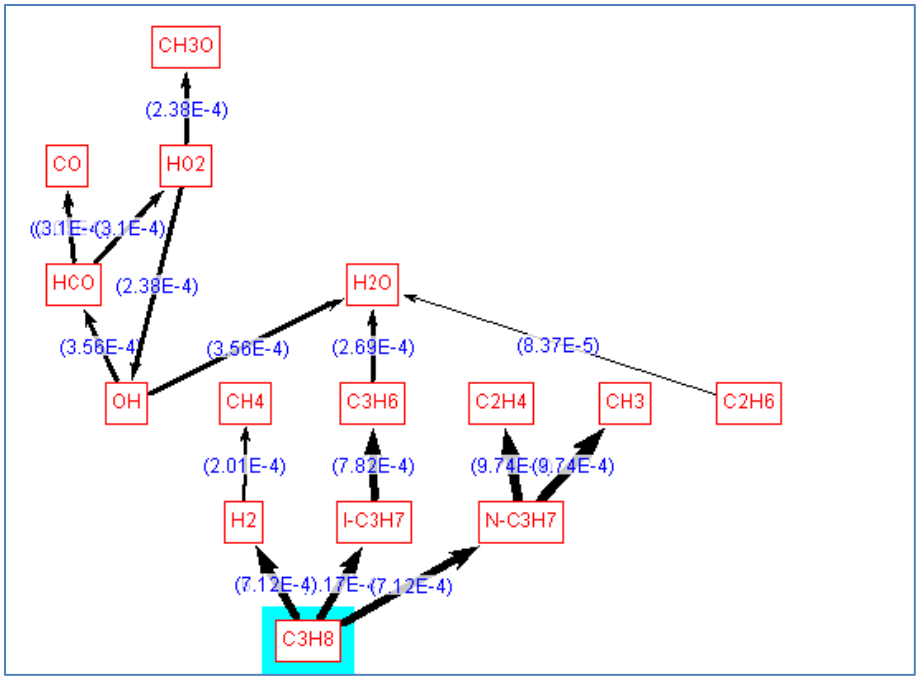

Figure 104 Reaction pathway of propane at 1300K, 2atm

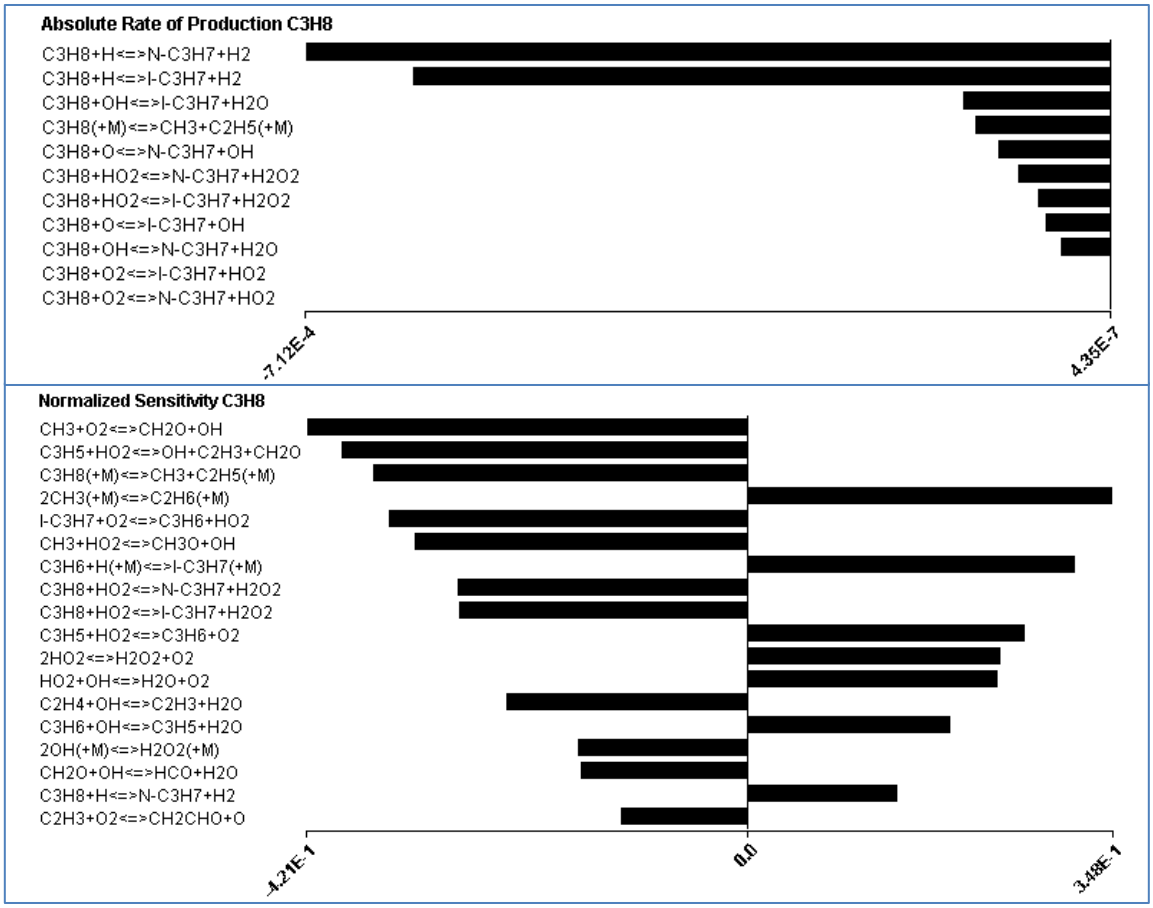

Figure 105 Absolute rate of production (upper) and normalized sensitivity (lower) of C3H8 at 1300K, 2atm

One of the major concerns in the reaction mechanism study is that increase in the initial pressure may cause the reaction mechanism to change. Therefore, to solve this problem, propane/air mixture is simulated at the same condition as above except the initial pressure is changed to 1atm.

As presented in Figure 106 and Figure 107, time to reach maximum temperature and maximum pressure is almost doubled compared with the time at 2atm condition while the reaction pathway is almost identical as shown in Figure 108. The normalized

sensitivity chart, which is indicated in Figure 109, shows the top 10 reactions that have influences on the heat release of the combustion are the same. However, the sensitivity value of each reaction is different and the rank sequence of the reaction is different. Therefore, change in the initial pressure will affect the reaction mechanism and the reaction rate, but the influences are mainly caused by reaction step sequences/rankings rather than different reaction steps.

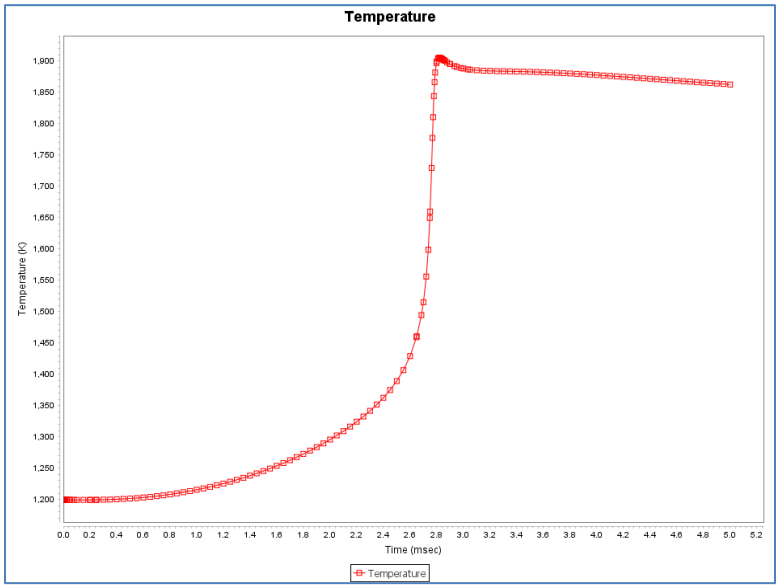

Figure 106 Temperature simulation profile of propane at 1atm, 1200K, 15vol% fuel

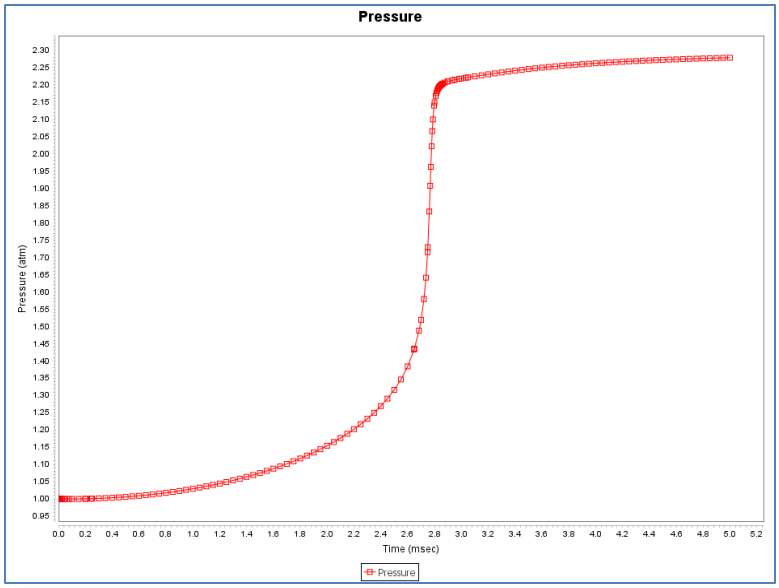

Figure 107 Pressure simulation profile of propane at 1atm, 1200K, 15vol% fuel

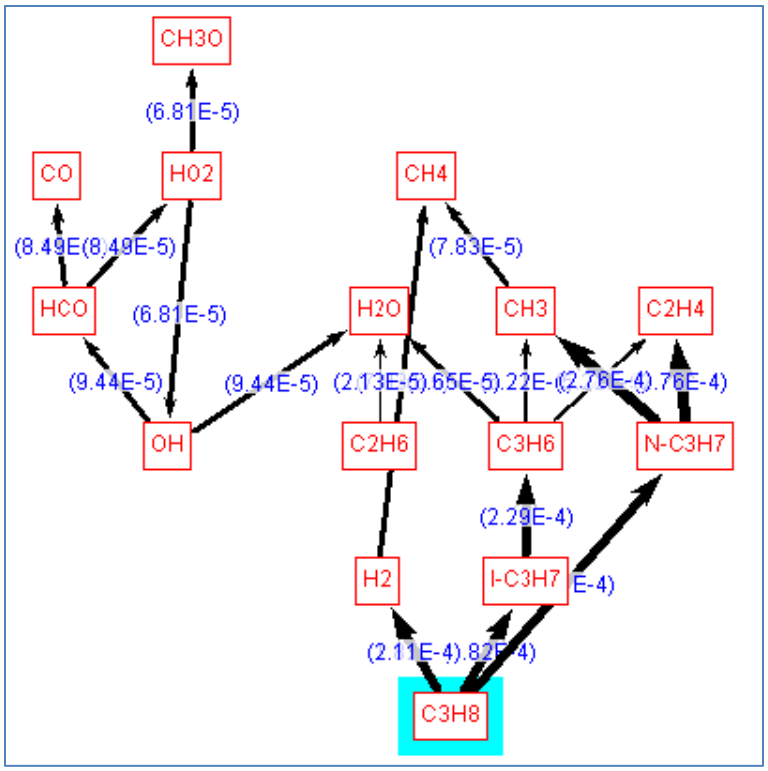

Figure 108 Reaction pathway of propane at 1300K, 1atm

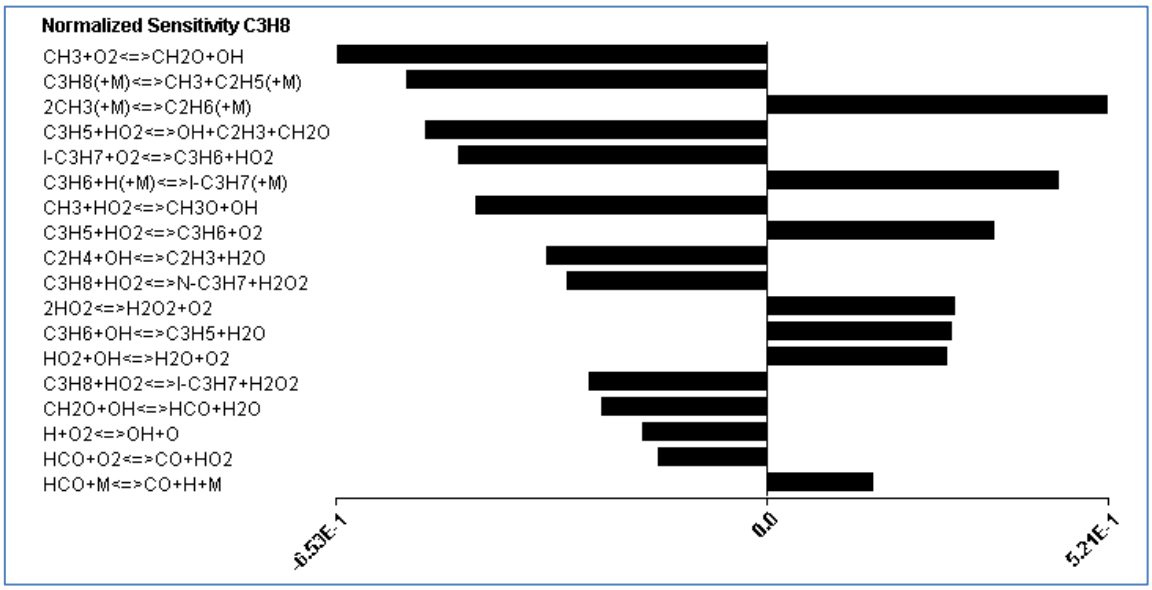

Figure 109 Normalized sensitivity of C3H8 at 1300K, 1atm

For ethylene, the combustion simulation in air is set at the condition of 1atm, 1,200K and 38vol%. The ethylene/air mixtures will reach its temperature maximum value of 1,700K and pressure maximum value of 1.72atm in less than 1ms, as presented in Figure 110 and Figure 111, which proves immediate ignition. For ethylene combustion, the major reactions take place within 0.1ms (0.82ms~0.92ms), as shown in Figure 112, no secondary reaction continues after oxygen is depleted. Similar to other pure hydrocarbon gases, ethylene reaction pathway is studied at the condition of 1,300K, 1atm as presented in Figure 113.

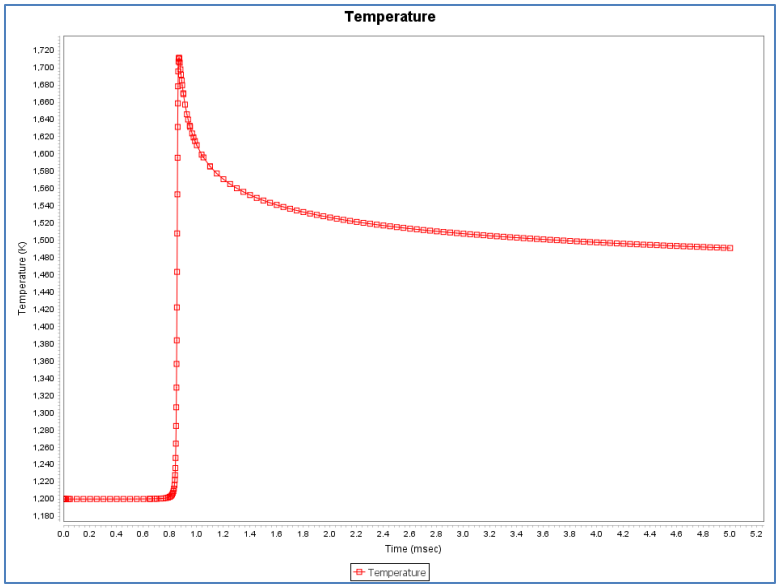

Figure 110 Temperature simulation profile of ethylene at 1atm, 1200K, 38vol%fuel

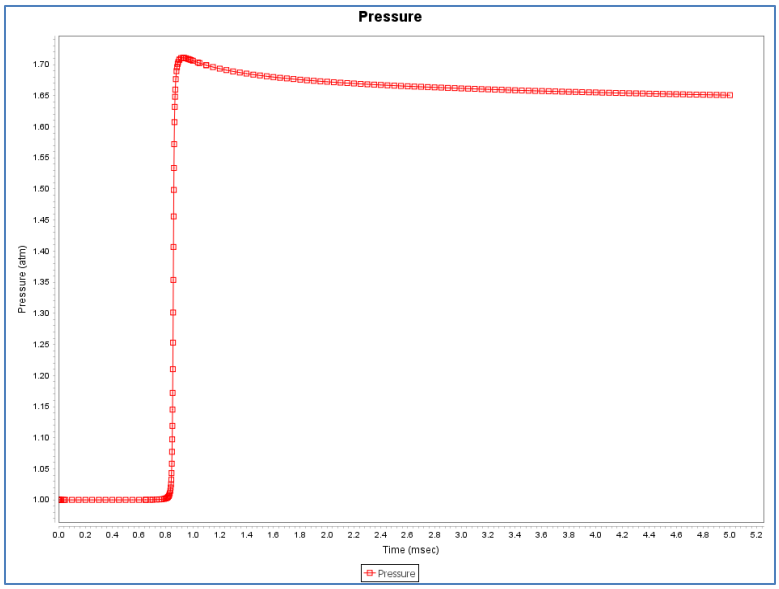

Figure 111 Pressure simulation profile of ethylene at 1atm, 1200K, 38vol%fuel

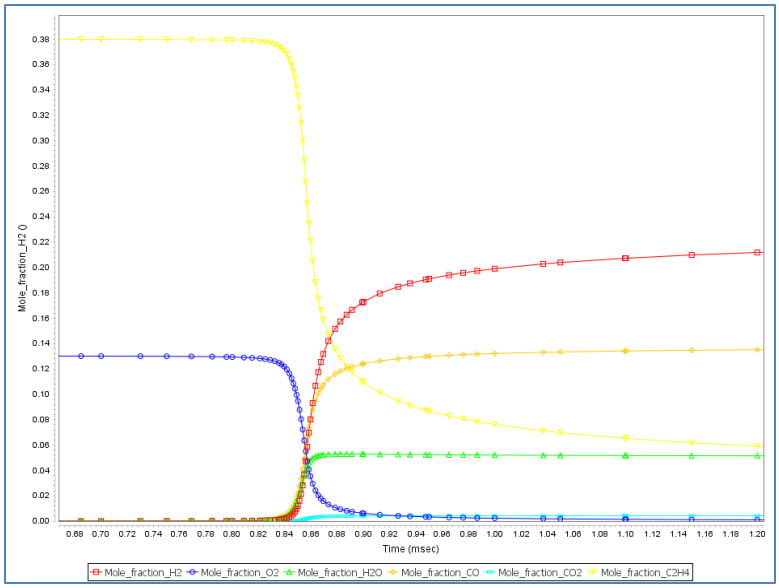

Figure 112 Mole fraction of major reactants and products profile of ethylene at 1atm, 1200K, 38vol% fuel

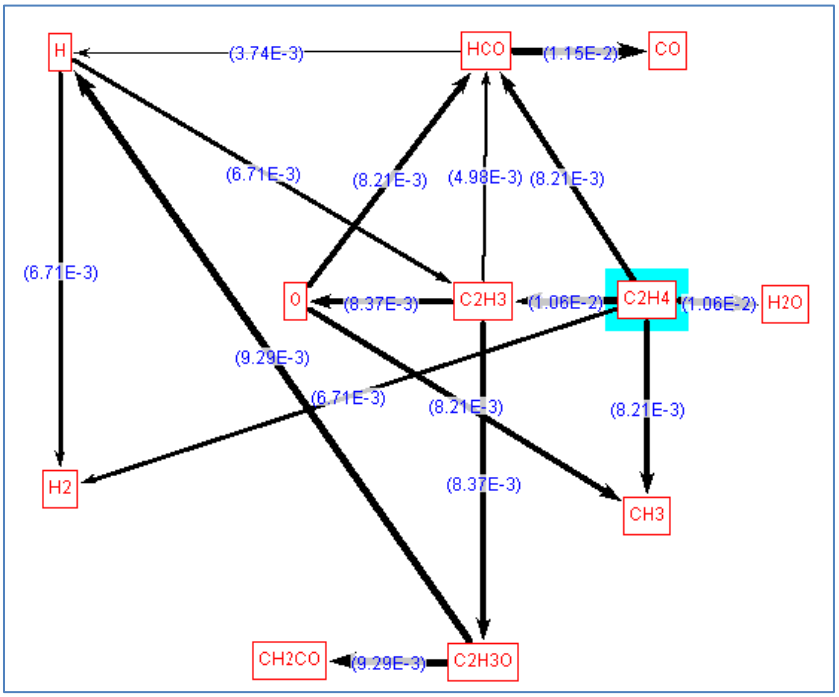

Figure 113 Reaction pathway of ethylene at 1300K, 1atm

As indicated in the normalized sensitivity analysis, the top 3 reactions that contributed to the heat release of the combustion reactions are: $C2H3 + O2 \rightarrow C2H3O + O$, $C2H4 + H \rightarrow C2H3 + H2$, $C2H4 + CH3 \rightarrow C2H3 + CH4$. The reaction that contributed least to the heat generation is the decomposition of C2H3. Therefore, it can be concluded that in the ethylene reaction at UFL, the heat release of the reaction are mainly promoted by the decomposition of oxygen, activation of C2H4 to form C2H3 using CH3 or H while the heat release is inhibited by the breaking of C=C bond.

6.3.3 Reaction pathway of binary mixtures

Binary mixtures of methane/ propane mixture (50% methane) at 2atm/1200K, methane/ethylene mixture (30% methane) at 1atm/1200K, and propane/ethylene (30% propane) at 1atm/1200K are selected due to the significant difference between experimental flammability data and predictions. GRI-Mech 3.0 is used as the chemistry set for all binary mixture simulation. Though GRI-Mech 3.0 is developed for methane combustion purpose, it contains minimal set of propane and ethylene oxidation kinetics.

6.3.3.1 Simulation of methane/propane mixture

The combustion simulation of methane/propane mixture is set at the condition of 2atm, 1,200K and 15.9vol% (50% methane). As shown in Figure 114, the temperature of the gas mixtures will increase to the maximum value of 2,150K in 5.4ms, which indicates that immediate ignition has taken place. Also Figure 115 confirms that an increment of 2.6atm in the combustion process has happened. In Figure 116, for the first

5.3ms, the mole fractions of C3H8 and O2 are decreasing, but the CH4 mole fraction remain unchanged, while the mole fractions of H2, CO, and H2O are increasing. After 5.3ms, the mole fraction of water starts to decrease with the increasing of H2, CO and CO2 mole fraction, which suggests secondary reaction. For this study, the reaction scope is set to the time when the reaction produces a temperature rise of 100K.

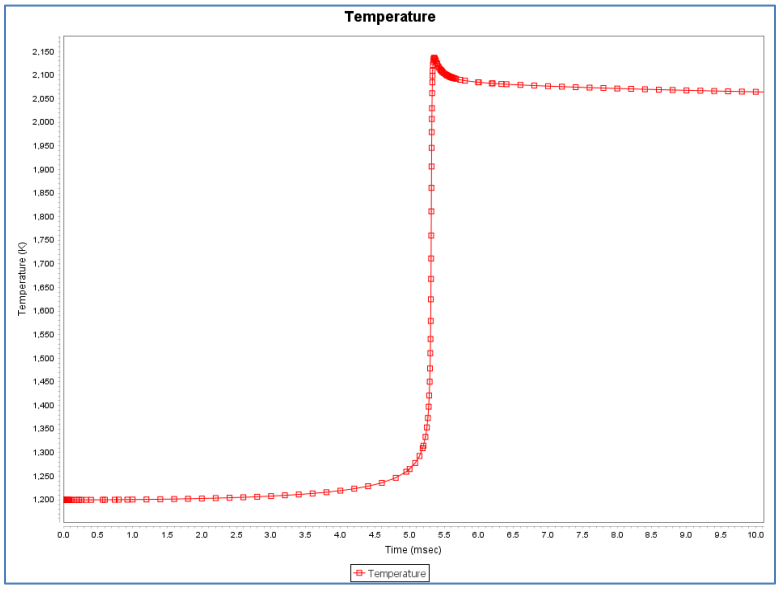

Figure 114 Temperature simulation profile of methane/propane (50:50) mixture at 2atm, 1200K, 15.9vol% fuel

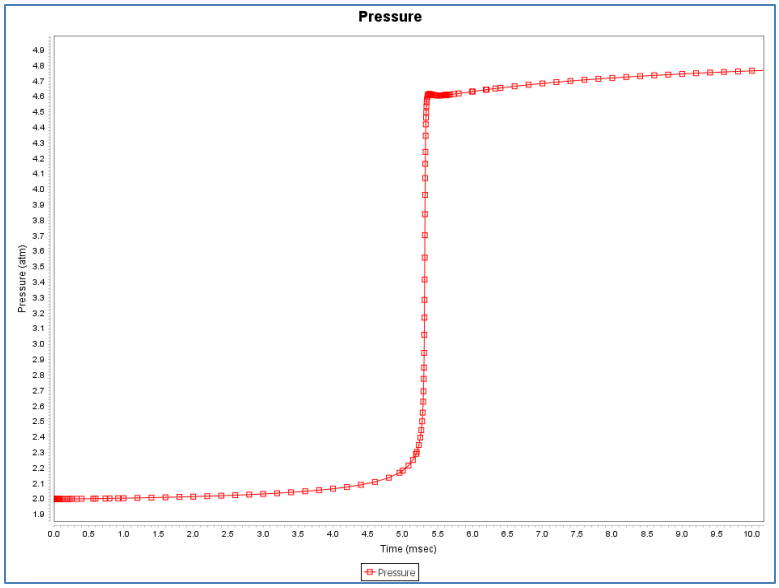

Figure 115 Pressure simulation profile of methane/propane (50:50) mixture at 2atm, 1200K, 15.9vol% fuel

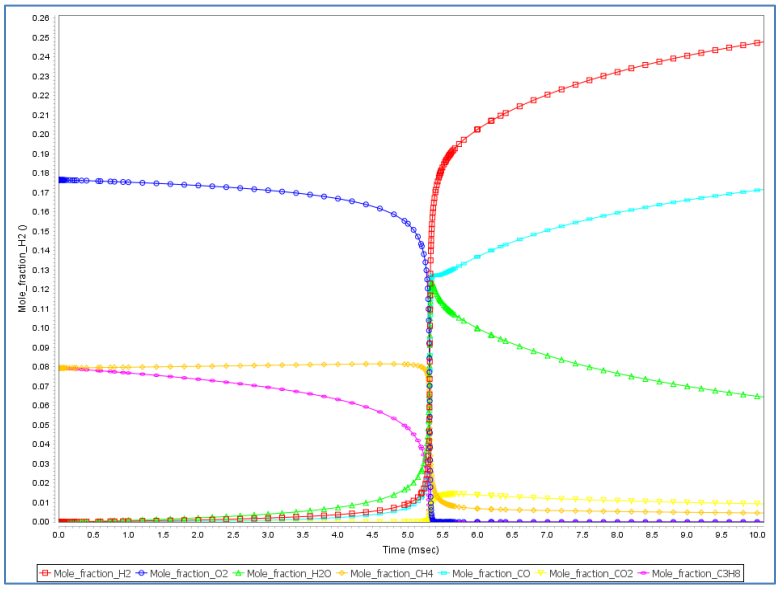

Figure 116 Mole fraction of major reactants and products profile of methane/propane (50:50) mixture at 2atm, 1200K, 15.9vol% fuel

As shown in Figure 117, the total reaction pathway of methane/propane mixture at 1,300K, 2atm is a complex reaction network. Figure 118 represents the absolute rate of production and normalized sensitivity of C3H8, which proves the top 3 reactions that contribute to the temperature rise in the combustion process are: $CH3 + C2H5(+M) \rightarrow C3H8(+M)$, $CH3O + O2 \rightarrow HO2 + CH2O$, and $CH3 + CH2O \rightarrow HCO + CH4$. Unlike pure methane combustion mechanism or pure propane combustion mechanism, the rate limiting steps are more likely to produce activated molecules instead of breaking C-H, C-C bonds.

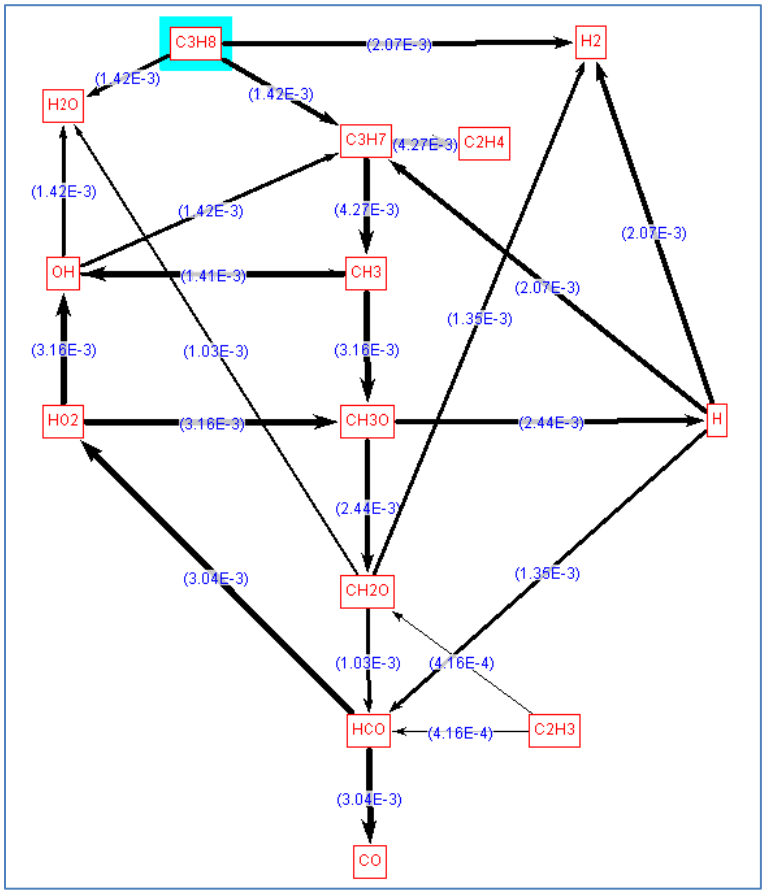

Figure 117 Reaction pathway of methane/propane (50:50) mixture at 2atm, 1300K

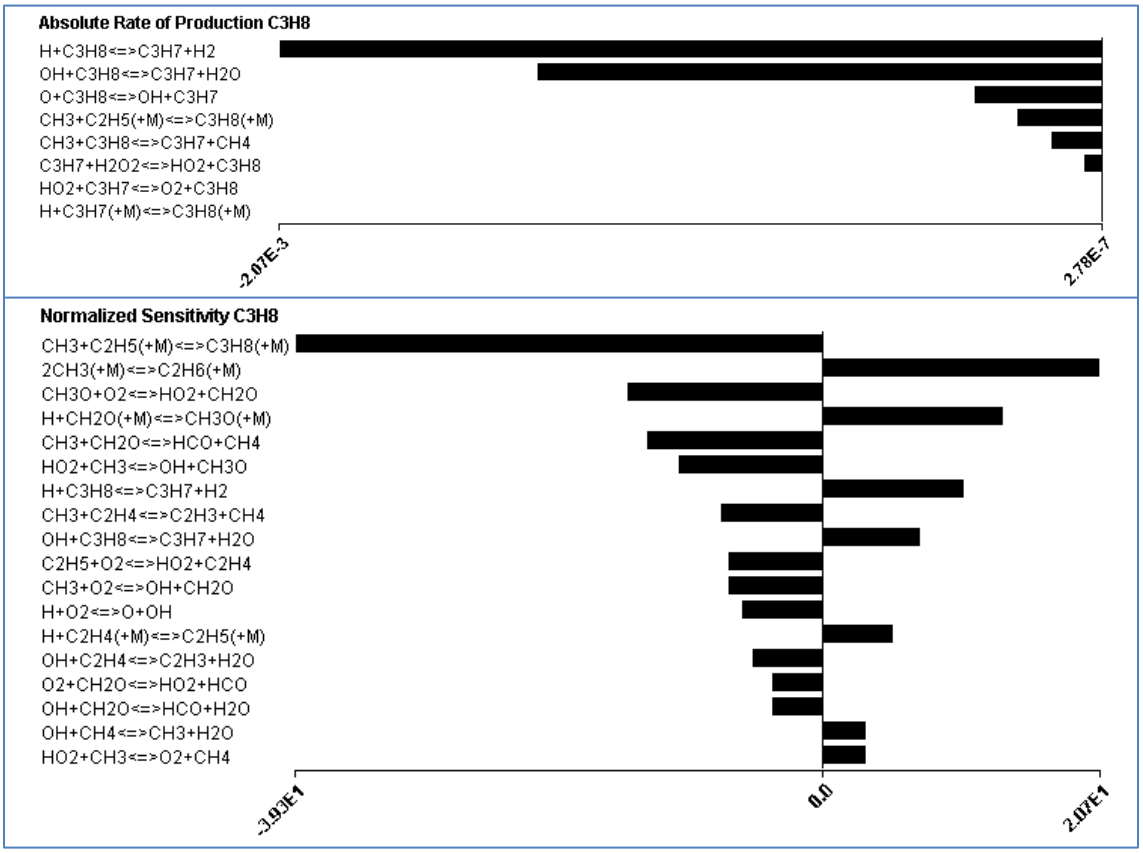

Figure 118 Absolute rate of production (upper) and normalized sensitivity (lower) of methane/propane (50:50) mixture at 2atm, 1300K

6.3.3.2 Simulation of methane/ethylene mixture

The combustion simulation of methane/ethylene mixture is set at the condition of 1atm, 1,200K and 33.1vol% (30% methane). The methane/ethylene mixtures reach its temperature maximum value of 1,820K and pressure maximum value of 1.84atm in less than 0.55ms, as presented in Figure 119 and Figure 120, which confirms the immediate ignition of the gas mixture. As shown in Figure 121, the reactants are heated for 0.43ms,

then the reaction takes place with a decreasing of C2H4, O2 and CH4 mole ratio, while the H2O, CO and CO2 mole ratios are increasing until the O2 is depleted. The reaction pathway of the methane/ethylene mixture at 1,300K, 1atm is presented in Figure 122. When the fuel mixture generates a temperature rise of 100K, the normalized sensitivity analysis is performed and compared for both CH4 and C2H4, as shown in Figure 123. The normalized sensitivities for CH4 and C2H4 are identical while the top 3 reaction steps that contributed most to the heat release are: $C2H3 + O2 \rightarrow O + CH2CHO$, $CH3 + C2H4 \rightarrow C2H3 + CH4$, $H + C2H4 \rightarrow C2H3 + H2$. And the reaction that contributed least to the heat generation is: $C2H3 + O2 \rightarrow HCO + CH2O$. The sensitivity analysis proves that, though the first rate limiting step of the methane/ethylene mixtures is different from ethylene UFL combustion; however, the major reaction rate limiting steps are similar to the ones of ethylene UFL combustion. When ethylene is mixed with methane for UFL test, the ethylene will be more reactive in the combustion process. Since unreacted methane takes certain percentage of the fuel, which dilutes the heat of the reaction, to propagate the flame, it requires more heat release from ethylene combustion, thus higher fuel concentration. Moreover, the methane prohibits some of the rate limiting reaction steps, which reduces the heat release and further dilutes the heat generated from ethylene combustion. Therefore, for methane/ethylene mixture UFL test, the experimental results tend to be higher than the predictions from mixture rules.

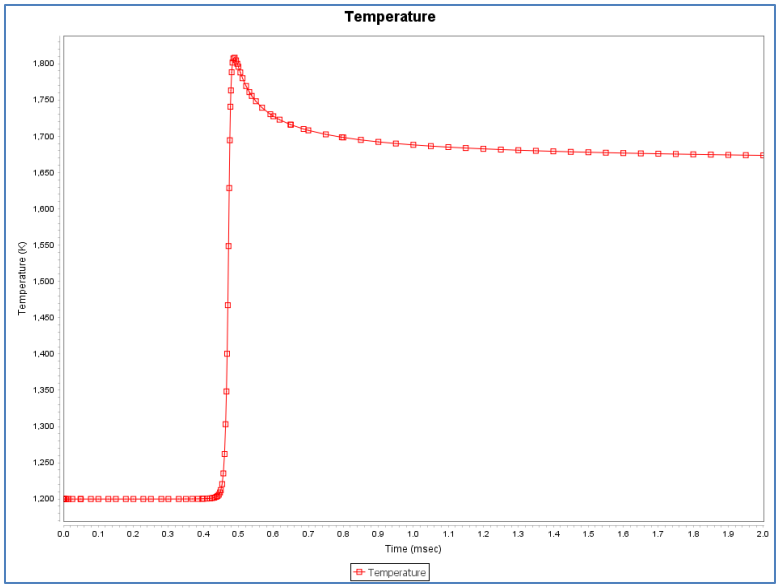

Figure 119 Temperature simulation profile of methane/ethylene (30:70) mixture at 1atm, 1200K and 33.1vol% fuel

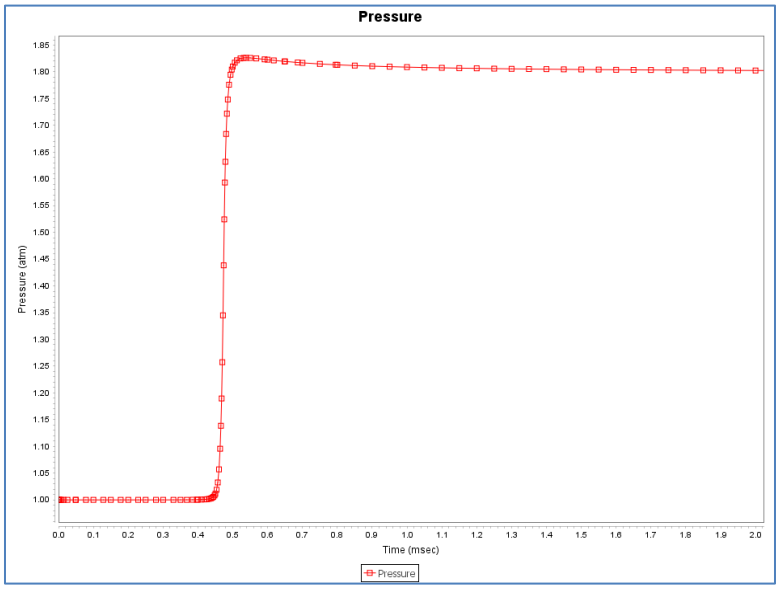

Figure 120 Pressure simulation profile of methane/ethylene (30:70) mixture at 1atm, 1200K and 33.1vol%fuel

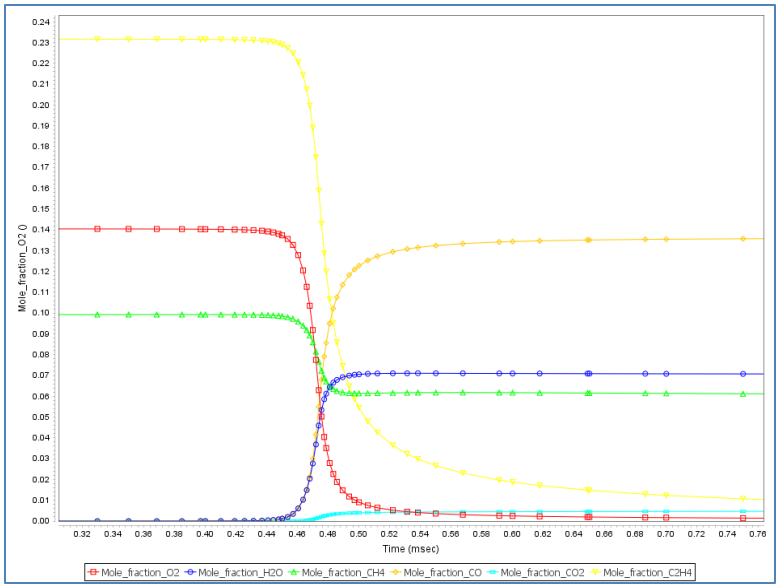

Figure 121 Mole fraction of major reactants and products profile of methane/ethylene (30:70) mixture at 1atm, 1200K and 33.1vol%

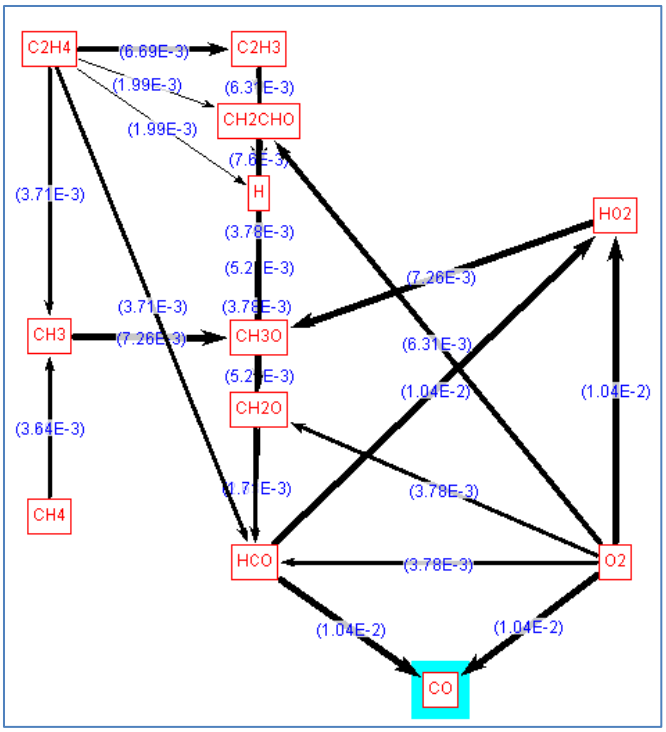

Figure 122 Reaction pathway of methane/ethylene (30:70) mixture at 1atm, 1300K

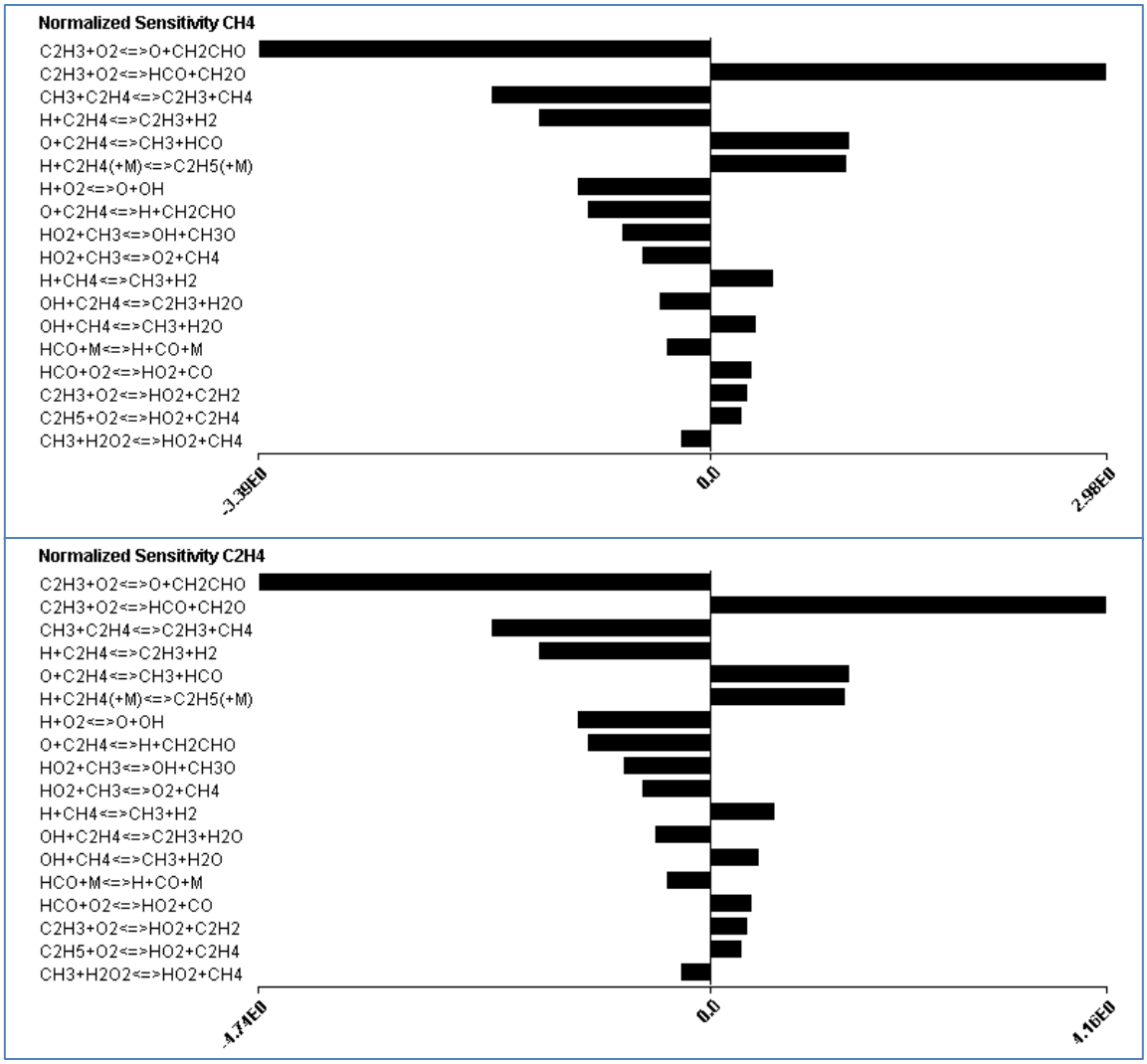

Figure 123 Normalized sensitivity analysis of methane/ethylene (30:70) mixture at 1atm, 1300K

6.3.3.3 Simulation of propane/ethylene mixture

The combustion simulation of propane/ethylene is also set at the condition of 1atm, 1,200K with 25.5vol% (30% propane). The propane/ethylene mixtures reach the maximum temperature of 1,770K and maximum pressure of 1.93atm in 0.35ms, as

presented in Figure 124 and Figure 125, correspondingly. As indicated in Figure 126, the combustion/oxidation reaction takes place in 0.32ms with decreasing of C3H8 and O2 mole fractions and rapid increasing of H2, CO, and H2O mole fractions. However, secondary reaction continues after 0.32ms, as the decomposition of C2H4 is still happening.

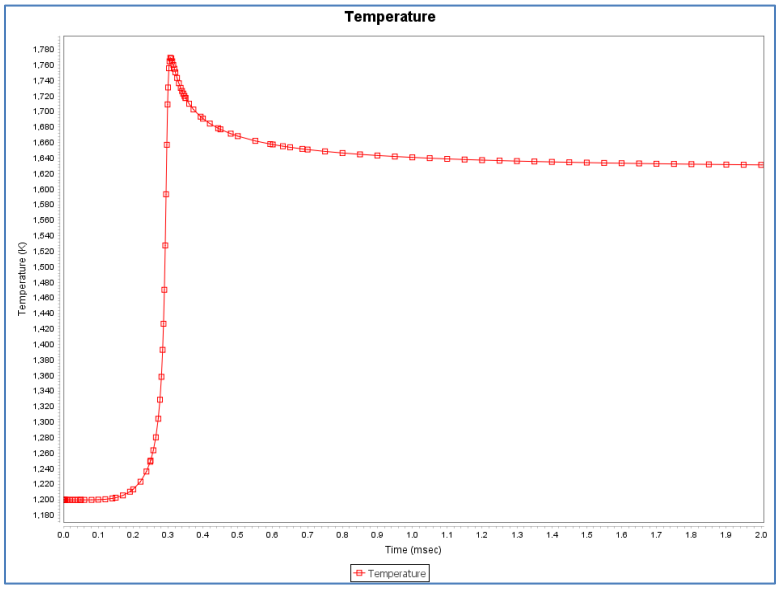

Figure 124 Temperature simulation profile of propane/ethylene (30:70) mixture at 1atm, 1200K and 25.5vol% fuel

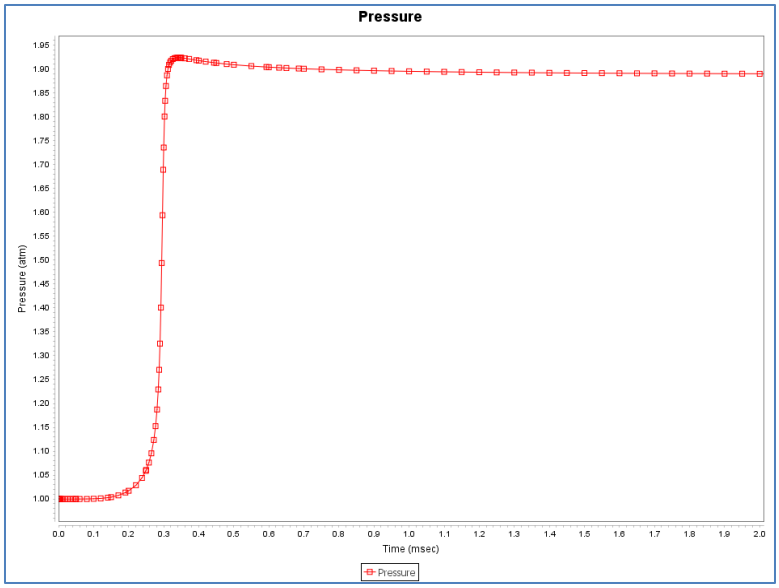

Figure 125 Pressure simulation profile of propane/ethylene (30:70) mixture at 1atm, 1200K and 25.5vol% fuel

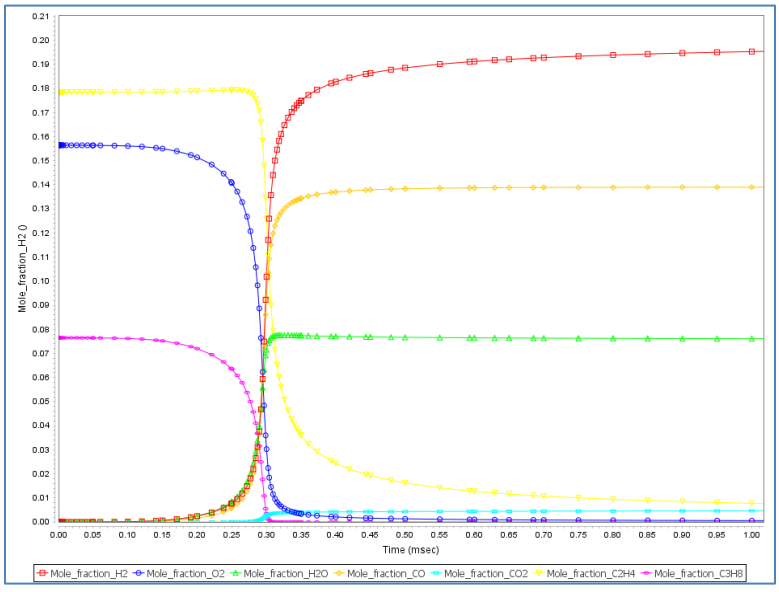

Figure 126 Mole fraction of major reactants and products profile of propane/ethylene (30:70) mixture at 1atm, 1200K and 25.5vol% fuel

The reaction pathway of propane/ethylene mixture is then studied at 1,300K, 1atm as presented in Figure 127. The reaction pathway shows that when the gas temperature reaches 1,300K, decomposition of propane is happening which generates shorter carbon chain products such as C2H3, C2H4, CH3, CH3O, etc.. The normalized sensitivity analysis is performed and compared for both C2H4 and C3H8, as shown in Figure 128. Though the reaction that contributed most and the reaction contributed least in the heat generation for C3H8 and C2H4 are the same, but the top 3 reactions that have the largest temperature sensitivities for C3H8 and C2H4 are different. This is mainly caused by the possible reactions of decomposition of C3H8 to form C2H4 during the initial stage of the combustion process. This can also be seen in the Figure 126, as the mole fraction of ethylene is actually increasing till 0.28ms. However, in the total normalized sensitivity analysis, the top 5 reactions that contributed to heat release are the same for both C3H8 and C2H4, which include: $OH + C2H4 \rightarrow C2H3 + H2O$, $HO2 + CH3 \rightarrow OH + CH3O$, $CH3 + C2H4 \rightarrow C2H3 + CH4$, $C2H3 + O2 \rightarrow O + CH2CHO$, $H + C2H4 \rightarrow C2H3 + H2$. The sensitivity analysis proves that the major reaction rate limiting steps are more similar to the ones of ethylene UFL combustion. Heat releases are more related to the activation of C2H4 to form C2H3 while the major endothermic reaction steps are more related to the decomposition of C3H8 to form C3H7. Therefore, although ethylene is more reactive than propane in the combustion process, ethylene will only have a greater impact when ethylene takes more than half of the fuel. When ethylene is on the lean side, the decomposition of propane, which consumes heat and generates hydrogen and extra ethylene, can also in turn support the combustion process,

thus fulfill the criterion of flammability limit. So for propane/ethylene mixture test, the experimentally measured UFL tend to be higher than the predictions only when ethylene is on the rich side.

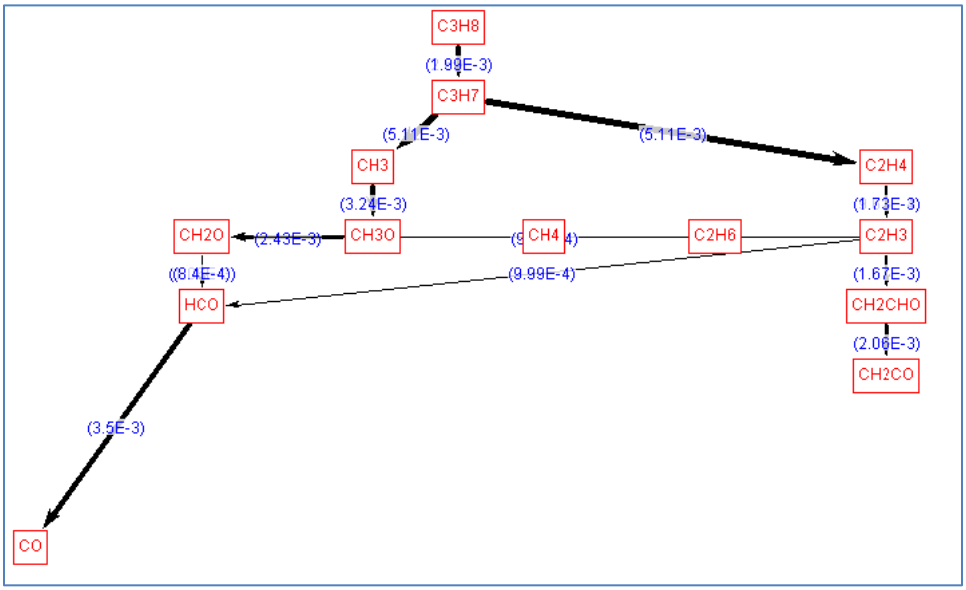

Figure 127 Reaction pathway of propane/ethylene (30:70) mixture at 1atm, 1300K

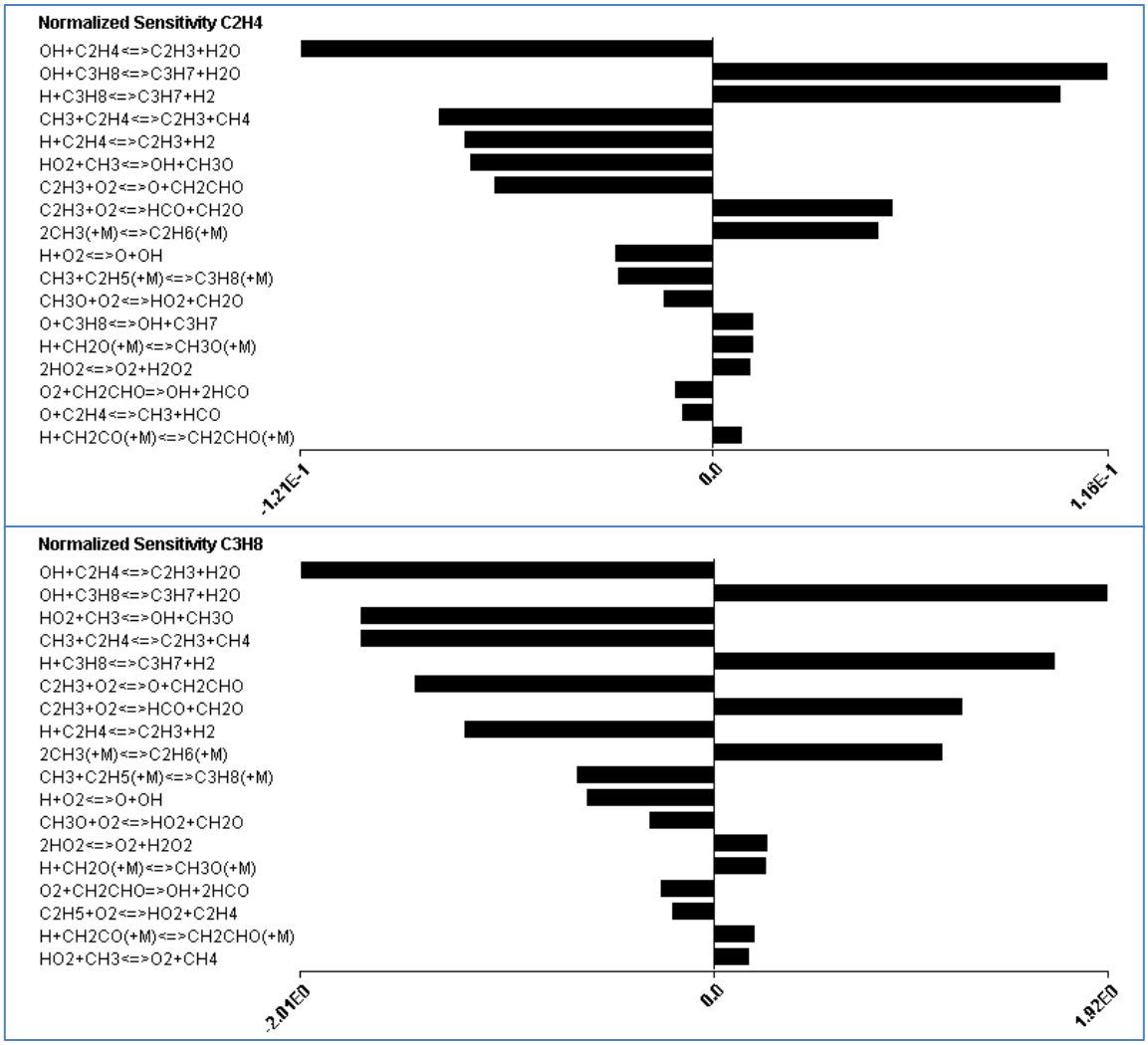

Figure 128 Normalized sensitivity analysis of ethylene (upper) and propane (lower) mixture at 1atm, 1300K

6.3.4 Reaction pathway analysis summary

Combustion reactions at upper flammability limit are complex. Upon using the ANSYS CHEMKIN software with accurate chemistry reaction kinetics and transport simulations, detailed reaction mechanism at UFL was investigated.

Due to the research study scope, the primary focus of this study is about the experimental measurement of flammability limit. The simulation study using CHEMKIN is a supportive tool to prove and analyze the large deviation between the experimental data and predictions. The usage of simulation program is very basic and none of the fundamental reaction kinetics or the thermodynamic properties is touched. The study here is section 6.3 is a good indicator that the CHEMKIN software can be used as a tool to solve reaction mechanism problems. And it is recommended that in the future, the simulation of reaction pathway for different light hydrocarbon mixtures can be an independent research work.

While based on the simulation study in this work, detailed UFL combustion mechanisms of pure methane, propane and ethylene are identified. Most temperature sensitive reaction steps are confirmed for the heat release and the flame propagation of each pure light hydrocarbon gas. Then, the UFL combustion mechanisms of binary mixtures are explored. Most and least temperature sensitive reaction steps are identified and compared with the rate limiting steps of pure light hydrocarbon gas combustions. It is proved that for UFL test, ethylene is more reactive than methane and propane in the combustion process. When ethylene is rich in the fuel mixtures, the activation of C2H4 to form C2H3 usually contribute the most heat release in the oxidation mechanisms.

However, even though the ANSYS CHEMKIN software is a robust program that has the capabilities to calculate kinetics and transport problems simultaneously, the simulation is still limited to the extent of CFD codes and assumptions. The CFD codes used for binary mixture are not primarily designed to study the UFL combustions

especially for mixtures involving propane and ethylene. Also in this study, the reaction mechanisms of nitrogen oxidation and soot formation are not taken into consideration. Therefore, for the future work, a more comprehensive kinetics file that includes reaction mechanism for methane, propane and ethylene is necessary. Also, more reaction conditions including lower reaction temperature and heat loss to surroundings should be added in the simulation.

6.4 Flammability limit predictions for binary mixtures

The comparison of experimental data and predictions from Le Chatelier's Rule proves that the Le Chatelier's rule works well for LFL predictions of saturated hydrocarbon mixtures. But when the hydrocarbon mixtures involve unsaturated hydrocarbons, the predictions start to deviate from experimental data, especially at elevated conditions. Therefore, a more accurate prediction method is needed.

As illustrated by Zhao [8], a feasible prediction method is to perform modification on the Le Chatelier's Rule [39] as presented in Equation 21,

$$\frac{1}{FL_{mix}} = \frac{y^{\mu}}{FL_{fuel\ I}} + \frac{(1-y)^{\theta}}{FL_{fuel\ II}} \quad (21)$$

where y is the mole fraction of fuel I in the fuel mixtures, and FL_{fuel} is the measured flammability limit of the fuel species in volume percent, FL_{mix} is the flammability limit of the gas mixtures, while μ and θ are the coefficient for each reaction condition and reactant species.

Figure 129-152 and Table 17-18 represent the calculation results using modified Le Chatelier's Rule and the comparison of experimental data with the predictions from

modified Le Chatelier's Rule. As shown in Table 17-18, the absolute deviation of the prediction from experimental data proves that this new prediction method is able to predict the flammability limit of binary mixtures with a maximum error of ±4.3%, which is a great improvement compared to the yield percentage in Table 13. The absolute deviation in Table 13 refers to the absolute value of difference between experimental value and predictions using modified Le Chatelier's rule.

However, it is important to mention that equation 21 is a best fitting calculation based on experimental measured results presented in this study without consideration of detailed reaction kinetics or thermodynamic property of the flammable gases. Therefore, the equation and the coefficient presented in this section can only work with the gas species of binary mixtures of methane, propane and ethylene with limited reaction conditions (Temperature: 20 ℃ or 200 ℃, Pressure: 1atm or 2atm). More study with different reaction conditions is needed to characterize the correlation between the coefficient μ, θ and temperature/pressure/gas species. The equation 21 may not be suitable for the prediction of mixture flammability involving other light hydrocarbon gases (such as ethane, propylene, acetylene).

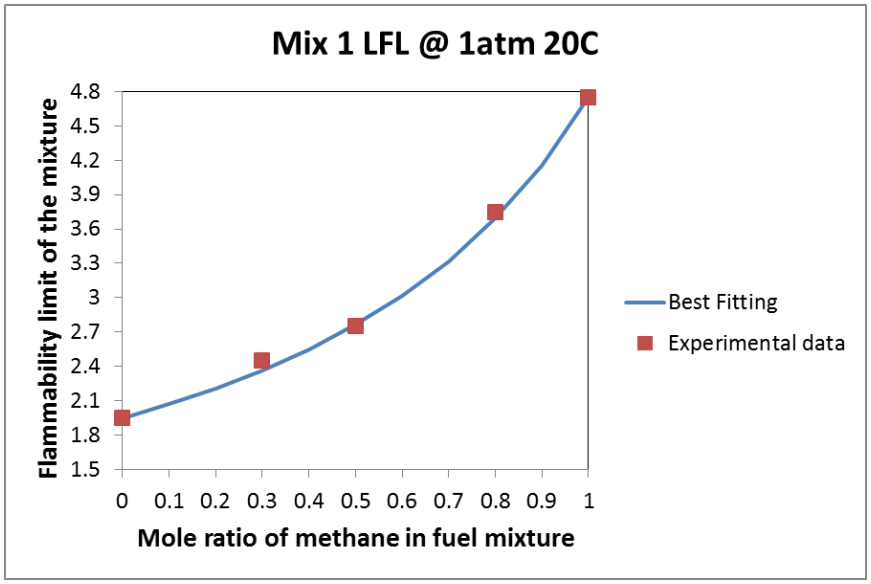

Figure 129 LFL of methane(30%, 50% 80%) /propane mixture and predictions from Le Chatelier's rule at 1atm 20 °C

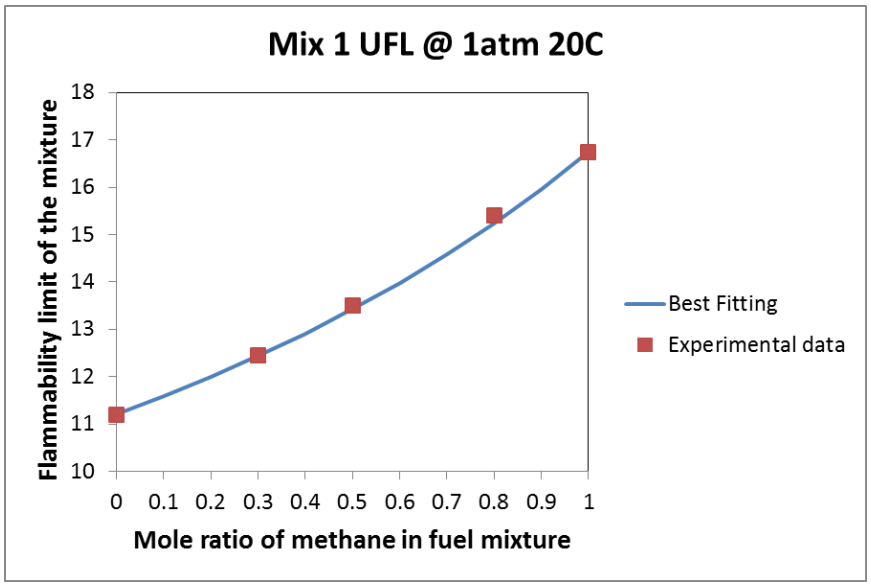

Figure 130 UFL of methane(30%, 50% 80%) /propane mixture and predictions from Le Chatelier's rule at 1atm 20 °C

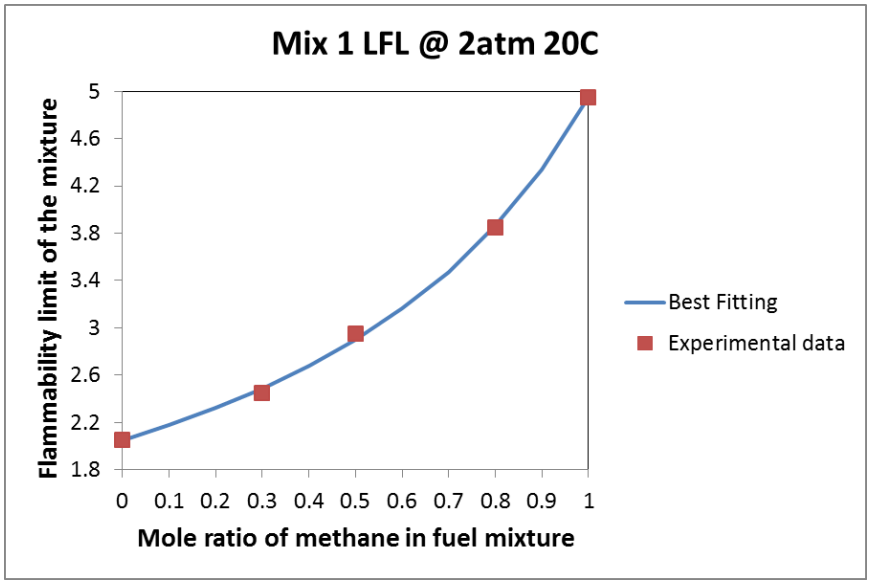

Figure 131 LFL of methane(30%, 50% 80%) /propane mixture and predictions from Le Chatelier's rule at 2atm 20 °C

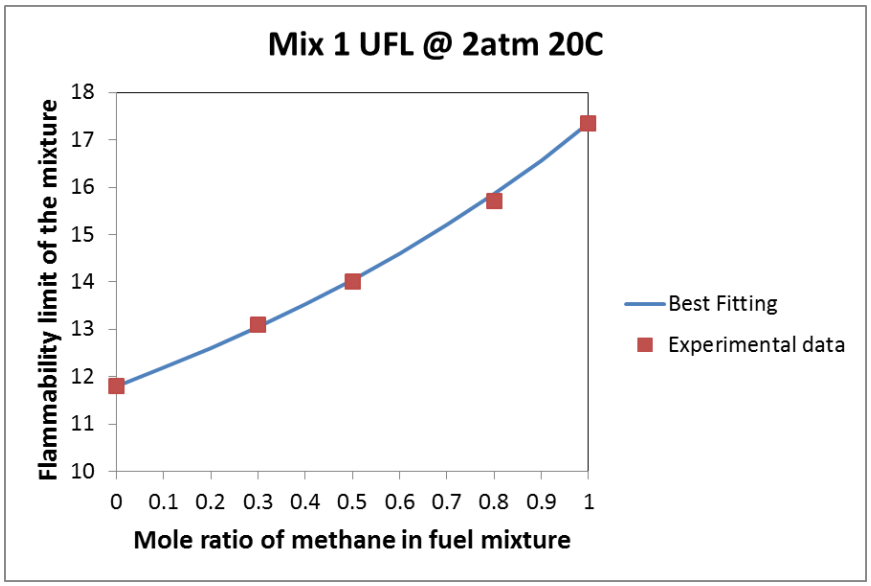

Figure 132 UFL of methane(30%, 50% 80%) /propane mixture and predictions from Le Chatelier's rule at 2atm 20° C

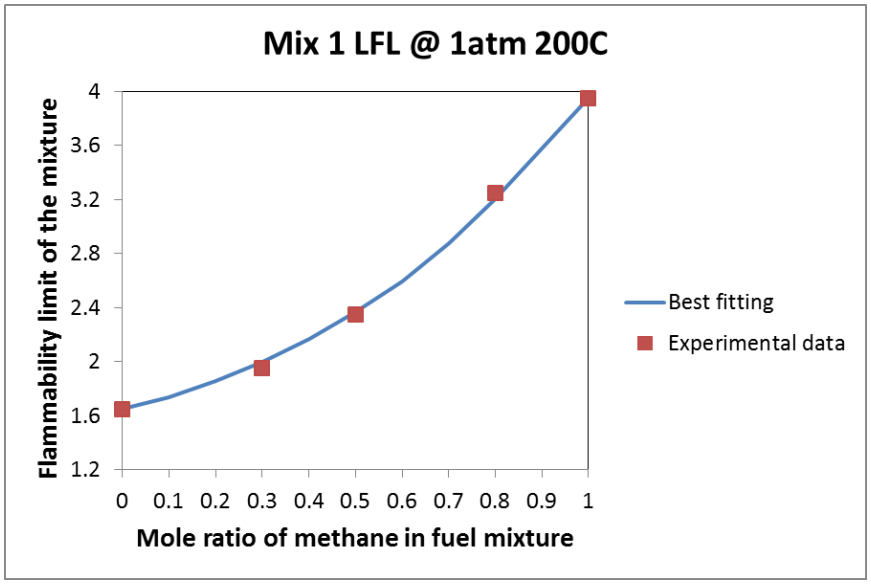

Figure 133 LFL of methane(30%, 50% 80%) /propane mixture and predictions from Le Chatelier's rule at 1atm 200 °C

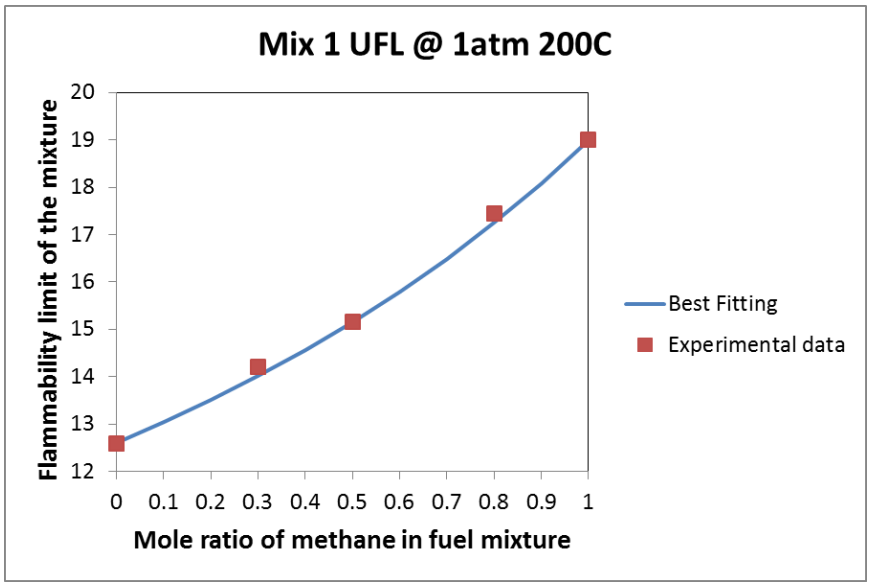

Figure 134 UFL of methane(30%, 50% 80%) /propane mixture and predictions from Le Chatelier's rule at 1atm 200° C

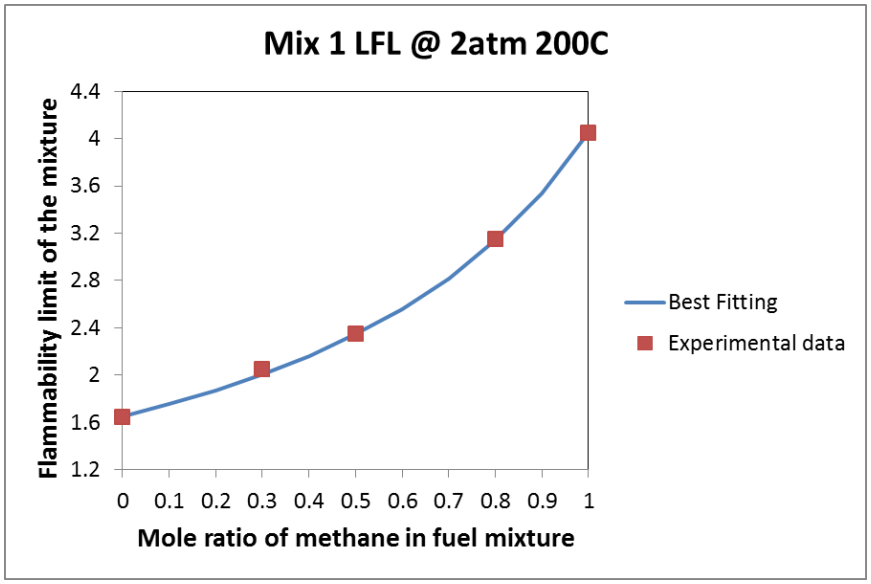

Figure 135 LFL of methane(30%, 50% 80%) /propane mixture and predictions from Le Chatelier's rule at 2atm 200 °C

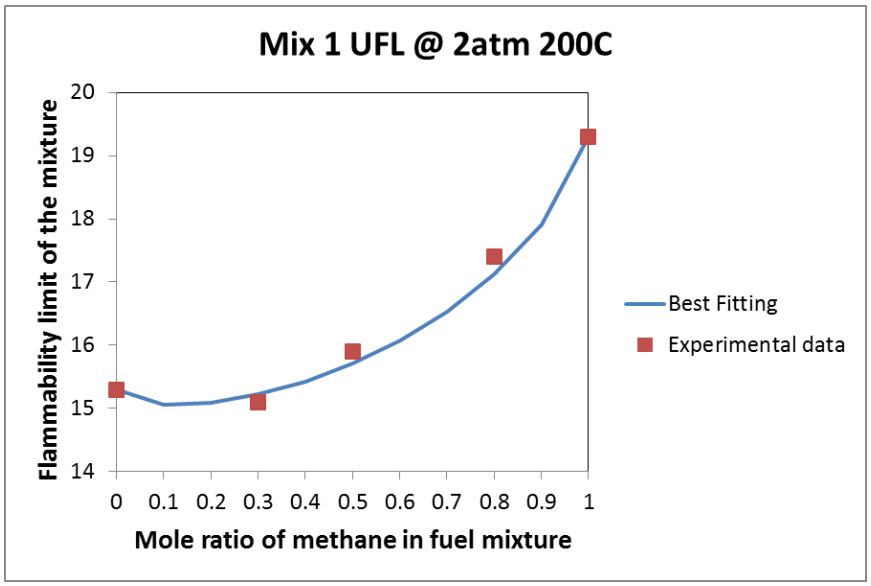

Figure 136 UFL of methane(30%, 50% 80%) /propane mixture and predictions from Le Chatelier's rule at 2atm 200° C

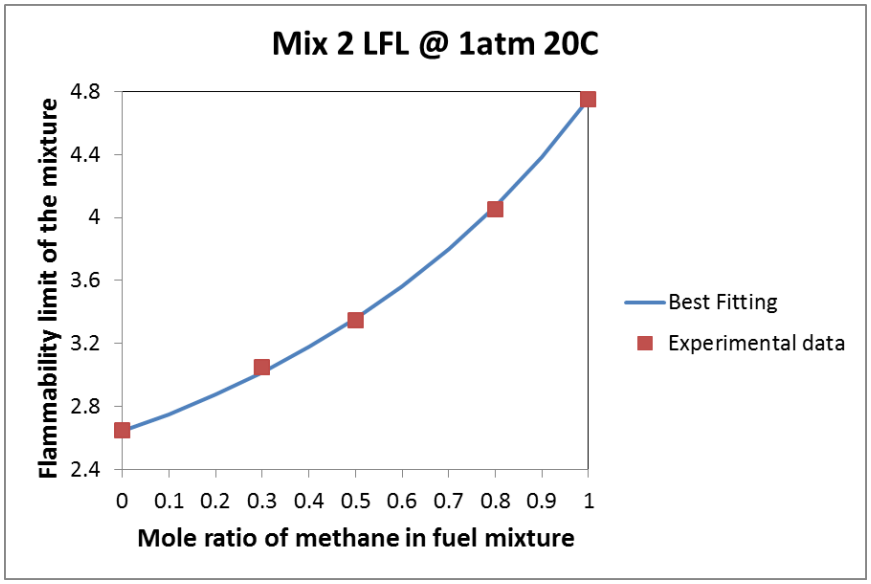

Figure 137 LFL of methane(30%, 50% 80%) /ethylene mixture and predictions from Le Chatelier's rule at 1atm 20 °C

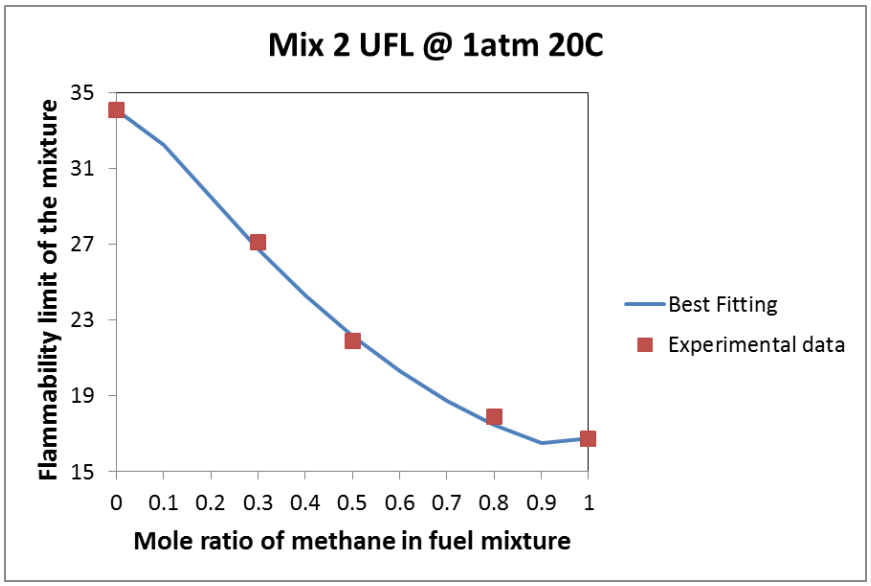

Figure 138 UFL of methane(30%, 50% 80%) /ethylene mixture and predictions from Le Chatelier's rule at 1atm 20° C

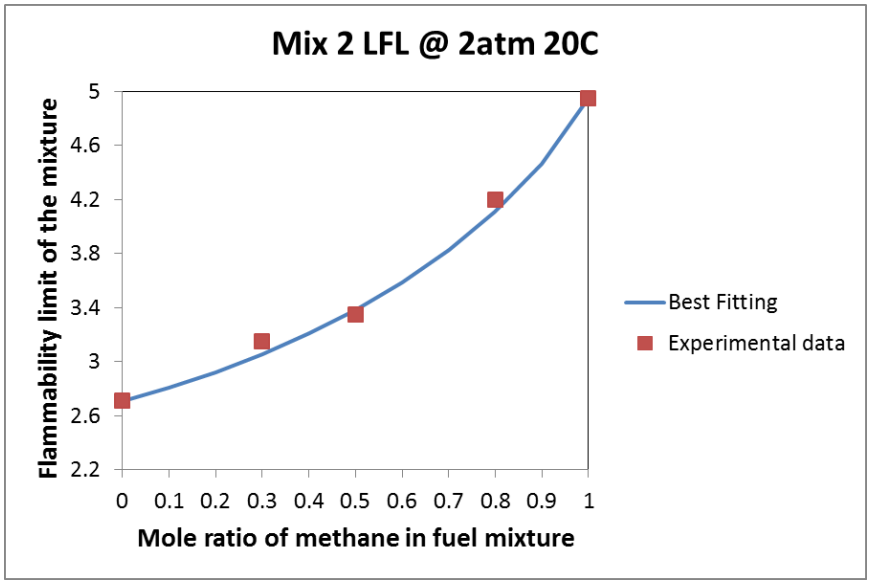

Figure 139 LFL of methane(30%, 50% 80%) /ethylene mixture and predictions from Le Chatelier's rule at 2atm 20 °C

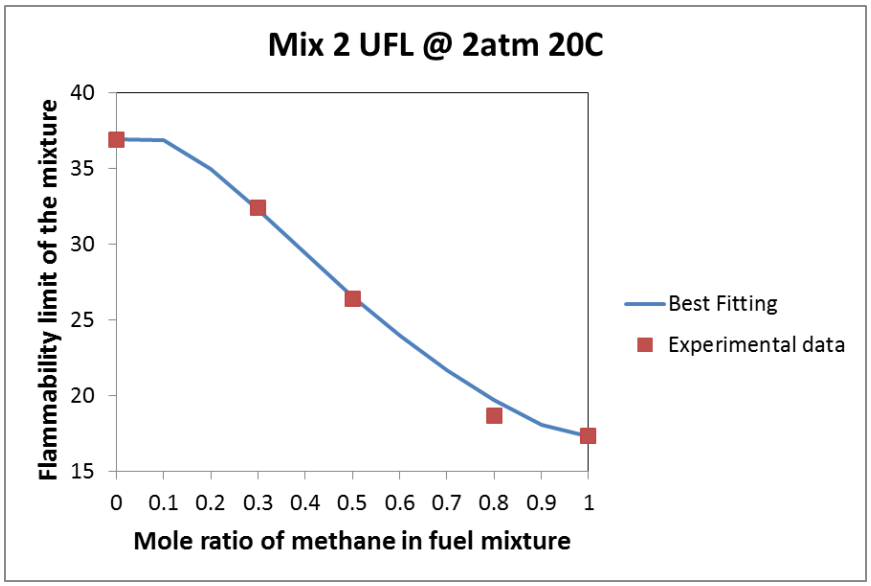

Figure 140 UFL of methane(30%, 50% 80%) /ethylene mixture and predictions from Le Chatelier's rule at 2atm 20° C

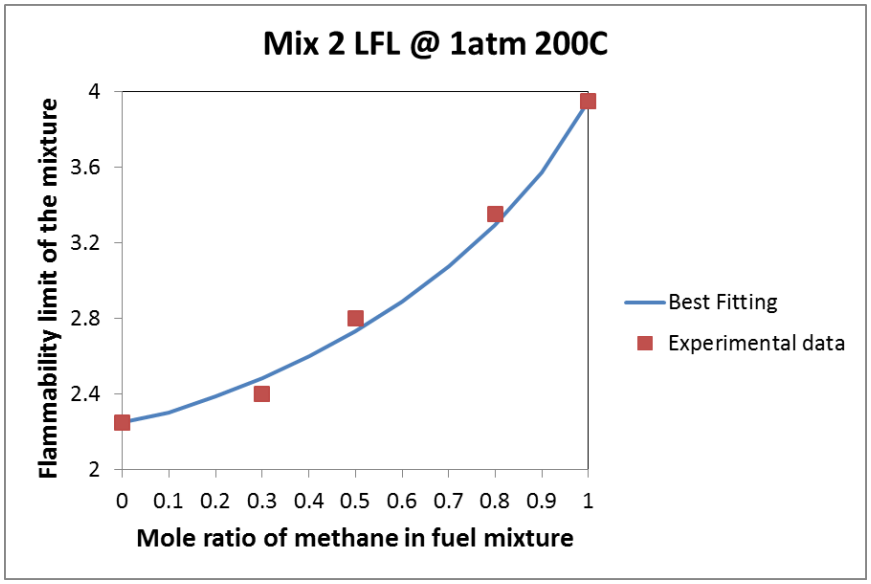

Figure 141 LFL of methane(30%, 50% 80%) /ethylene mixture and predictions from Le Chatelier's rule at 1atm 200 °C

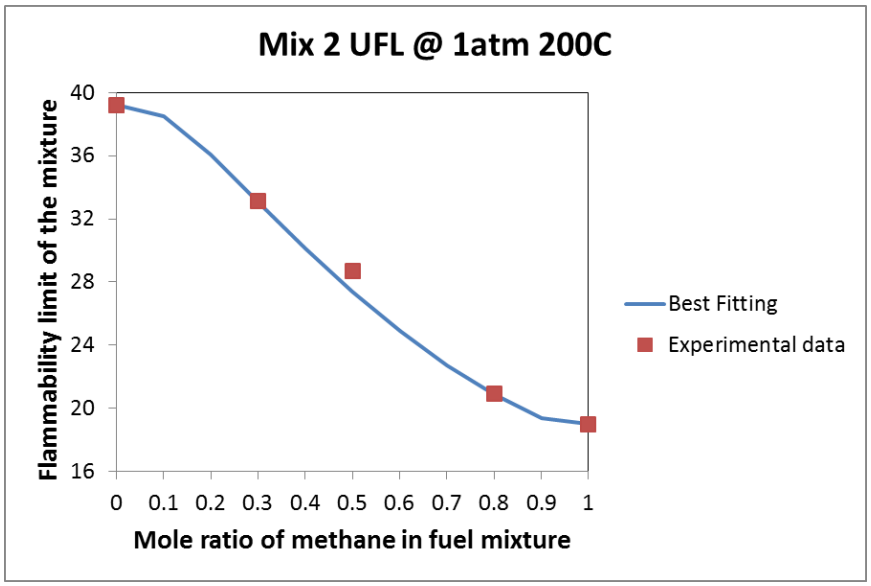

Figure 142 UFL of methane(30%, 50% 80%) /ethylene mixture and predictions from Le Chatelier's rule at 1atm 200° C

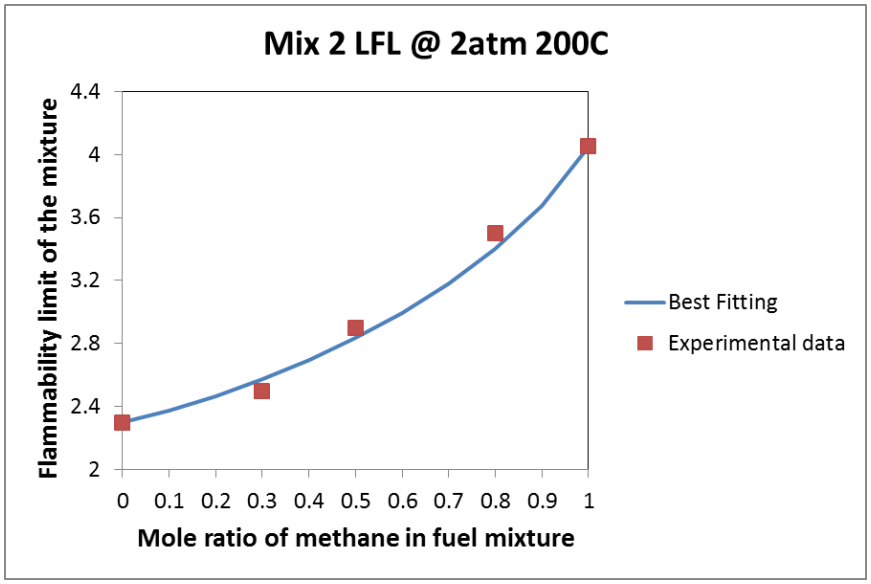

Figure 143 LFL of methane(30%, 50% 80%) /ethylene mixture and predictions from Le Chatelier's rule at 2atm 200 °C

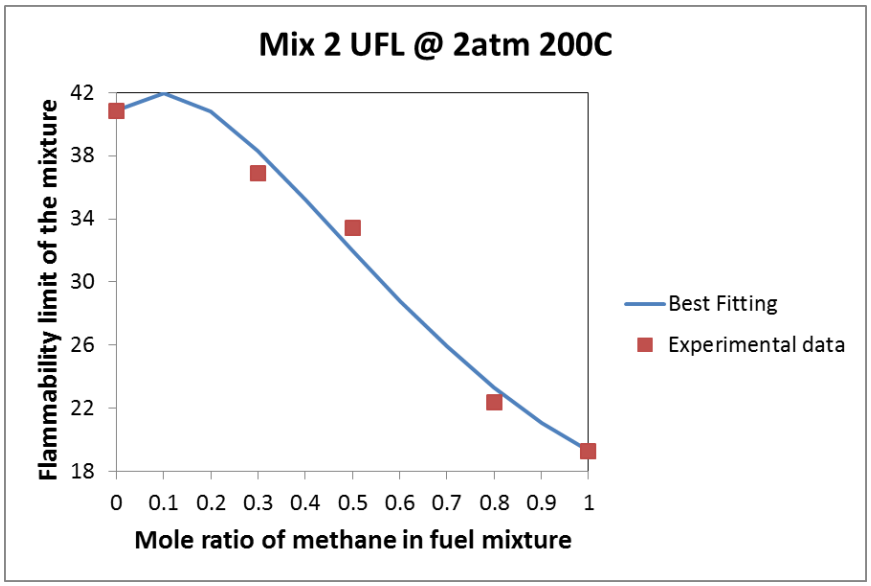

Figure 144 UFL of methane(30%, 50% 80%) /ethylene mixture and predictions from Le Chatelier's rule at 2atm 200° C

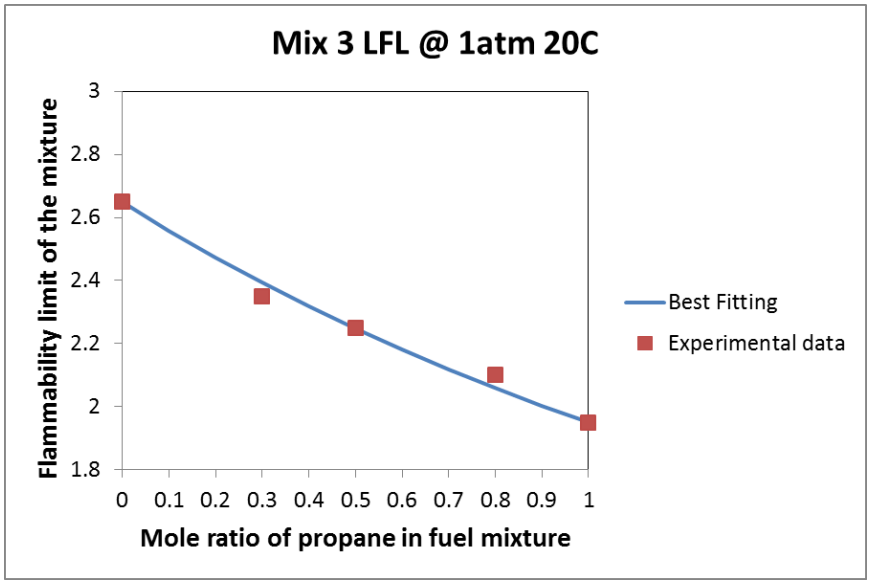

Figure 145 LFL of propane(30%, 50% 80%) /ethylene mixture and predictions from Le Chatelier's rule at 1atm 20 °C

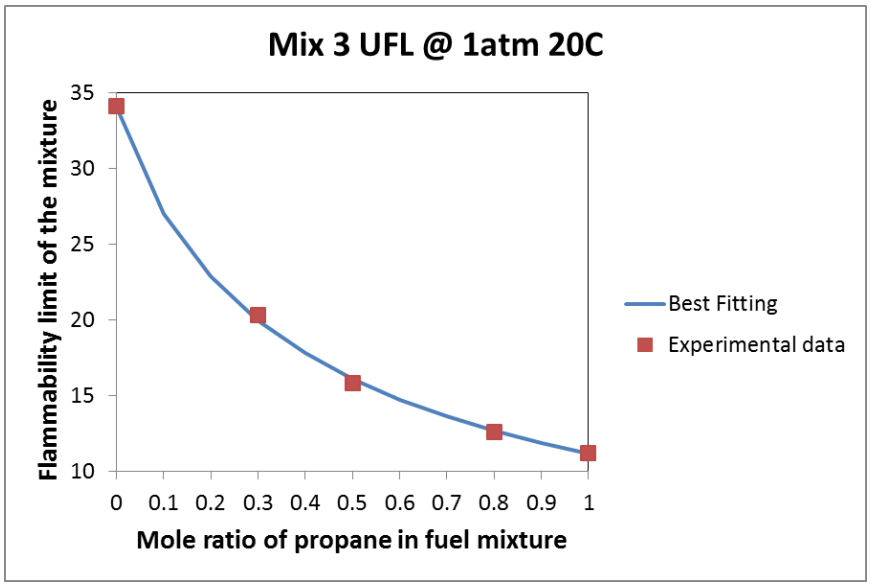

Figure 146 UFL of propane(30%, 50% 80%) /ethylene mixture and predictions from Le Chatelier's rule at 1atm 20° C

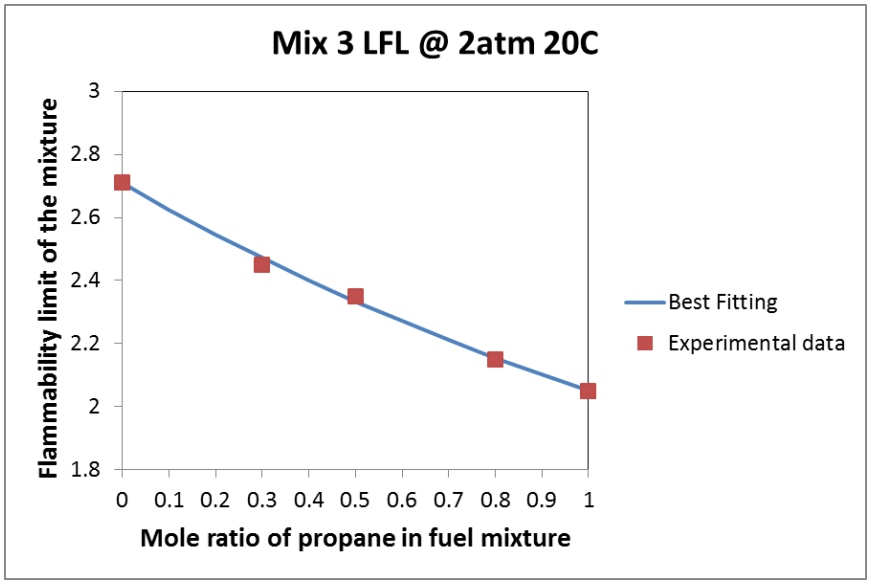

Figure 147 LFL of propane(30%, 50% 80%) /ethylene mixture and predictions from Le Chatelier's rule at 2atm 20 °C

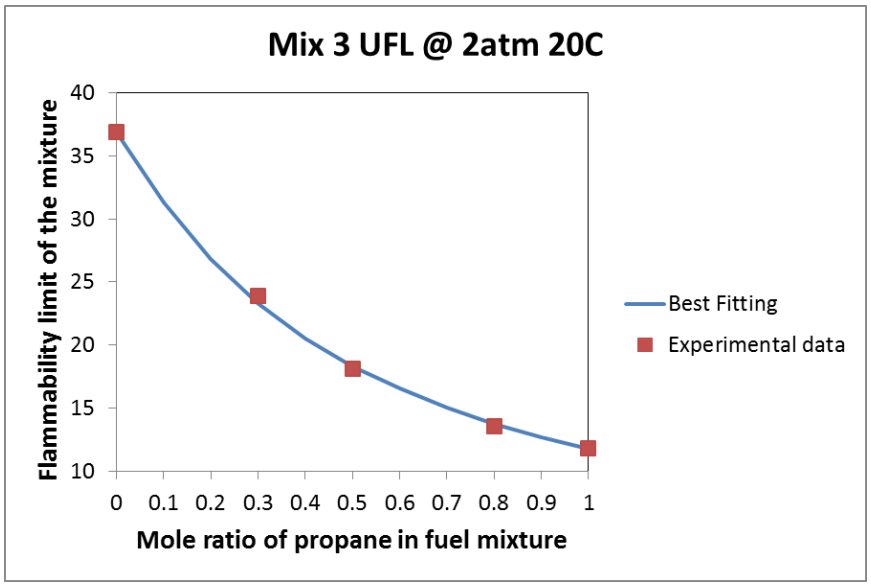

Figure 148 UFL of propane(30%, 50% 80%) /ethylene mixture and predictions from Le Chatelier's rule at 2atm 20° C

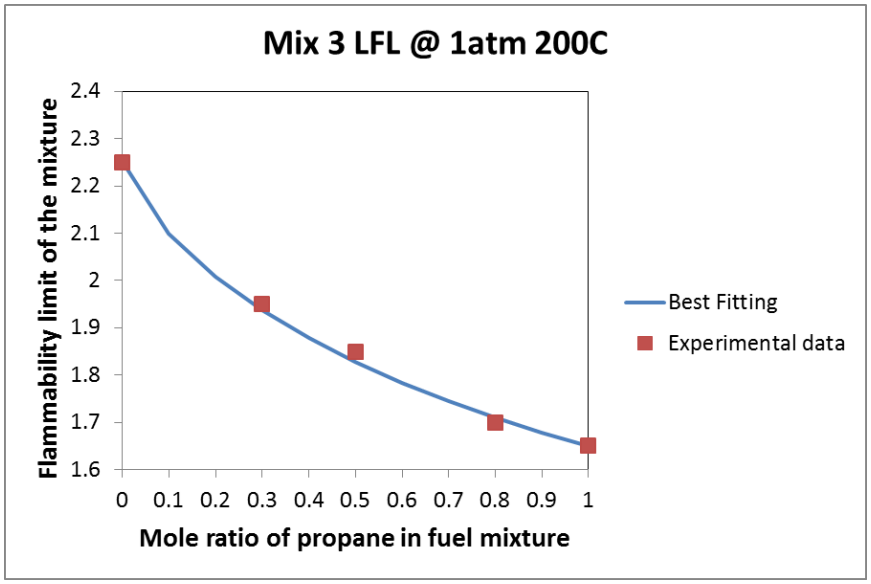

Figure 149 LFL of propane(30%, 50% 80%) /ethylene mixture and predictions from Le Chatelier's rule at 1atm 200 °C

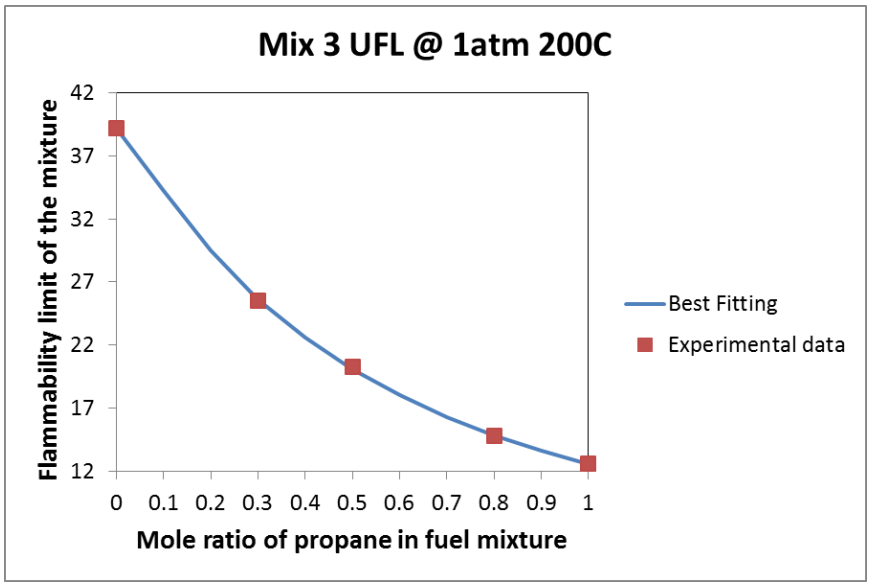

Figure 150 UFL of propane(30%, 50% 80%) /ethylene mixture and predictions from Le Chatelier's rule at 1atm 200° C

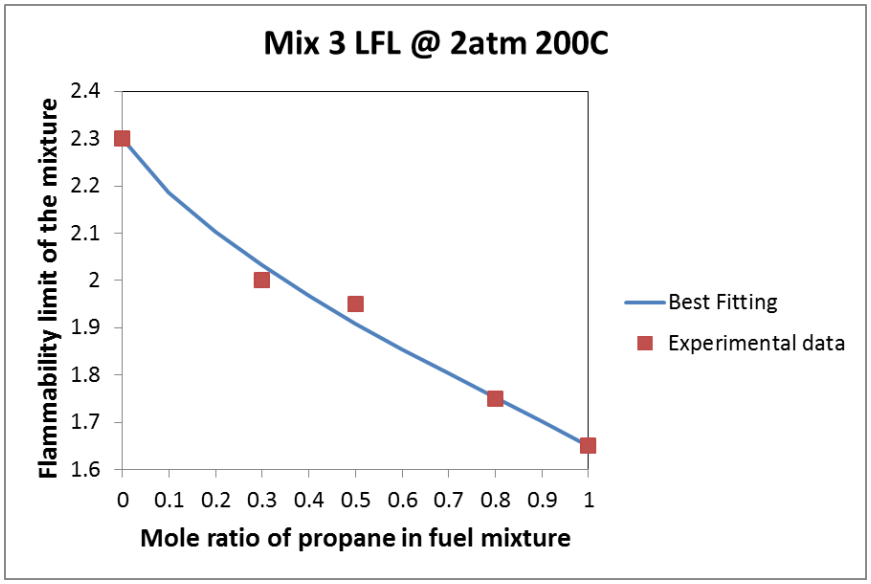

Figure 151 LFL of propane(30%, 50% 80%) /ethylene mixture and predictions from Le Chatelier's rule at 2atm 200 °C

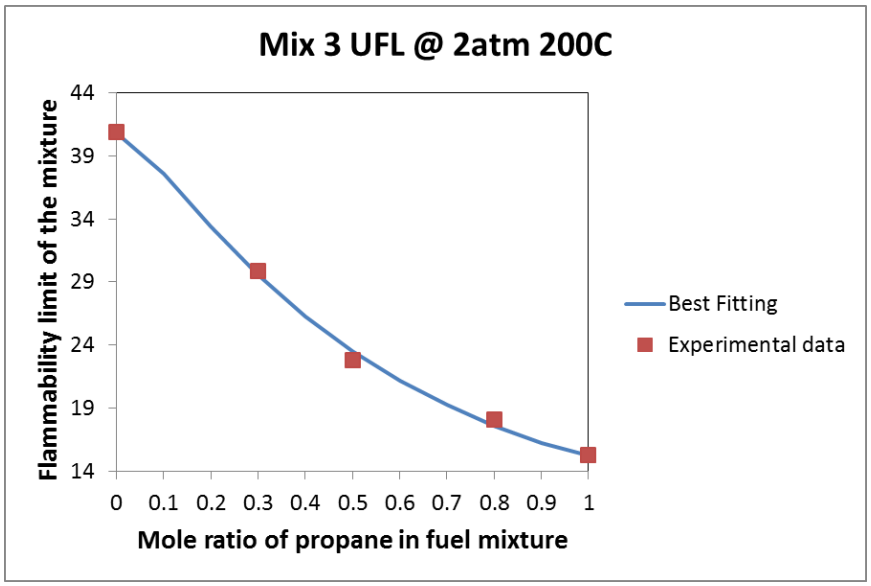

Figure 152 UFL of propane(30%, 50% 80%) /ethylene mixture and predictions from Le Chatelier's rule at 2atm 200 °C

Table 17 Modified Le Chatelier's rule prediction and coefficient for methane and propane mixture

Mix I	CH4 & C3H8		Experimental data					Coefficient		Modified Le Chatelier's Rule Prediction			Absolute Dev from experimental data		
	T (℃)	P (atm)	0	30%	50%	80%	100%	μ	θ	30%	50%	80%	30%	50%	80%
LFL	20	1	1.95	2.45	2.75	3.75	4.75	1	1	2.37	2.76	3.69	3.3%	0.5%	1.6%
	20	2	2.05	2.45	2.95	3.85	4.95	1	1	2.49	2.90	3.86	1.5%	1.7%	0.2%
	200	1	1.65	1.95	2.35	3.25	3.95	0.85	1.1	2.00	2.36	3.20	2.5%	0.6%	1.6%
	200	2	1.65	2.05	2.35	3.15	4.05	1	1	2.01	2.34	3.14	2.1%	0.2%	0.4%
UFL	20	1	11.2	12.45	13.5	15.4	16.75	1	1	12.44	13.42	15.24	0.1%	0.6%	1.0%
	20	2	11.8	13.1	14	15.7	17.35	1	1	13.05	14.05	15.86	0.4%	0.3%	1.0%
	200	1	12.6	14.2	15.15	17.45	19	1	1	14.02	15.15	17.25	1.3%	0.0%	1.2%
	200	2	15.3	15.1	15.9	17.4	19.3	0.88	0.88	15.22	15.71	17.11	0.8%	1.2%	1.6%

Table 18 Modified Le Chatelier's rule prediction and coefficient for methane and ethylene mixture

Mix II	CH4 & C2H4		Experimental data					Coefficient		Modified Le Chatelier's Rule Prediction			Absolute Dev from experimental data		
	T (℃)	P (atm)	0	30%	50%	80%	100%	μ	θ	30%	50%	80%	30%	50%	80%
LFL	20	1	2.65	3.05	3.35	4.05	4.75	0.95	1	3.02	3.36	4.07	1.0%	0.3%	0.5%
	20	2	2.71	3.15	3.35	4.2	4.95	0.95	0.95	3.06	3.38	4.11	3.0%	1.0%	2.2%
	200	1	2.25	2.4	2.8	3.35	3.95	0.9	0.95	2.49	2.73	3.30	3.6%	2.3%	1.6%
	200	2	2.3	2.5	2.9	3.5	4.05	0.95	0.95	2.57	2.83	3.40	3.0%	2.3%	2.8%
UFL	20	1	34.1	27.1	21.9	17.9	16.75	1.25	0.55	26.77	22.16	17.46	1.2%	1.2%	2.5%
	20	2	36.9	32.4	26.4	18.7	17.35	1.5	0.65	32.30	26.56	19.70	0.3%	0.6%	5.3%
	200	1	39.2	33.1	28.7	20.9	19	1.45	0.62	33.11	27.37	20.87	1.9%	2.8%	0.8%
	200	2	40.85	36.9	33.4	22.4	19.3	1.55	0.85	38.32	31.97	23.31	3.9%	4.3%	4.1%

Table 19 Modified Le Chatelier's rule prediction and coefficient for propane and ethylene mixture

Mix III	C3H8 & C2H4		Experimental data					Coefficient		Modified Le Chatelier's Rule Prediction			Absolute Dev from experimental data		
	T (℃)	P (atm)	0	30%	50%	80%	100%	μ	θ	30%	50%	80%	30%	50%	80%
LFL	20	1	2.65	2.35	2.25	2.1	1.95	1	1	2.39	2.25	2.06	1.8%	0.1%	2.0%
	20	2	2.71	2.45	2.35	2.15	2.05	1	1	2.47	2.33	2.15	0.9%	0.7%	0.2%
	200	1	2.25	1.95	1.85	1.7	1.65	0.9	1	1.94	1.83	1.71	0.7%	1.2%	0.6%
	200	2	2.3	2	1.95	1.75	1.65	0.95	1.05	2.03	1.91	1.75	1.6%	2.1%	0.2%
UFL	20	1	34.1	20.3	15.8	12.6	11.2	0.93	0.95	19.98	16.12	12.67	1.6%	2.0%	0.6%
	20	2	36.9	23.9	18.1	13.6	11.8	1.05	1	23.31	18.36	13.80	2.5%	1.4%	1.5%
	200	1	39.2	25.5	20.3	14.8	12.6	1.1	1	25.66	20.09	14.88	0.6%	1.0%	0.6%
	200	2	40.85	29.9	22.8	18.1	15.3	1.2	0.8	29.57	23.52	17.62	1.1%	3.2%	2.7%

7. CONCLUSIONS AND FUTURE WORK

7.1 Summary and conclusions

The primary objective of this study was to design and conduct experiments to measure the flammability limits of pure light hydrocarbons (methane, propane, and ethylene) and binary mixtures at both normal conditions and elevated conditions. For this purpose, different experimental criteria (combustion behavior, flame propagation distance, maximum explosion pressure and maximum temperature rise) were used to identify the best flammability limit criterion for non-standard reaction apparatus. It was found that both pressure criteria and flame propagation criterion were suitable for the flammability limit experimental measurement. However, the flame propagation criterion could involve probabilistic uncertainty due to random errors in the propagation distance measurement and flame turbulence, especially at the upper flammability limit where the flame was developing slowly and asymmetrically after the ignition. Therefore, 7% pressure criterion, which is a conservative standard, was applied for the determination of flammability limit in this work.

With the determined criterion, the experimental measurement for the flammability limit started with pure light hydrocarbons including methane, propane and ethylene. The tests were conducted at the initial condition of temperature from ambient to maximum 300 ℃ and pressure up to 2 atm. Measurement results were plotted and compared with theoretical predictions to study the apparatus effect, temperature effect and initial pressure effect on pure light hydrocarbons. It was found that:

- For the apparatus effect, when the concentration of fuel was close to stoichiometric ratio, the maximum explosion pressure values generated using cylindrical vessel and spherical vessel were similar. When the concentration was away from the stoichiometric ratio and getting close towards the flammability limits, the cylindrical vessel generated higher explosion pressure. However, once the concentration of fuel reached exactly flammability limit boundary, the maximum explosion pressure was the same again. Also, cylindrical vessel would generate wider flammability range for saturated light hydrocarbons.
- For temperature dependence, it was confirmed that both LFL and UFL varies linearly with temperature rise. Temperature dependence coefficient c and calculated coefficient α were compared with previous literature. Experimental data proved that the modified Burgess and Wheeler law only works with lower flammability limit and the temperature dependence coefficient are also related to the gas species and the test initial pressure.
- For pressure effect, experimental data showed that as the initial pressure increases, both LFL and UFL increase, and predicted values from literature were significantly higher than the experimental results.

With the study of temperature effect and pressure effect, an estimation equation used for the flammability limit prediction of pure methane, propane and ethylene at elevated conditions was developed.

Experimental measurements were also carried out for binary mixtures at normal and elevated conditions. Experimental data were compared with predictions from Le

Chatelier's Rule to validate its application at elevated reaction conditions. It was proved that Le Chatelier's rule works well for LFL predictions of saturated hydrocarbon mixtures. But when the hydrocarbon mixtures involved unsaturated hydrocarbons, the LFL predictions started to deviate from experimental data, especially at elevated conditions. For UFL predictions, Le Chatelier's rule only worked for normal conditions, large deviations from experimental data were discovered for all elevated conditions, especially for the binary mixtures rich in ethylene.

The explanation of the difference between predictions and experimental data were analyzed through the investigation of binary mixture temperature dependence and combustion reaction pathway. The reaction pathway analysis was conducted using ANSYS CHEMKIN software. Detailed UFL combustion mechanisms of pure methane, propane and ethylene were identified. Most temperature sensitive reaction steps were confirmed for the heat release and the flame propagation. Also, the UFL combustion mechanisms of binary mixtures were explored to identify the most and least temperature sensitive reaction steps. It was shown that in the UFL test, ethylene was more reactive than methane and propane in the combustion process. When ethylene was rich in the fuel mixtures, the activation of C2H4 to form C2H3 usually contributed the most heat release in the oxidation reaction mechanisms.

Finally, for better prediction of binary mixture flammability limit, modification of Le Chatelier's Rule was improved. Then, the calculated results from modified Le Chatelier's Rule were compared with experimental data. It was the validated that the

modified Le Chatelier's Rule is capable to predict the flammability limit of hydrocarbon mixtures with a maximum error of ±4.3%.

7.2 Future work

In this study, due to limited timeframe and the research scope, the experiments conducted only include methane, propane and ethylene. For better predictions of pure components flammability limit at elevated conditions, it is recommended to include other gas species such as ethane, butane, propylene and acetylene. Also, though the reaction vessel has the capability to test flammability for the entire temperature range from room temperature to 300 ℃, the temperature selection in this study are limited to 20 ℃, 50 ℃, 100 ℃, 200 ℃, 300 ℃ for pure fuel, 20 ℃ and 200 ℃ for binary mixtures. For better understanding of temperature effect on the flammability limit, a smaller temperature increment steps is necessary. More data at the elevated conditions would not only help by providing extra data information, but would also enhance the reliability of the prediction model. For binary mixture study, more data are needed for different fuel mixture ratios (10:90, 40:60, 75:25, etc.).

The experimental data generation speed is mainly constrained by the manual operation of the equipment. Repetitive experiment at same reaction conditions can be time consuming. Therefore, an upgrade in the flammability apparatus to make the equipment automated could benefit future experiments. Using actuated parts such as solenoid valves, actuated valves and pressure sensors for automatic control of gas loading can greatly reduce the time needed for the gas sample preparation.

The other proposed study is related to the investigation of the combustion product. Analysis of the combustion products, especially the products from UFL test, would greatly benefit the study of reaction mechanism of partial oxidation and fuel decomposition. For this purpose, gas sample, which is collected from the reaction vessel, should be further analyzed using GC-MS to identify the concentration of each component. With appropriate design and modification on equipment, an on-line GC-MS can be installed.

Except the future work in the experimental measurement, the simulation work of reaction mechanism can also be extended. Since in this study, the CFD codes used for binary mixture are not primarily designed to study the UFL combustions of propane and ethylene, a more comprehensive kinetics file that includes reaction mechanism for methane, propane and ethylene is necessary. Also, more reaction conditions including lower reaction temperature and heat loss to surroundings should be added in the simulation to better study the real oxidation process that take place during the combustion process in the experiment.

REFERENCES

1. Wen P-j, Shu C-m, Chang Z-c, Chen S-C, Shyu M-L. Effects of Initial Pressure on the Flammability Limit of OX-Air Mixture with 20-L-Appartus. 2001.

2. News TA. Williams Olefins contests OSHA findings stemming from explosion at Geismar plant. The Advocate News.

3. Zabetakis MG. Flammability Characteristics of Combustible Gases and Vapors. U.S. Department of the Interior, Bureau of Mines; 1965.

4. Britton LG. Two Hundred Years of Flammable Limits. Process Safety Progress. 2002;21(1):1-12.

5. Mashuga CV. Determination of the combustion behavior for pure components and mixtures using a 20 L sphere. Michigan: Michigan technological University; 1999.

6. Crowl DA, Louvar JF. Chemical process safety : fundamentals with applications. 3rd ed. Daniel A. Crowl, Joseph F. Louvar. Prentice-Hall international series in the physical and chemical engineering sciences. Upper Saddle River, NJ : Prentice Hall, [2011] 3rd ed.; 2011.

7. Safelincs-Ltd. Information about the Fire Triangle/Tetrahedron and Combustion. https://www.firesafe.org.uk/information-about-the-fire-triangletetrahedron-and-combustion/.

8. Zhao F, Rogers WJ, Mannan MS. Experimental measurement and numerical analysis of binary hydrocarbon mixture flammability limits. Process Safety & Environmental Protection. 2009;87(2):94-104. doi:10.1016/j.psep.2008.06.003.

9. ASTM. ASTM E681 Standard Test Method for Concentration Limits of Flammability of Chemicals (Vapors and Gases). ASTM; 2015.

10. Coward HF, Jones GW. Limits of Flammability of Gases and Vapors Bulletin 503. Washington, DC: US Bureau of Mines; 1952.

11. White AG. XCVI.-Limits for the propagation of flame in inflammable gas-air mixtures. Part III. The effects of temperature on the limits. J Chem Soc. 1925;127(0):672-84. doi:10.1039/CT9252700672.

12. Kuchta JM. Investigation of fire and explosion accidents in the chemical, mining, and fuel-related industries - a manual. Bulletin. 1986.

13. Zabetakis MG, Lambiris S, Scott GS. Flame temperatures of limit mixtures. Symposium (International) on Combustion. 1958;7(1):484-7. doi:https://doi.org/10.1016/S0082-0784(58)80082-X.

14. Wu X, Yang Z, Wang X, Lin Y. Experimental and theoretical study on the influence of temperature and humidity on the flammability limits of ethylene (R1150). Energy. 2013;52:185-91. doi:https://doi.org/10.1016/j.energy.2013.01.042.

15. Kondo S, Takizawa K, Tokuhashi K. Effects of temperature and humidity on the flammability limits of several 2L refrigerants. Journal of Fluorine Chemistry. 2012;144:130-6. doi:https://doi.org/10.1016/j.jfluchem.2012.08.004.

16. Zhao F. Inert Gas Dilution Effect on the Flammability Limits of Hydrocarbon Mixtures: Texas A&M University; 2011.

17. Mitu M, Giurcan V, Razus D, Oancea D. Inert gas influence on the laminar burning velocity of methane-air mixtures. Journal of Hazardous Materials. 2017;321:440-8. doi:https://doi.org/10.1016/j.jhazmat.2016.09.033.

18. SAFEKINEX. Report on the experimentally determined explosion limits, explosion pressures and rates of explosion pressure rise: German Federal Institue for Materials Research and Testing (BAM)2002.

19. Zabetakis MG. Fire and explosion hazards at temperature and pressure extremes. 1965.

20. Takahashi A, Urano Y, Tokuhashi K, Kondo S. Effect of vessel size and shape on experimental flammability limits of gases. J Hazard Mater. 2003;105:27-37. doi:10.1016/j.jhazmat.2003.07.002.

21. Zhao F, Rogers W, Mannan MS. Calculated flame temperature (CFT) modeling of fuel mixture lower flammability limits. Journal of hazardous materials. 2010;174(1-3):416-23.

22. Vidal M, Wong W, Rogers WJ, Mannan MS. Evaluation of lower flammability limits of fuel–air–diluent mixtures using calculated adiabatic flame temperatures. Journal of hazardous materials. 2006;130(1-2):21-7.

23. Wong WK. Measurement of flammability in a closed cylindrical vessel with thermal criterion. College Station: Texas A&M University.

24. ASTM. ASTM E 918-83 Standard practice for determining limits of flammability of chemicals at elevated temperature and pressure. ASTM; 2005.

25. L Cashdollar K, A. Zlochower I, M Green G, A Thomas R, Hertzberg M. Flammability of Methane Propane and Hydrogen Gases. 2000.

26. Kondo S, Takizawa K, Takahashi A, Tokuhashi K, Sekiya A. A study on flammability limits of fuel mixtures. Journal of Hazardous Materials. 2008;155(3):440-8. doi:https://doi.org/10.1016/j.jhazmat.2007.11.085.

27. BSI. BS EN 1127 Explosive atmospheres. Explosion prevention and protection. Basic concepts and methodology. BSI; 2011.

28. Sadlier AG, Wolfe CA, Reese MM, Says I. Automated Alarms for Managing Drilling Pressure and Maintaining Wellbore Stability New Concepts in While-Drilling Decision Making Society of Petroleum Engineers. 2011. doi:10.2118/146298-MS.

29. Giménez-López J, Millera A, Bilbao R, Alzueta MU. Experimental and kinetic modeling study of the oxy-fuel oxidation of natural gas, CH4 and C2H6. Fuel. 2015;160:404-12. doi:10.1016/j.fuel.2015.07.087.

30. Heffington WM, Parks GE, Sulzmann KGP, Penner SS. Studies of methane-oxidation kinetics. Symp (International) on Combustion. 1977;16(1):997-1011. doi:https://doi.org/10.1016/S0082-0784(77)80391-3.

31. Suzuki T. Note: Empirical relationship between lower flammability limits and standard enthalpies of combustion of organic compounds. Fire and Materials. 1994;18(5):333-6.

32. Suzuki T, Koide K. Short Communication: Correlation between Upper Flammability Limits and Thermochemical Properties of Organic Compounds. Fire and Materials. 1994;18(6):393-7.

33. Zabetakis MG, Lambiris S, Scott GS. Flame temperatures of limit mixtures. Symp (International) on Combustion. 1958;7(1):484-7. doi:https://doi.org/10.1016/S0082-0784(58)80082-X.

34. Shebeko YN, Fan W, Bolodian IA, Navzenya VY. An analytical evaluation of flammability limits of gaseous mixtures of combustible–oxidizer–diluent. Fire Safety Journal. 2002;37(6):549-68. doi:https://doi.org/10.1016/S0379-7112(02)00007-3.

35. ANSYS. ANSYS Chemkin-Pro. https://www.ansys.com/products/fluids/ansys-chemkin-pro.

36. Smith GP, Golden DM, Frenklach M, Moriarty NW, Eiteneer B, Goldenberg M et al. GRI-Mech 3.0. http://www.me.berkeley.edu/gri_mech/.

37. Center for Energy Research (CER), University of California SD. Propane/Air Mechanism. http://www-mae.ucsd.edu/~combustion/cermech/.

38. Appel J, Bockhorn H, Frenklach M. Kinetic modeling of soot formation with detailed chemistry and physics: laminar premixed flames of C2 hydrocarbons. Combustion and Flame. 2000;121(1):122-36. doi:https://doi.org/10.1016/S0010-2180(99)00135-2.

39. Kondo S, Takizawa K, Takahashi A, Tokuhashi K. Extended Le Chatelier's formula and nitrogen dilution effect on the flammability limits. Fire Safety Journal. 2006;41(5):406-17. doi:https://doi.org/10.1016/j.firesaf.2006.03.002.